Norwegian Public Roads Administration

Standardized pile shoes on steel pipe piles

Status of R&D project June 2011

VD report | Directorate of Public Roads | No 34E

Directorate of Public Roads
Traffic safety, Environment and Technology
Geotechnical
June 2011

VD rapport

Tittel
Standardiserte hule pelspisser for stålrørspel

Undertittel
Status FOU-prosjekt juni 2011

Forfatter
Grete Tvedt og Tewodros Tefera

Avdeling
Trafikksikkerhet, miljø- og teknologiavdelingen

Seksjon
Geoteknikk og skred

Prosjektnummer
601863

Rapportnummer
Nr. 34E

Prosjektleder
Grete Tvedt

Godkjent av
Frode Oset og Eldar Høysæter

Emneord
Oslo spiss, stålrørspel, pelspiss, sveising, fullskalaforsøk, dynamisk beregning, støtbølge, rammespenning, diskontinuitet

Sammendrag
Statens vegvesen er blant de største byggherrene i Norge som fundamenterer konstruksjoner på stålrørspeler. Ettersom bergspissene er kostbare og viktig for pelens bæreevne har Statens vegvesen startet FOU-prosjektet. Dette i håp om å kunne redusere pris, redusere antall vrakpeler og øke kunnskapen om problemstillinger knyttet til bergspissene og oppnå en optimalisert dimensjonering med sikte på standardiserte spisser som kan anvendes i de fleste tilfeller. Dette pågående FOU-prosjektet har skjedd i samarbeid med Aas-Jakobsen, Geovita og Ruukki. NTNU, Institutt for konstruksjonsteknikk har gjennomført to mastergradsoppgaver i FOU-prosjektet. Fullskalaforsøket som omtales i denne rapport er foreløpig det siste i dette pågående FOU-prosjektet, og det er en del av en masteroppgave til Svein Jørgensen Tveito NTNU, Institutt for konstruksjonsteknikk, i våren 2010.

Antall sider 108

Dato Juni 2011

VD report

Title
Standardized pile shoes on steel pipe piles

Subtitle
Status of R&D project June 2011

Author
Grete Tvedt and Tewodros Tefera

Department
Traffic safety, Environment and Technology

Section
Geotechnical

Project number
601863

Report number
No. 34E

Project manager
Grete Tvedt

Approved by
Frode Oset and Eldar Høysæter

Key words
Oslo point, steel pipe pile, pile shoe, welding, full scal test, dynamic calculation, sress wave, driving stress, discontinuity

Summary
The Norwegian Public Roads Administration is among the largest clients in Norway who have structures founded on steel pipe piles. Since the pile shoes are expensive and important part of the steel pipe piles on rock, the Norwegian Public Roads Administration has started this R&D project. This ongoing R&D Project with the purpose of standardizing the pile shoes for steel pipe piles aims to increase the knowledge related to steel pipe pile shoes on rock and optimise the design in order to standardize the dimensions. This ongoing R&D Project is carried out in collaboration with the Norwegian C.E. consultants; Aas-Jacobsen, Geovita and the Finnish steel supplier Ruukki. In collaboration with NTNU, Department of Structural Engineering, two master projects were conducted. The full-scale experiment in this report is the current stage of this R&D project and is part of the master thesis by Sveinung Jørgensen Tveitoat NTNU, spring 2010.

Pages 108

Date June 2011

Table of Contents version

0 Symbols and acronyms 4
1 Purpose and background of the project 5
2 Historical review of the Oslo point 5
3 Calculation of pile shoes according to the Norwegian Piling Handbook 7
3.1 Assumption for calculations 7
3.2 Assessment of the size of dowel and inside diameter of hollow bar/pipe 8
3.3 Design of the hollow bar 9
3.4 Design for static long term load (after 100 years) 10
4 Dynamic loads and stresses in the pile and shoe 11
4.1 Stress wave theory 11
4.2 Evaluation of dynamic loads during driving 15
4.3 Design of dynamic load from PDA measurements 16
4.4 Design of dynamic load according to the Norwegian Piling Handbook 18
5 Full-scale test of steel pipe pile shoe driven on rock 20
5.1 Test location and companies involved 20
5.2 Shoe types 22
5.3 Instrumentation 25
5.4 Driving test piles 25
5.5 Results from full scale test 26
5.6 Related costs of the full scale test 40
6 Theoretical calculation using the finite element method 41
6.1 Material models 41
6.2 Comparison of results with the physical test 44
7 Laboratory tests with small scale pile shoes 50
8 Summary of all tests 58
8.1 Driving stresses in pile shoe parts 58
8.2 Dynamic amplification factor 59
8.3 Stresses in steel with rapid load application as during pile driving 62
9 Conclusions and recommendations 63
9.1 Proposed changes to the Norwegian Piling Handbook 65
9.2 Pile spacing 66
10 Suggestions for further work 66
10.1 Design of pile shoe for piles with a diameter of 800 mm 66
10.1.1 Parameter study in Abaqus 66
10.1.2 Thickness of the welding 66
10.1.3 Evaluation of hardening, shaping and build-up welding on the rock shoe 67
10.1.4 What is the best end face on the hollow bar, concave or straight end face? 67
10.2 The rock type and stress occurring in the shoe 67
10.3 Full-scale test with solid shoes 68
10.3.1 Other pile dimensions - can we just scale up and down? 68
11 References 68

Attachments

A. PDA report
B. Driving procedure and driving protocol

0 Symbols and acronyms

Symbol	Explanation
A	Area
c	wave velocity (for steel, c = 5172 m/s)
d	Dowel diameter
d_i	Shoe/hollow bar's internal diameter
d_y	Shoe/hollow bar's outside diameter
D	Pile diameter
E	Modulus of elasticity (for steel, E = 210,000 N/mm^2)
f_o	Impedance constant
f_a	Reduction factor
f_{di}	Discontinuity factor for the initial wave
f_{dr}	Discontinuity factor for the reflected wave
f_u	Rupture stress
f_y	Yield stress
f_w	Amplification factor
F_d	Design load
g	Gravitational acceleration
h	Drop height
L	Total length of pile shoe
N_d	Design capacity
$N_d^{corroded}$	Design capacity reduced due to corrosion
$N_\gamma^{DRIVING}$	Dynamic force (load)
N_i	Installed capacity
R	Length of stiffening plates
R_{ck}	Characteristic bearing capacity
t	Thickness
v	velocity
S	Free length of pile shoe
t_r	Thickness of stiffening plates
T	Thickness of bottom plate
W	Section modulus
Z	Acoustic impedance
Ø	Pile diameter
γ_t	Partial factor for total resistance of a pile
γ_m	Material factor
ρ	Density (for steel, ρ = 7850 kg/m^3)
σ_{dr}	Dynamic stress
σ_o	Front stress (stress wave theory)
σ_{max}	Maximum stress with stress wave

1 Purpose and background of the project

The Norwegian Public Roads Administration (NPRA) currently has an on-going R&D project regarding steel pipe piles with hollow rock shoes. This report summarizes the results of this R&D work so far with a special focus on the latest results from the master thesis by Sveinung Jørgensen Tveito carried out at NTNU, Department of Structural Engineering in 2010.

The purpose of the R&D project is to standardize the pile shoes for steel pipe piles. Steel pipe piles are becoming larger and larger with increasingly higher loads per pile. The NPRA want to verify that the pile shoe can withstand this load. It is difficult to calculate the dynamic load that the pile shoe is subjected to, and therefore it is rarely (never) done. If a pile becomes overloaded during driving and in doing so is destroyed, it is rather expensive. Thus the objective is to dimension a standardized robust pile shoe. In this way economic benefit can be obtain through “mass production” of the same type of pile shoes as well as reduces or avoids pile shoe damage due to undersized pile shoe.

The R&D project was divided into several phases and in the earlier phases of the study the dimensions of the pile shoes were calculated in different ways:

- Phase 1: Calculation according to empirical models in the Norwegian Piling Handbook 2005 and 1991 [2] and [3]. The calculations were performed by Geovita in 2007/2008. [1]
- Phase 2: Static calculation using the finite element software ANSYS.
  The calculations were performed by Aas-Jakobsen 2007/2008. [1]
- Phase 3: Dynamic calculation using ABAQUS.
  Calculations performed in the master theses by Andreas K. Forseth 2009 [4] and Sveinung J. Tveito 2010 [5].
- Phase 4: Full scale test and laboratory tests were performed by the NPRA in collaboration with RUUKKI and NTNU in the thesis by Sveinung J. Tveito in 2010 [5].
- Phase 5: Additional calculation to the full scale test performed in the master thesis by Sveinung J. Tveito 2010 [5].

2 Historical review of the Oslo point

L. Bjerrum published in 1957 the Norwegian experience with steel piles to rock, NGI Publication No. 23 [7]. The paper reviews 25 years of Norwegian experience of the use of steel piles for foundations. The first building in Oslo with steel pile foundations was built around 1930.

The first piles, which were driven in 1931, were already supplied with a special point and careful considerations were given to its form in order to safeguard against the sliding of the pile on an inclined rock surface. The pile shoes were equipped with a specially designed shoe that would prevent the pile sliding against the sloping rock. The final solution was to make the point of a round steel bar the lower end of which was hollow ground. In this way the sharp edges of the bar should be able to secure a hold in the rock immediately after the initial rock contact. This type of pile shoe has since been called an ‘Oslo point’.

Initially H-beams and railway tracks were used as piles. Figure 2-1, a) H-section steel piles with points and caps as required by the Building Authority of Oslo in 1957 and as can be seen the diameter of the round steel is between 70 mm and 100 mm. Figure 2-1, b) shows a full-scale test of 4 piles driven to rock and afterwards extracted for inspection.
The study showed hollow ground steel bar shoes were the best choice for the hard rock that the shoes were driven into in Oslo. Oslo points were solid steel rods and the shoes that were the best in the test were those in which the lower 100 mm (4 inches) was hardened to between 400 and 600 Brinell.

The hollow ground shoe corresponds to what we call the shoe with a concave end face is referred as Oslo point in a number of subsequent international publications. The tests and analysis summarized in the NGI publ. No. 23 [7] is basis for a further development of the Oslo point to make it hollow to mount dowels.

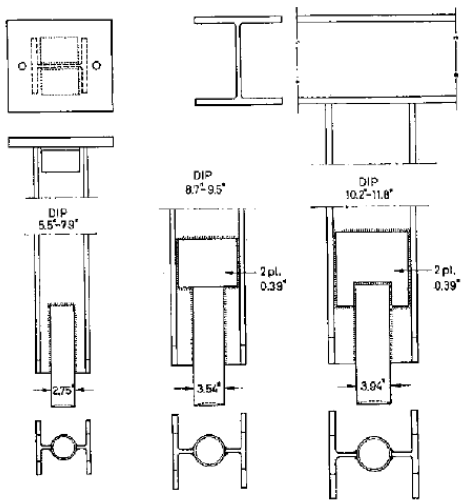

(A) H-section steel piles with points and caps as required by the Building Authority of Oslo in 1957.

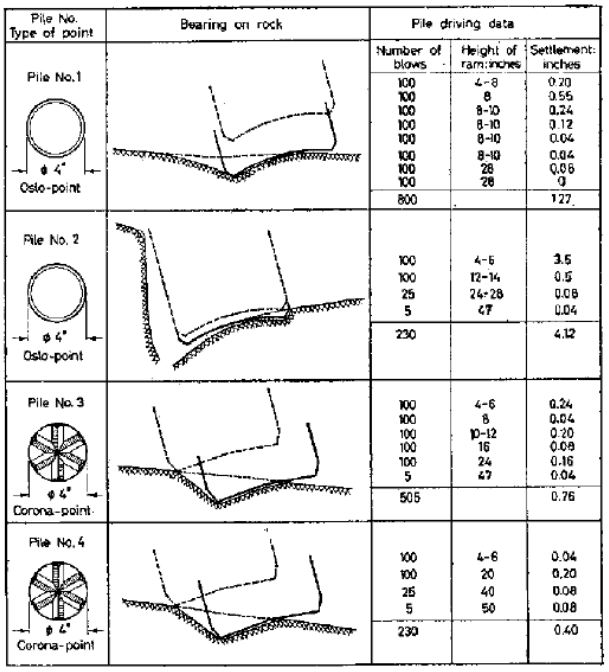

Pile No. Type of point	Bearing on rock	Pile driving data		
		Number of blows	Height of ram: inches	Settlement: inches
Pile No. 1 (φ 4", Oslo-point)		100	4-8	0.20
		100	8	0.55
		100	8-10	0.24
		100	8-10	0.12
		100	8-10	0.04
		100	8-10	0.04
		100	28	0.06
		100	28	0
		800		1.27
Pile No. 2 (φ 4", Oslo-point)		100	4-6	3.5
		100	12-14	0.5
		25	24-28	0.08
		5	47	0.04
		230		4.12
Pile No. 3 (φ 4", Corona-point)		100	4-6	0.24
		100	8	0.04
		100	10-12	0.20
		100	16	0.08
		100	24	0.16
		5	47	0.04
		505		0.76
Pile No. 4 (φ 4", Corona-point)		100	4-6	0.04
		100	20	0.20
		25	40	0.08
		5	50	0.08
		230		0.40

(b) Point bearings of four batter steel piles driven to rock and afterwards extracted for inspection.

Figure 2-1: Examples of the use and test of the Oslo point from 1957 [7]

In 1950, the maximum permitted stress was 100 kPa for piles shorter than 12 -15 m. For longer piles the permitted stress was lower. Since then loads have become greater and greater as well as pile dimensions have increased accordingly. Steel materials have improved, and have higher yield stress. Therefore it's time to develop new experiences.

3 Calculation of pile shoes according to the Norwegian Piling Handbook

Geovita and Aas-Jakobsen performed static calculations of piles and pile shoes [1] according to the pile design flow chart, Figure 1.1 in the Norwegian Piling Handbook 2005 [2]. Ahead of the calculations number of practical options e.g. dimensions of pile and dowel were given, and this gave some assumptions and driving conditions for the calculations. The calculations in this report are revised in relation to the dimensions of the piles in the full scale test.

For a clear understanding of terminologies used in this report, the different parts of the pile shoe are shown in Figure 3-1.

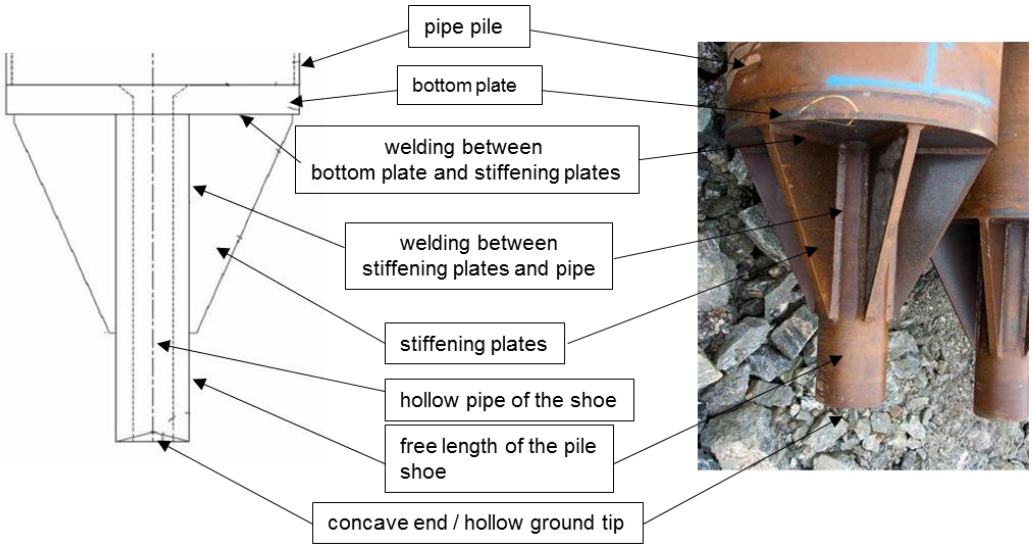

Figure 3-1: Terminologies for parts of the pile shoe's component used in this report

3.1 Assumption *for calculations*

Design load transferred to the pile shoe after installation, F_d = 5000 kN. The design load includes any supplementary loads and the deadweight of the pile. The steel pipe pile have a diameter of 814 mm and a wall thickness of 14.2 mm. The steel pipe has an area, A = 35,635 mm^2.

Reduction factor (f_a)for the project has been set to f_a = 0.85.

The partial factor for uncertainty linked to the determination of characteristic bearing capacity is set to, γ_t = 1.6. With the design load F_d = 5000 kN, the bearing capacity, which then be verified becomes $R_{ck} = F_d * \gamma_t$ = 5000 kN * 1.6 = 8000 kN.

It is generally known that the yield stress of steel is dependent on the wall thickness as shown in Table 3-1. This must be taken into account in the design of individual structural components of the pile shoe.

Wall thickness, t (mm)	Yield stress, f_y (MPa)
$t < 16$	355
$16 < t \leq 40$	345
$40 < t \leq 63$	335
$63 < t \leq 80$	325
$80 < t \leq 100$	315
$100 < t \leq 150$	295

Table 3-1: Minimum yield stress of steel for different wall thickness (EN 10025-2: 2004)

3.2 Assessment of the size of dowel and inside diameter of hollow bar/pipe

In the project order the chosen dowel had a diameter, d = 80 mm. The basses for the assessment is that the dowel must be so strong that it resists a punch, yet the larger it becomes the larger the shoe that needs to dislodge the rock. A rock drill bit with a diameter of 96 mm was chosen after talks with NSP, Dagfinn Dybvik.

The maximum shear capacity of the dowel is $R \approx 0{,}7 \cdot f_y \cdot A$. When there is a gap between the shoe and the rock, the dowel capacity will be reduced because of the moment developed in the dowel. The capacity of the dowel R is then determined based on the following formula [6].

$$R = \frac{2 \cdot W \cdot f_y}{\Delta \cdot \gamma_M}$$

where: W = dowel section modules,
f_y = yield stress of steel,
Δ = gap between the shoe and the rock, and
γ_M = partial factor for material strength of steel.

By combining the two formulas we get a design diagram for the dowel shown in Figure 3-2. We have then assumed that the steel has the yield stress $f_y = 355$ N / mm^2. If the rock has 45° angle to the horizontal plane, for the test shoe there will be 58 to 108 mm gap between the shoe tip and the rock surface.

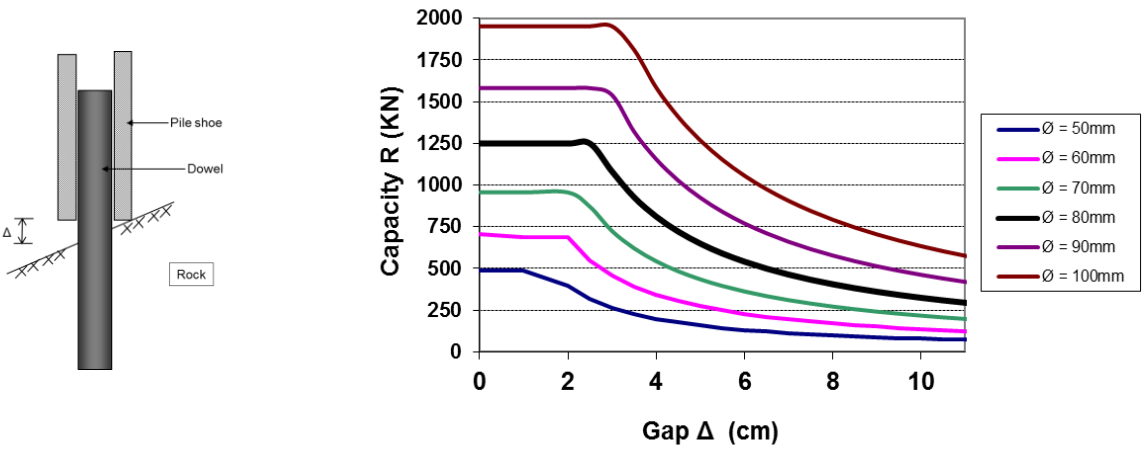

Figure 3-2: Dowel capacity

Hollow steel pile shoes have large tolerance deviations, typically more than 5 mm both inside and outside diameter. However, the steel area is always equal to or greater than the theoretical. In the specification of the hollow bar of the pile shoes the requirement is therefore to the minimum measurement for the inner diameter (where the tolerance deviation has been included) and steel area.

Furthermore, there must be a few millimetres of clearance between the inner hollow bar and the rock drill bit, estimated with a minimum of 5 mm clearance around.

⇨ Minimum internal diameter of the hollow bar:

d_{min} = 80 (dowel) + 10 (deviation hollow bar) + 20 (clearance dowel/hollow bar) = 110 mm
Inside diameter of the hollow bar used in full-scale tests d_i = 119 mm.

Initially, it is not required that the hollow bar of the pile shoe to have the same area (capacity) as the pile pipe. This is because the steel thickness of the pile pipe for long piles is usually increased due to technical reasons when driving, i.e. in order to verify the necessary characteristic bearing capacity. The capacity of the shoe is therefore controlled by the design load (F_d):

3.3 Design of the hollow bar

$R_{ck} = F_d * \gamma_t$ = 5000 kN * 1.6 = 8000 kN.

In Phase 1 of the project a steel pipe pile was calculated with the dimension Ø814x14.2 mm [1] according to figure 1.1 in the Norwegian Piling Handbook (2005) [2].

In the Norwegian Piling Handbook (1991) [3] chapter 9.5:

> *"For up to approx. 10 control blows in order to make a dynamic loading test, σ_{dr} can normally be exceeded by up to 25%."* The same is stated in *the* Norwegian Piling Handbook (2005) [2] chapter 4.7. (This is a correction text from the Norwegian version of the report). We have looked at this in detail in a literature study in this report in section 8.3.

REQUIREMENTS: $\sigma_{\max} \leq 1{,}25 \cdot \sigma_{dr} = 1{,}25 \cdot \frac{f_y}{1{,}05}$

Based on the above requirements the pile and the pile shoe should then withstand:

$$R_{c;k} = 8000\,kN \leq 1{,}25 \cdot N_d \quad (\text{"}Dynamic\ load\text{"})$$

Driving stress is controlled without the use of f_a factor and γ_m = 1.05.
The stress is allowed to exceed the yield stress by 25%, and the necessary shoe area is then:

$$R_{c;k} \leq A_{shoe} \cdot \frac{f_y}{\gamma_m} \cdot 1{,}25$$

$$\Rightarrow \quad A_{shoe} \geq \frac{1}{1{,}25} \cdot R_{c;k} \cdot \frac{\gamma_m}{f_y} = \frac{1}{1{,}25} \cdot 8000 \cdot \frac{1{,}05}{335} \cdot 10^3 = 20060\,mm^2$$

With $d_i \geq 110$ mm the minimum d_y = 195 mm

If the stress is not allowed to exceed the yield stress the necessary shoe area will be:

⇨ $$A_{shoe} \geq \frac{1}{1{,}0} \cdot R_{c;k} \cdot \frac{\gamma_m}{f_y} = \frac{1}{1{,}0} \cdot 8000 \cdot \frac{1{,}05}{335} \cdot 10^3 = 25074\ mm^2$$

Selected hollow bar in the full-scale test for NPRA-shoe is therefore:

d_y = 219 mm, d_i = 119 mm ⇨ $$A = \frac{\pi}{4}(d_y^2 - d_i^2) \quad = \quad 26546 \quad mm^2$$

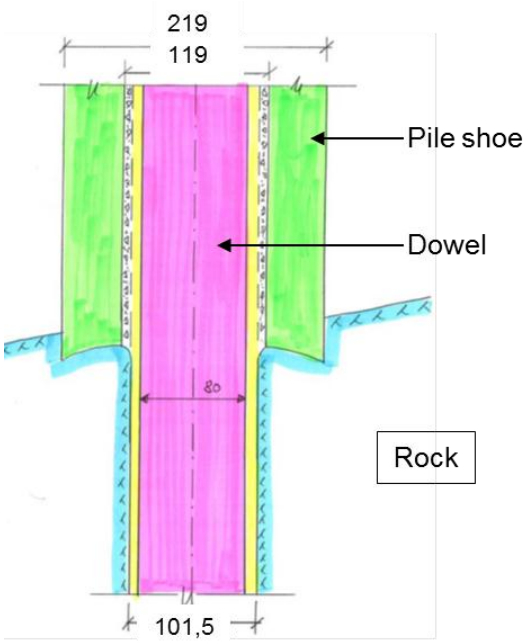

Figure 3-3: Section of the shoe and dowel in rock with the dimensions used in the full-scale test

3.4 Design for static long term load (after 100 years)

Verifying the selected hollow bar of the pile shoe (d_y = 219 mm, d_i = 119 mm) against the static load after 100 years. Bridges are usually designed for a life time of 100 years.

- ⇨ The pile is reinforced and casted with concrete to make sure that the reinforcement and concrete bear the load
- ⇨ There is grouting between the hollow bar and dowel. Corrosion is therefore assumed only externally.

Recommended corrosion rate specified in the Norwegian Piling Handbook 2005 section 6.1.5 [2] is 0.015 mm/year.
We have chosen a higher corrosion rate: 0.025 mm/year · 100 years = 2.5 mm.

$$A_{shoe}^{corroded} = \frac{\pi}{4} \cdot \left(214^2 - 119^2\right) = 24846\ mm^2$$

Dimensioning the cross-section capacity of corroded cross-section of the hollow bar:

$$N_d^{corroded} = A^{corroded} \cdot \frac{f_y}{\gamma_m} \quad ; \quad \gamma_m = 1{,}05 \text{ According to NS-EN 1993-1-1 2005/NA-2008}$$

$$N_d^{corroded} = 24846 \cdot \frac{335}{1{,}05} \cdot 10^{-3} = 7926\ kN$$

The installed capacity will then be:

$$N_i^{corroded} = f_a \cdot N_d^{corroded} = 0{,}85 \cdot 7566 = 6737\ kN$$

$$N_i^{corroded} > F_d = 5\,000\ kN \qquad OK$$

Loading during driving will be the design load.

4 Dynamic loads and stresses in the pile and shoe

4.1 Stress wave theory

The theory of stress wave for piles is summarised in the master thesis 2010 [5].
Since the piles are long slender bodies the following assumptions were made:

1. The stress condition is one dimensional
2. All particles in the same section have the same deformation u(x,t)
3. The material is isotropic and linearly elastic

One dimensional wave velocity is defined as: $c = \sqrt{\frac{E}{\rho}}$

The stress with stress wave is:

$$\sigma(x,t) = \frac{E}{c} v(x,t) = c\rho v(x,t)$$

During pile driving v(x,t) is replaced by $v = \sqrt{2gh}$, i.e. the velocity of the incoming hammer.
The force will then be:

$F = \sigma(x,t) \cdot A = \frac{EA}{c} v(x,t) = Zv(x,t)$ where $Z = \frac{EA}{c}$ is defined as the acoustic impedance.

This shows that for a wave which propagates in a positive direction, the force is directly proportional to the particle velocity.

Stress is doubled with a fixed end. Depending on the strength of the material that the pile shoe penetrates into, the degree of fixity will be a position between a permanently fixed end and a

free end. For a pile shoe that penetrates into rock the rock will offer resistance and thus reflect a pressure wave with lower amplitude than the incoming.

Wave reflections occur in areas where the cross section or material properties change. This is relevant, for example, at the transition from pile pipe to pile shoe, or on the hollow bar above or below the end of the stiffening plates. When a stress wave (σ_i) hits a discontinuity (see Figure 4-1), part of it will continue to propagate (σ_t), and part of it is reflected (σ_r).

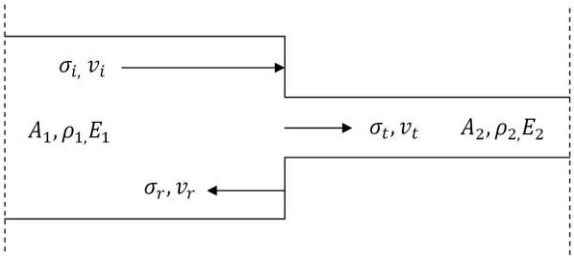

Figure 4-1: Discontinuity in cross-section

In the event of a cross-section change there must be equilibrium of forces and the particle velocity across the transition must be equal to:

$$A_1 \cdot (\sigma_i + \sigma_r) = A_2 \cdot \sigma_t \qquad \text{and} \qquad v_i - v_r = v_t$$

In the case when the density ρ and modulus of elasticity E are equal for the two materials one can with an intermediate calculation arrives at the following relations:

$$\sigma_t = \frac{2A_1}{A_1 + A_2} \cdot \sigma_i = f_{di} \cdot \sigma_i \qquad \text{and} \qquad \sigma_r = \frac{A_2 - A_1}{A_1 + A_2} \cdot \sigma_i = f_{dr} \cdot \sigma_i$$

f_{di} is the discontinuity factor for the initial wave and f_{dr} is the discontinuity factor for the return wave.

In order to make calculations for pile driving by hand, certain simplifications must be made. The hammer here is considered as a rigid body with the mass M_0 and the drop speed v_0 when it hits the pile. The pile is assumed to have a pipe cross-section with the material properties E, A and ρ, where the end against the rock is seen as fixed. The pile shoe is ignored. The model is outlined in Figure 4-2. By setting up the dynamic equilibrium of forces of the hammer, one can establish the stress process over time at the pile head, i.e., x = 0.

The calculations we have made with the discontinuity in this report are simplified. We have looked at the area on the shoe and pipe. We have for simplicity's sake cut out the discontinuity over the base plate. We have also only seen the initial wave and not the return wave.

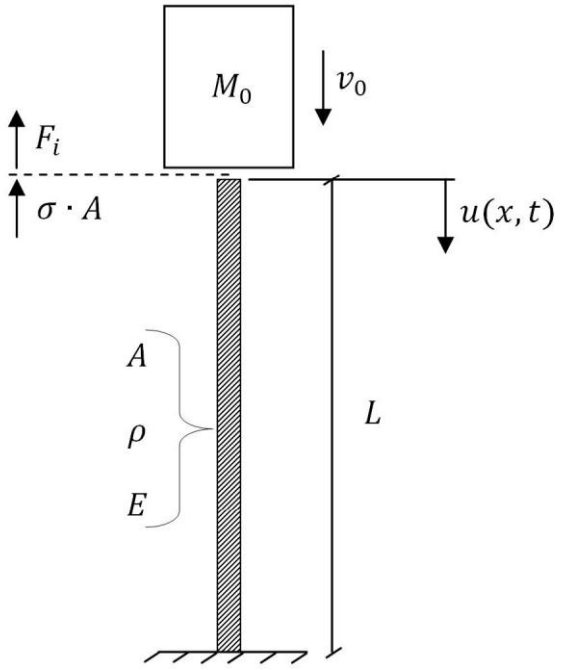

Figure 4-2: Idealized model of the pile driving

$$\sigma A + F_i = c\rho v A + M_0 \frac{dv}{dt} = 0$$

After some intermediate calculations we arrive at:

$\sigma = \sigma_0 e^{-\frac{\rho c A}{M_0} \cdot t}$ where $\sigma_0 = \rho c v_0$ is the value of the initial stress front.

Finally, you can use that the mass of the pile is $M = \rho AL$:

$$\sigma = \sigma_0 e^{-\frac{M}{M_0} \cdot \frac{c}{L} t}$$

The equation above give the stress at the point x = 0 for varying t < 2L/c. But since the stresses run like a wave down in the pile, the stress σ_0 that was at the point x = 0 at t = 0 has moved to x = $c\Delta t$ after t = Δt.

At the time t = Δt the stress in x = 0 becomes: $\sigma = \sigma_0 e^{-\frac{M}{M_0} \cdot \frac{c}{L} \Delta t}$

In this way, the wave moves down the pile with σ_0 at the front, while it draws the stress history from point x = 0 as a tail, as in Figure 4-3. When t = L/c the wave has moved down to the pile toe. There the wave becomes reflected and continues up again with the same sign of operation as the end is fixed. The total stress in a cross-section is given by the sum of the forward wave and the reflected wave. At t = 2L/c the wave front moves to the pile head again and the stress becomes:

$$\sigma = \sigma_0 + \sigma_0 e^{-\frac{2M}{M_0} \cdot}$$

The different material parameters are shown in Table 4-1 for the idealised model in Figure 4-2. We have chosen parameters used in the full scale test. The mass of the pile is M = ρAL. Initial speed of the hammer is set to $v = \sqrt{2gh}$ = 2.43 m/s for h = 0.3 m.

L (m)	D_y (mm)	t (mm)	ρ (kg/m^3)	E (N/mm^2)	c (m/s)	M_0 (kg)	M (kg)
7.52	813	14.2	7850	210,000	5172	9000	2104

Table 4-1: Geometry and material properties used for theoretical calculations of the full-scale test.

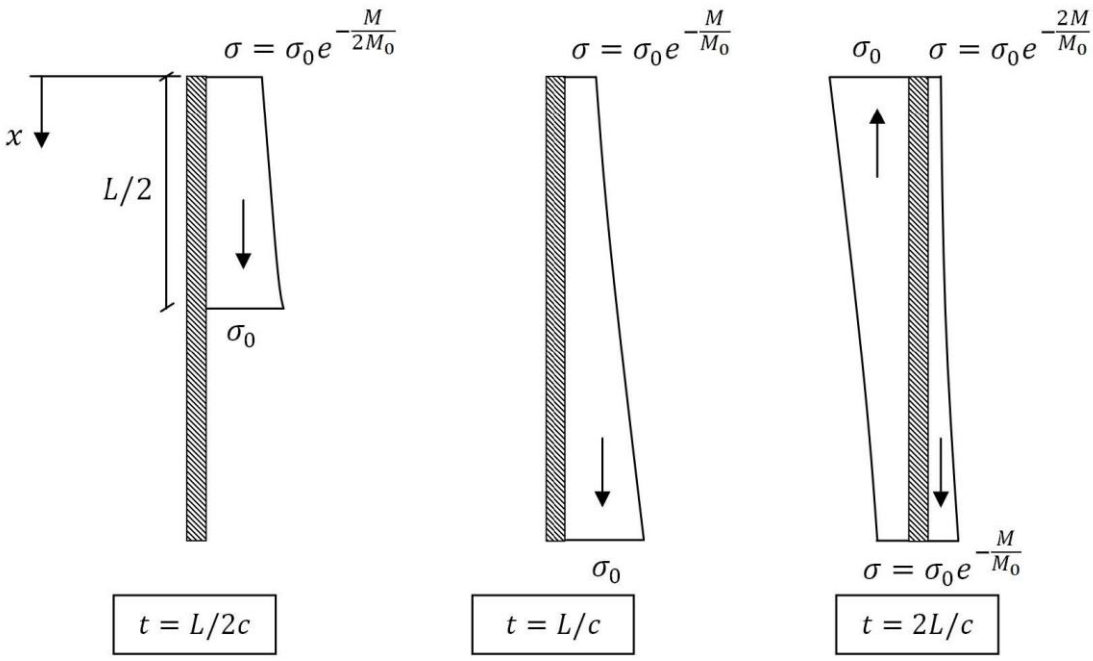

Figure 4-3: Stress state at different times

Figure 4-3 illustrates how the stress at the top of the steel pipe pile changes over time

At t = 0: $\sigma(x=0) = \sigma_0 e^{-\frac{M}{M_0}\cdot\frac{c}{L}t} = \sigma_0 = c\rho v = 98.5$ MPa

At t = L/c = 0.0015 s: $\sigma(x=0) = \sigma_0 e^{-\frac{M}{M_0}} = 78.0$ MPa

At t = 2L/c = 0.0029 s: $\sigma(x=0) = \sigma_0 e^{-\frac{2M}{M_0}} = 61.7$ MPa

The total stress at t = 2L/c with continuous initial stress will then be:

σ_{max} (t = 2L/c, x = 0) = 98.5 + 61.7 = 160.2 MPa

$$\sigma_t = \frac{2A_1}{A_1 + A_2}\cdot\sigma_0 = \frac{2\cdot 35635}{26546 + 35635}\cdot\sigma_0 = 1{,}14\cdot\sigma_0 = 1{,}14\cdot 160{,}2\ MPa = 182{,}6\ MPa$$

The same calculations were performed for different drop heights, and the results are given in

Table 4-2 and Table 4-3.

h (m)	v (m/s)	σ at t = 0 (MPa)	σ at t = L/c (MPa)	σ at t = 2L/c (MPa)	σ_{max} at t = 2L/c (MPa)
0.3	2.43	99	78	62	160
0.6	3.43	139	110	87	226
1.0	4.43	180	142	113	292
1.4	5.24	213	168	133	346

Table 4-2: Calculation of theoretical maximum stress in the steel pipe at the pile head by stress wave theory

h (m)	Pile pipe σ_{max} at t = 2L/c (MPa)	Pile shoe σ_{max} at t = 2L/c (MPa)
0.3	160	183
0.6	226	258
1.0	292	333
1.4	346	395

Table 4-3: Calculation of theoretical maximum stress in the pile pipe and the pile shoe by the discontinuity formula (f_{di} = 1.14)

The stress wave has a wavelength many times longer than the length of the pile. This is controlled by the condition $M/M_0 = \rho AL/M_0$. The larger the mass condition, the shorter the wavelength. The condition also helps to control the length of the blow. The lower the condition, the longer it takes for the stroke to finish.

For information a hydraulic hammer is usually driven one blow every 0.1 seconds.
In comparison, the stress wave in 75 m long piles propagates and reflects in runs of 0.03 seconds.

4.2 Evaluation of dynamic loads during driving

In order to ensure that the pile reaches the characteristic bearing capacity or safe rock anchoring, it is verified with a few blows (typically 2 to 10 blows). In this case, it is verified with R_{ck} = 8000 kN.

One can calculate the stress in the shoe, to ensure that the pile or shoe is not overdriven, with the help of the following methods:

- Stress wave theory
- Wave equation
- PDA measurements
- Pile movement/sink measurements

⇨ The methods provide an estimate of σ_0

σ_0 can, to some extent, be controlled based on the selection of the hammer. Favourable are high, slender and heavy hammer.

As the stress wave reaches the pile shoe, the wave is reflected through the pile as a pressure wave. In the event of large shoe resistance, a pressure stress spike occurs at the pile shoe (σ_{max}) when the downward and upward wave overlaps:

$\underline{\sigma_{\max} = f_w \cdot \sigma_0}$ where f_w is the amplification factor for stress waves

f_w varies from 1.0 - 1.8 (most typically between 1.3 and 1.5) depending on the method, shoe tip resistance and pile length. It provides guidelines for selection of f_w in Table 4-4.

f_w can also be estimated from PDA curves, but this is not an officially recognized method. Besides it is not all PDA-curves that can be interpreted in this way, for example, it is difficult for relatively short piles.

4.3 Design of dynamic load from PDA measurements

The full-scale test has been carried out on short piles and PDA measurements are difficult to interpret.

We therefore show an example how to determine f_w based on PDA-curves from the project "Bjørvika - Sørenga" where HP 305 x 186 with steel grade S460M piles were driven. A hammer load of 120 kN with the efficiency of about 1.0 and a drop height of 1.0 metres were used.

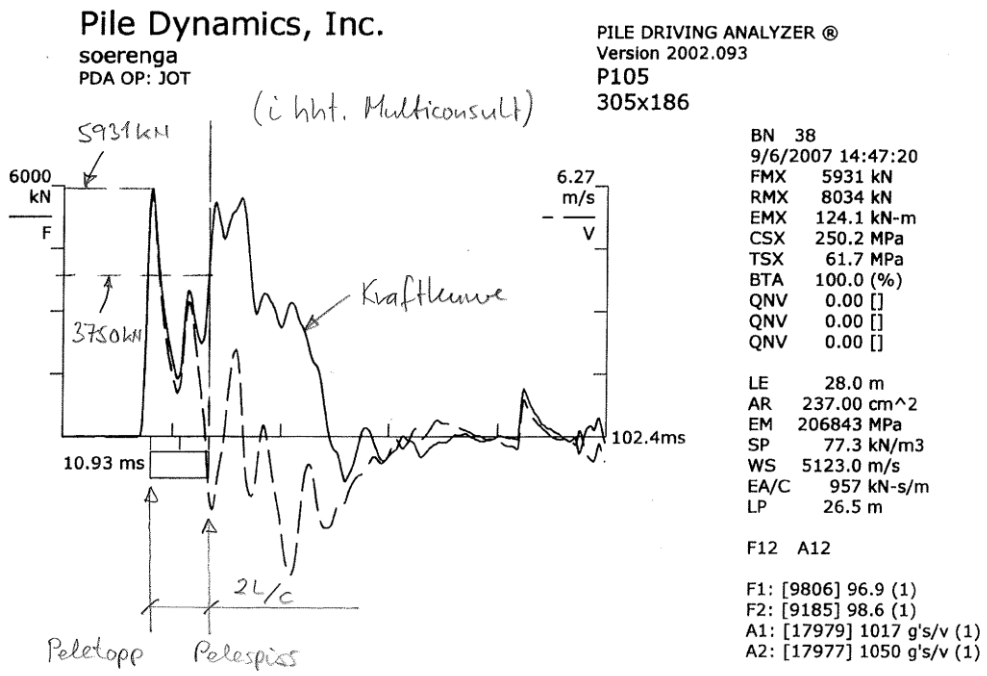

Figure 4-4: Determination of f_w based on PDA curves for HP piles in the Bjørvika project [1]

Measured force at the pile head, FMX = 5931 kN (corresponding to CSX, stress at the top of the pile).

$$f_w = \frac{5931 + 3750}{5931} = 1{,}63$$

Stress in the pile shoe during dynamic testing will then be:

$$\sigma_{max} = f_w \cdot \sigma_0 = 1{,}63 \cdot 250{,}2 = \underline{408\ MPa}$$

Note! The compressive stress σ_{max} is the stress due to overlapping of the downward and reflected stress wave in the toe of the pile pipe/pile shoe.

Although it is difficult to interpret the full scale test as the piles are short, we have shown an example below:

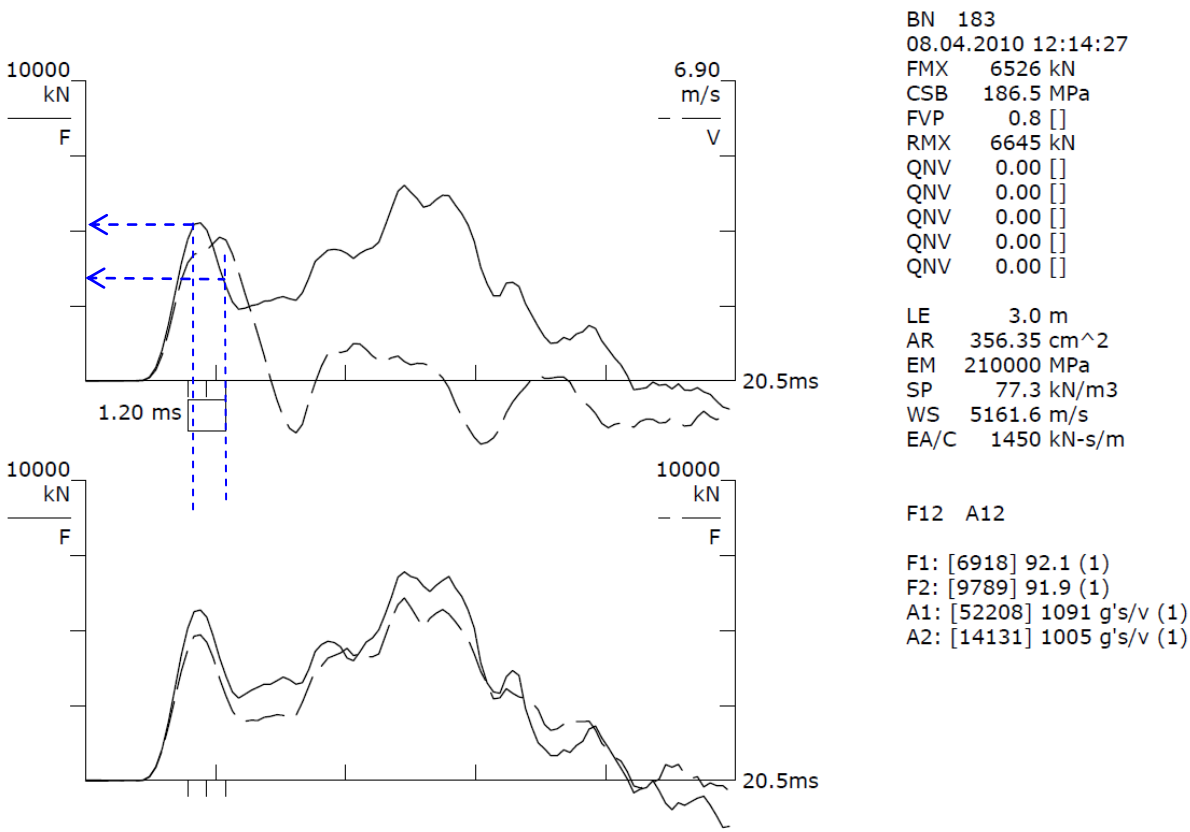

Figure 4-5: Determination of f_w based on PDA curves for full scale test on steel pipe pile 1 in the Dal- Boksrud project

Measured force at the pile head, FMX = 6526 kN

$$f_w = \frac{6526 + 2750}{6526} = 1{,}42$$

4.4 Design of dynamic load according to the Norwegian Piling Handbook

When the hammer hits the pile head, a stress wave occurs with front stress:

$$\sigma_o = f_o \cdot \sqrt{\rho \cdot g \cdot h \cdot E} \qquad \text{where:} \qquad f_0 = f_i \cdot \eta \cdot \sqrt{2} \approx 0{,}9 \cdot 1{,}0 \cdot \sqrt{2} = \underline{1{,}27}$$

f_i = 0.9 (impedance state between the hammer and pile where 0.9 is a commonly used factor)

$$\sigma_0 = 1{,}27 \cdot \sqrt{7{,}85 \cdot 9{,}81 \cdot h \cdot 2{,}1 \cdot 10^8} \cdot 10^{-3} = 161{,}5 \cdot \sqrt{h}$$

As the stress wave reaches the pile shoe, the wave is reflected through the pile as a pressure wave if the shoe tip resistance is high.

$$\sigma_{\max} = f_w \cdot \sigma_0$$

Amplification factor for stress wave f_w gives an increase in the stress σ_0 to σ_{max} depending on the side friction on the pile and sink in the rock. From the full-scale test in chapter 5, we choose values for f_w in relation to the sink according to the Norwegian Piling Handbook [2] Table 4-4. The pile in the experiment is short with little side friction, but the sink is about 1 mm.

The table in the Norwegian Piling Handbook gives values for sink greater than 5 mm and less than 1 mm. With the final blows the sink is usually between 1 and 3 mm. The table is therefore difficult to interpret in this range. We have chosen some variations of f_w from small to large depending on the shoe tip resistance, and calculated the stress in the pile pipe and in the hollow bar, Table 4-5.

	During downward driving Moderate driving resistance s > 5 mm/blow			During final driving Significant shoe resistance s < 1 mm/blow		
Friction resistance	Small	Medium	Large	Medium		Small
Tip resistance	Small	Medium		Moderate	Large	Very large
Compression	1.0	1.0	1.0	1.2 to 1.3	1.3 to 1.5	1.5 to 1.8
Tension	-1.0 to -0.8	-0.8 to -0.4	-0.4 to -0.3	Stress can occur in the reflected wave when the pile head See 4.6.3 [2]		

Table 4-4: Recommended values for f_w the factor in the Norwegian Piling Handbook [2]

The calculated front stress σ_0 and the maximum stresses $\sigma_{max\ (pipe)}$ in the pile pipe due to the overlapping of the upward and downward stress waves are shown in Table 4-5.

Because of the area of the NPRA pile shoe being smaller than the area of the pile pipe, greater stress occurs in the shoe according to the discontinuity formula:

$$\sigma_t = \frac{2A_1}{A_1 + A_2} \cdot \sigma_0 = \frac{2 \cdot 35635}{26546 + 35635} \cdot \sigma_0 = 1{,}14 \cdot \sigma_0$$

where σ_0 is the initial stress in the pile pipe and σ_t is the stress in the hollow bar. The maximum stress in the hollow bar is amplified accordingly.

$\sigma_{max\ (shoe)} = 1.14\ \sigma_{max\ (pipe)}$ i.e. that $f_{di} = 1.14$

h (m)	measured s (mm/blow)	f_w	σ_0 MPa	$\sigma_{max(pipe)}$ MPa	$\sigma_{max(shoe)}$ MPa
0.3	1.0	1.0	88	88	101
0.6	0.7	1.0	125	125	143
1.0	1.1	1.0	161	161	184
1.4	1.3	1.0	191	191	218
0.3	1.0	1.25	88	110	126
0.6	0.7	1.25	125	156	178
1.0	1.1	1.25	161	202	230
1.4	1.3	1.25	191	239	272
0.3	1.0	1.5	88	133	151
0.6	0.7	1.5	125	188	214
1.0	1.1	1.5	161	242	276
1.4	1.3	1.5	191	287	327
0.3	1.0	1.8	88	159	181
0.6	0.7	1.8	125	225	257
1.0	1.1	1.8	161	291	331
1.4	1.3	1.8	191	344	392

Table 4-5: Calculated front stress and maximum stress for the NPRA-shoes according to the Norwegian Piling Handbook section 4.6.2

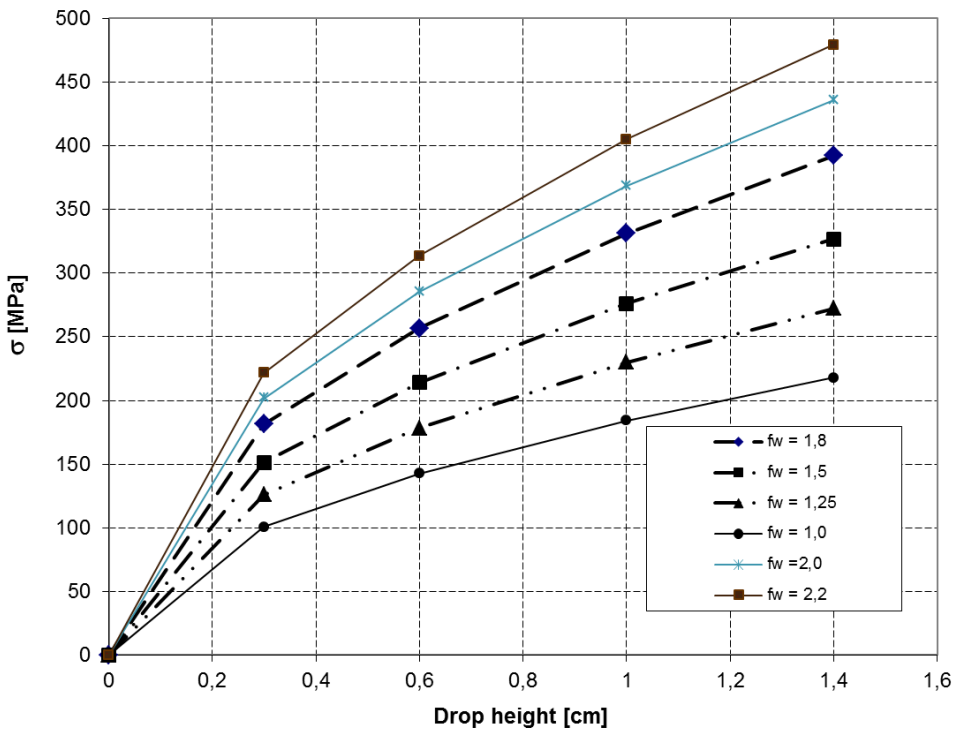

Figure 4-6: The plot shows the maximum stress in the NPRA shoes according to the Norwegian Piling Handbook [2] section 4.6.2 with varying amplification factor for stress waves f_w.

REQUIREMENTS: $$\underline{\sigma_{\max} \leq 1{,}25 \cdot \sigma_{dr} = 1{,}25 \cdot \frac{f_y}{1{,}05}} = 1{,}25 \cdot \frac{355}{1{,}05} = 422{,}6 MPa$$

$\sigma_{max\ (pipe)}$ = 344 MPa ⇨ OK for pile pipe

REQUIREMENTS: $$\underline{\sigma_{\max} \leq 1{,}25 \cdot \sigma_{dr} = 1{,}25 \cdot \frac{f_y}{1{,}05}} = 1{,}25 \cdot \frac{335}{1{,}05} = 398{,}8 MPa$$

$\sigma_{max\ (shoe)}$ = 392.1 MPa ⇨ OK for pile shoe

The yield stress of the material is determined by the wall thickness. A pile driving rig often in production pile driving uses 70% energy. That is, with the drop height 1.0 m if there is any resistance to driving in the ground.

The last blows are driven at full energy, usually a maximum of 2 -10 blows.

The NPRA pile shoes withstand a maximum energy with an amplification factor of 1.8 if one allows the yield stress to be exceeded by 25% due to high strain rate (ref. Figure 8-7). If the pile shoe is driven with full energy (1.4 m fall height) without the pile shoe having full contact with the rock surface, this will give an eccentric load. The yield stress will then be exceeded. The RUUKKI shoe has a greater area than the NPRA shoe and will therefore also have sufficient capacity.

5 Full-scale test of steel pipe pile shoe driven on rock

Full scale pile driving tests was performed by the NPRA in collaboration with RUUKKI and NTNU. This full scale test on driving steel pipe pile shoes on rock at Akershus was part the master thesis at NTNU 2010 [5].

5.1 Test location and companies involved

The NPRA drove three steel pipe piles at the E6 Dal - Boksrud project site directly on rock. We would like to thank the E6 project for the support they showed before and during the test period.

In this full scale test the following companies and individuals were involved.

NPRA :	Hans Inge Kristiansen the site engineer at E6 Dal - Boksrud project, Tewodros Haile Tefera (Vegdirektoratet).
Entreprenørservice:	Harald Amble, Egil Arntzen and Thomas Hansen.
Multiconsult:	Joar Tistel performed PDA measurements.
NTNU:	Arne Aalberg, Trond Auestad and Jørgensen Tveito Sveinung Master's candidate.
Ruukki:	Harald Ihler and Jan Andreassen.

The test piles were driven in connection with the construction of the foundations for the Holmsjordet Bridge, Figure 5-1. A suitable site for the full scale test was found with rock outcrop by the bridge site. The rock type was gneiss (corrected in the master thesis) with distinct crack patterns. The blocks were approximately 2 x 2 x 1 m. E-module of gneiss is 50,000 MPa according to NFF Handbook 2 “Engineering geology and rock engineering”

Point load test were carried out at the NPRA, Vegdirektoratet by Tewodros Haile Tefera on rock samples collected from the test site. The test result showed the following parameters [8]:

Equivalent sample diameter, D_e [mm]	Measured load at fracture, P [kN]	Point load strength, I_s ($I_s = P/ D_e^2$)	Factor, k	Compressive strength, σ_c $\sigma_c = k \times I_s$ [MPa]
50	26.5	10.6	20	212
30	9.0	10.0	20	200
30	8.0	8.9	20	178
30	5.2	5.8	16	92
30	17.0	18.9	25	472
50	31.0	12.4	25	310
50	20.0	8.0	20	160
50	31.0	12.4	25	310
Average				242

Table 5-1: Measured compressive strength of samples of the calculated “point load test”.

The Norwegian Piling Handbook does not include rock parameters for Gneiss in fig. 12.2 [2], but the granite has 150 to 250 MPa in compressive strength.

The site was located on top of a cut that was blasted in connection with the road construction. The cut can be seen from the lower side in Figure 5-2. The rock blasting may have created weaknesses on the front edge of rock cut.

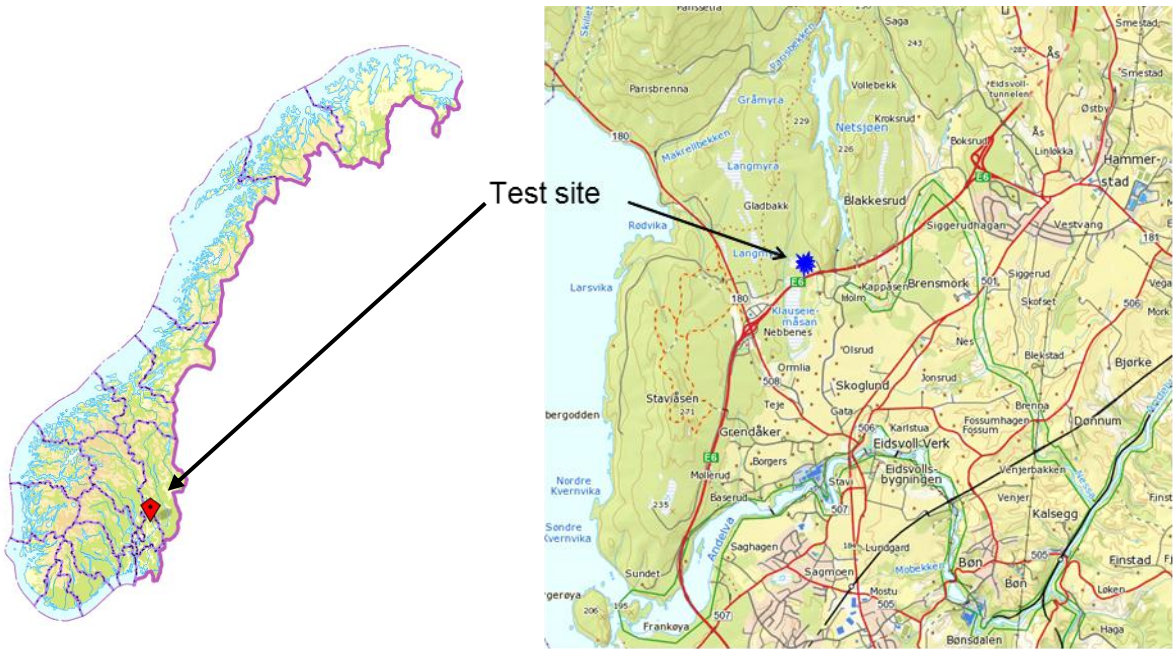

Figure 5-1: The site where the test was performed (Norgeskart.no)

Figure 5-2: The rock outcrop where piling was performed.

5.2 Shoe types

Three steel pipe pile rock shoes were driven on rock, Figure 5-3, in this full scale test.

Shoe no. 1 and no. 2 were designed in accordance with the guidelines in the Norwegian Piling Handbook. The stiffening plates and base plate material was grade S355J2N. The hollow pipe of the shoe was grade S355J2H. All welding were 10 mm and were inspected visually and with ultrasound. The hollow pipe tip of the shoe was hardened by carburization to 60 HRC (Hardness Rockwell) at the surface decreasing to 50,4 HRC 1.2 mm deep into hollow ,Figure 5-4. The tip of the shoe was bevelled with a 10% angle. The pile show was welded on a 2 m long steel pipe with a wall thickness of 14.2 mm when they arrived on site. The pile pipe shaft was extended to a total pile length from shoe to top as shown in Table 5-3 in the column L_{tot}.

Shoe no. 3 was a model designed by RUUKKI. The stiffening plates and base plate in the pile shoe was of steel grade S355J2N. The shoe blank was in the grade S355J2G. All welding thicknesses were 6 mm. Instead of bevelling and hardening the shoe tip was designed with a build-up weld with a height of 1 cm and a width at the root of 2 cm, Figure 5-4. The remainder of the shoe surface was flat. The Ruukki shoe was supplied with a factory welded pipe of the specified length. The pile pipe's wall thickness was 12.5 mm.

The steel area of the NPRA shoe was 26,546 mm^2 at the hollow bar and 47,066 mm^2 at the upper strain gauge. Area of the NPRA pile pipe was 35,653 mm^2. The steel area of the RUUKKI shoe was 37,385 mm^2 at the hollow bar and 40,823 mm^2 at the upper strain gauge. Area of the RUUKKI pile pipe was 31,436 mm^2.

Dowels were inserted into predrilled holes at the locations where the piles were driven. The dowels function is to keep the pile from lateral sliding during driving. The dowels were 3 m long round steel bars with a diameter of 80 mm and steel grade S355J2G3. Predrilling was performed using a 101.5 mm diameter rock drill pit.

Shoe no. 1 and 2 with shoe area 0.027 m^2

Shoe no. 3 with shoe area 0.037 m^2

Shoe no. 1 and 2 have a base plate thickness of 80 mm

Shoe no. 3 has a base plate thickness of 70 mm

Hardened shoe no. 1 and 2 with concave end-face

Shoe no. 3 with build-up weld on flat end

Figure 5-3: The three piles that were used in the test.

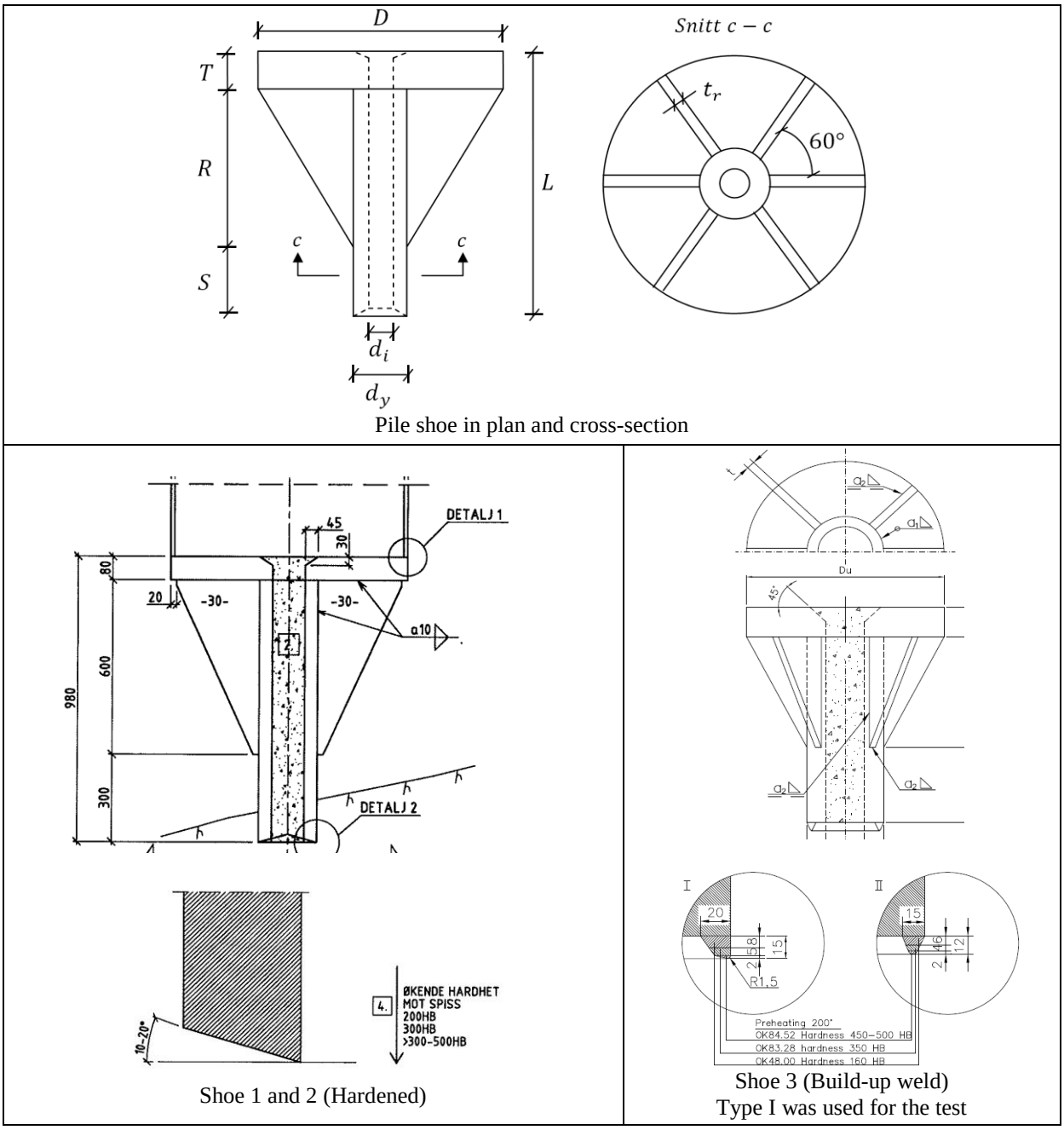

Figure 5-4: Pile shoe geometry.

Pile	D (mm)	T (mm)	R (mm)	S (mm)	L (mm)	d_y (mm)	d_i (mm)	t_r (mm)	welding (mm)	L_{tot} (mm)
Norwegian Piling Handbook 2005	Ø	0.1*Ø	Ø-d_y	1.5*Ø	T+R+S			0.035*Ø	No recommendation	
NPRA shoe no 1 (Hardened)	813	80	600	300	980	219	119	30	10	7520
NPRA shoe no 2 (Hardened)	813	80	600	300	980	219	119	30	10	6980
RUUKKI shoe no. 3 (Build-up weld)	813	70	600	260	930	240	100	20	6	7450

Table 5-2: Pile shoe measurements and the total length of the pile and shoe (L_{tot})

5.3 Instrumentation

All three piles were equipped with extensometers (strain gauges) and PDA gauges. Placement of the gauges is shown in Figure 5-1 and Table 5-3. Shoe movement was also filmed using a high-speed camera during some of the blows.

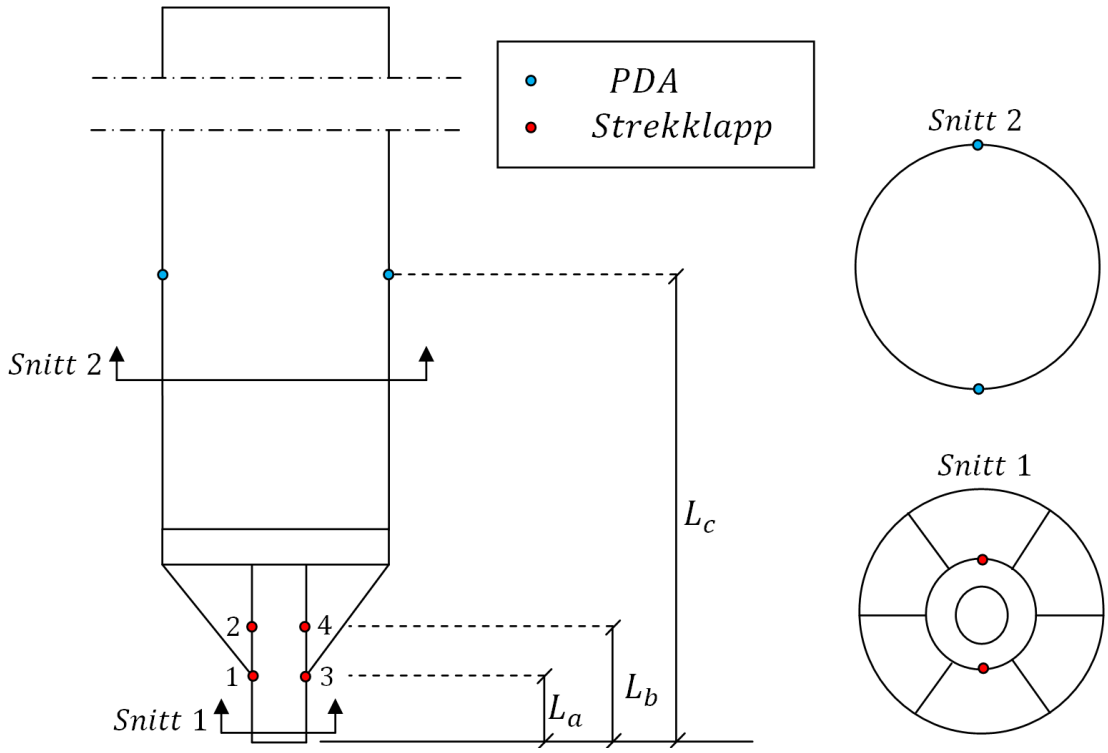

Figure 5-5: Placement of the strain gauges and PDA gauges on the piles. See table 5-3 for values for L_a, L_b and L_c.

Pile	L_a(mm)	L_b(mm)	L_c(mm)
Shoe no. 1	270	500	3000
Shoe no. 2	270	500	3000
Shoe no. 3	240	490	3000

Table 5-3: Placement of the strain gauges and PDA gauges. L_a, L_b and L_c relate to the measurements in 5-5.

5.4 Driving test piles

The piles were driven one by one a few metres apart. A piling rig of the type Junttan PM 25 with hydraulic double-acting hammer with a 9 ton hammer load was used for pile driving. Each pile was first raised to a vertical position over the predrilled hole in which the dowel was inserted. In this position the PDA gauges were screwed into the predrilled holes and the strain gauges and PDA gauges were connected to logging equipment, the high-speed camera was set up and connected to PC and equipment to measure the penetration in the rock was installed and set up. As the piles were driven into relatively flat rock surface, they did not have the side support that the surrounding soil usually provides. Dowels were therefore necessary to prevent lateral displacement. The predrilled holes for the dowels were 2 m deep. When inserted the 3 m-long dowels protruded 1 m above the ground and into the pile shoes. The piles were then supported at the bottom by the dowel and the top by the pile rig.

PDA gauge being fitted

PDA gauge fitted on the pile, extensometer to the left and accelerometer to the right

Strain gauge

protected strain gauges with tap

Figure 5-6: Instrumentation on the piles

5.5 Results from full scale test

There was considerable difference in the drop history between the piles, which is shown in Table 5-4. This may be due to local differences in rock and the rock's fracturing mechanisms, but also due to different shoe behaviour and driving history. For shoe no. 1 the fractures appeared already after the first blows. This meant that there was much more drop at the start, unlike the other two. It is difficult to say whether shoe design was the cause of the fastest penetration from only 3 tests.

Drop height (cm)	No. of blows			Penetration(mm)			Penetration/blow (mm)		
	Shoe 1	Shoe 2	Shoe 3	Shoe 1	Shoe 2	Shoe 3	Shoe 1	Shoe 2	Shoe 3
10	90	240	40	207	160	28	2.3	0.7	0.7
20	30	20	70	10	7	48	0.3	0.3	0.7
30	130	130	170	125	98	195	1.0	0.7	1.1
40	60	80	90	9	33	29	0.1	0.4	0.3
50	60	10	20	38	1	6	0.6	1.0	0.3
60	20	10	30	14	14	6	0.7	1.4	0.2
100	10	20	20	11	19	32	1.1	1.0	1.6
140	20	10	10	26	16	54	1.3	1.6	5.4

Table 5-4: Driving data for piles

The rock surface before the shoe was driven.

Fractured rock after the show had been driven down.

Figure 5-7: Photos of the rock in various stages before and after driving shoe no. 1.

The rock with predrilled holes with the dowel driven for Shoe no. 1.

The rock after Shoe no. 1 has been chiselled in and then extracted.

Figure 5-8: Photos of the rock and dowel in various stages before and after driving shoe no. 1.

Lower edge of shoe surface before the shoe was driven.

Lower edge of shoe surface after the shoe was driven.

Figure 5-9: Photos of Shoe no. 1 before and after driving

Lower edge of shoe surface before the shoe was driven.

Lower edge of shoe surface after the shoe was driven.

Figure 5-10: Photos of Shoe no. 2 before and after driving

Figure 5-11: Photos of the rock in various stages before and after driving shoe no. 3.

Lower edge of shoe surface before the shoe was driven.

Lower edge of shoe surface after the shoe was driven.

Figure 5-12: Photos of Shoe no. 3 before and after driving

Plastic deformation of NPRA shoe 1

Plastic deformation of NPRA shoe 2

Figure 5-13: Visual inspection of plastic deformation.

There are two main mechanisms that take place when the shoes work down into the rock. These are cracking and crushing, Figure 5-7 and Figure 5-11. At the beginning of chiselling pieces of the rock surface were hammered loose and thin fractures started to spread. In areas with direct contact with the shoe zones were formed where the rock was crushed into powder. The cracks move on towards weaknesses in the surrounding rock such as fractures, surface, edges or weaker zones in the rock.

Data was logged from a total of 15 blow series, 9 from shoe no. 1, and 6 from shoe no. 3. The data shows a slightly varied response not just from series to series, but also from blow to blow within each series. The differences come from different energy supplied from the hammer, different behaviour in the rock, and any yield in the shoe material. Strain gauges were also disturbed by the surrounding crushed rock.

Strain gauges 1 and 3 are the lower gauges positioned about 0.3 m from the toe, and 2 and 4 are the upper gauges placed 0.5 from the toe, as shown in Figure 5-5 and Table 5-3. It is natural that the numbers 2 and 4 register lower stress levels, since they lie between the stiffening plates on the pile shoe, and can then distribute the force over a larger area than is the case for numbers 1 and 3. From the results for shoe no. 1 it was found that the stress is about. 42 - 57% lower in the area around the ribs in relation to the shoe.

Measurement results for the strain gauges are shown in Table 5-5. Strain gauges for NPRA-shoe 1 gave good results for all drop heights. The stress increased in strain gauges corresponding to the drop height of the hammer. Strain gauges for the RUUKKI shoe did not work so well. The stress for strain gauges increased incrementally for the lowest increments. When the drop height was 60 cm and higher the results do not seem credible either for the upper or lower strain gauges. The stress decreased at drop heights above 50 cm, and we did not achieve stresses above 100 MPa. This seems unlikely in relation to that measured on NPRA shoe 1 and the theoretical calculations.

We perform further analysis and conclusions based on the measurements made on the NPRA shoe 1. The results for the two lowest drop heights for the RUUKKI shoe are shown.

As the strain gauges are located approximately 0.3 and 0.5 m from the toe of the shoe, the return wave comes very quickly, in fact, less than 0.0001 seconds, if theoretical calculations are made with L/c = 0.5/5172. We cannot distinguish between the down and return wave when measuring with the strain gauges, and therefore have not analysed the amplification factor merely by looking at measurements from the strain gauges mounted on the shoe. The first highest point we have on the stress-time curve is thus the maximum stress σ_{max}.

The stress in the hollow bar below the stiffening plates exceeds the yield stress at the drop height 1.0 and 1.4 m. It exceeds both the ordinary yield stress of 335 MPa and the corrected yield stress for the strain rate of 450 MPa. The visual inspection shows, however, some plastic deformation at the shoe tips, Figure 5-12 and Figure 5-14.

When comparing the upper and lower strain gauges on the two uppermost drop heights, we see that the stress in the upper strain gauges flattens out. This may indicate that there is greater deformation in the hollow bar so that the stiffening plates receive a larger share of the loads than at the lower drop heights. The stiffening plates were not instrumented, so that this theory has not been verified.

Drop height (cm)	NPRA shoe 1 σ (MPa)		RUUKKI shoe σ (MPa)	
	upper strain gauge	lower strain gauge	upper strain gauge	lower strain gauge
10	69	120	122	196
20	112	199	138	223
30	129	223	-	-
40	153	267	-	-
60	191	317	-	-
100	223	460	-	-
140	218	503	-	-

Table 5-5: Maximum stress in the shoes measured for each drop height at the upper and lower strain gauges

Drop height (cm)	NPRA shoe 1		RUUKKI – shoe		NPRA shoe 2	
	Degree of efficiency η	$\sigma_{(pipe)}$ MPa	Degree of efficiency η	$\sigma_{(pipe)}$ MPa	Degree of efficiency η	$\sigma_{(pipe)}$ MPa
10	0.96	106.2	1.17	143.8	1.10	116.7
20	0.91	138.1	1.02	181.0	1.40	159.8
30	1.29	184.7	1.08	218.1	1.12	172.3
60	1.06	253.1	0.90	237.3	0.79	211.3
140	1.04	341.1	0.79	292.3	0.89	312.7

Table 5-6: Registered values of stresses measured with PDA measurements. The degree of efficiency is calculated from the stated drop height against the measured stress from the PDA.

We refer to chapter 4.4 regarding the calculation of stresses from stress waves according to the Norwegian Piling Handbook [2]. We have calculated $\sigma_0 = 161{,}5 \cdot \eta \cdot \sqrt{h}$. We have then taken values from the strain gauges measurements and PDA measurements. Strain gauge stresses have been converted from shoe stresses to pipe stresses with a theoretical discontinuity factor f_{di} = 1.14 for NPRA shoe and f_{di} = 0.91 for RUUKKI shoe.

Measured discontinuity factor from measured values: $f_d = \sigma_{strain\ gauge\ (shoe)} / \sigma_{PDA(pipe)}$
Estimated total amplification factor in pipes is calculated: $f_{wtot} = \sigma_{PDA(pipe)} / \sigma_{0(pipe)}$
Amplification factor for shock waves will then be: $f_w = f_{wtot} / f_d$

Total amplification factor is here defined as: $f_{wtot} = f_w \cdot f_d$
If f_w = 1.4 – 1.9 and f_{di} = 1.14 then f_{wtot} = 1.6 – 2.2

Drop height (cm)	Drop/ blow (mm)	Degree of efficiency ή	$\sigma_{0(pipe)}$ MPa	Strain gauge		PDA measu.	Calculated from measured values		
				$\sigma_{max(shoe)}$ MPa	$\sigma_{max(pipe)}$ MPa	$\sigma_{PDA(pipe)}$ MPa	f_d	f_{wtot}	f_w
10	4.5	0.96	49	120	105	106.2	1.12	2.2	1.93
20	0.07	0.91	66	199	174	138.1	1.44	2.1	1.45
30	2.0	1.29	114	223	195	184.7	1.21	1.6	1.34
60	1.0	1.06	132	317	278	253.1	1.25	1.9	1.53
140	1.0	1.04	199	503	441	341.1	1.47	1.7	1.17

Table 5-7: Estimated f_w from the measured maximum stress from strain gauges and PDA measurements for NPRA shoe 1

Table 5-7 shows that the total amplification of the stress wave in the pipe for the NPRA shoe is between 1.6 and 2.2. This is in the same range as the theoretical calculations. The discontinuity factor varies between 1.12 and 1.47. The discontinuity factor is generally somewhat higher than that calculated theoretically, and this is partly because we have not included the reflected wave.

The calculated amplification factors based on measured values show that the total amplification factor is between 1.7 and 2.2. There is something strange in it being the highest amplification factor with lowest drop height and the largest drop. The tendency is that the amplification factor decreases with increasing energy. This was an unexpected result.

A source of error may be that the PDA measurement and strain gauge measurement were not read for the same blow or logged at the same time.

Drop height (cm)	Drop/ blow (mm)	Degree of efficiency ή	$\sigma_{0(pipe)}$ MPa	Strain gauge		PDA measu.	Calculated from measured values		
				$\sigma_{max(shoe)}$ MPa	$\sigma_{max(pipe)}$ MPa	$\sigma_{PDA(pipe)}$ MPa	f_d	f_{wtot}	f_w
10	2.3	1.17	56	196	215	143.8	1.36	2.56	1.89
20	0.3	1.02	73	223	245	181.0	1.23	2.47	2.01

Table 5-8: Estimated f_w from the measured maximum stress from strain gauges and PDA measurements for RUUKKI shoe

For the RUUKKI shoe the calculated values of the amplification factor do not correspond with the theoretical values. The cause of this may be faulty strain gauges measurements even at the lowest drop heights. It may appear that discontinuity formula does not apply when the area of the shoe is larger than the pipe.

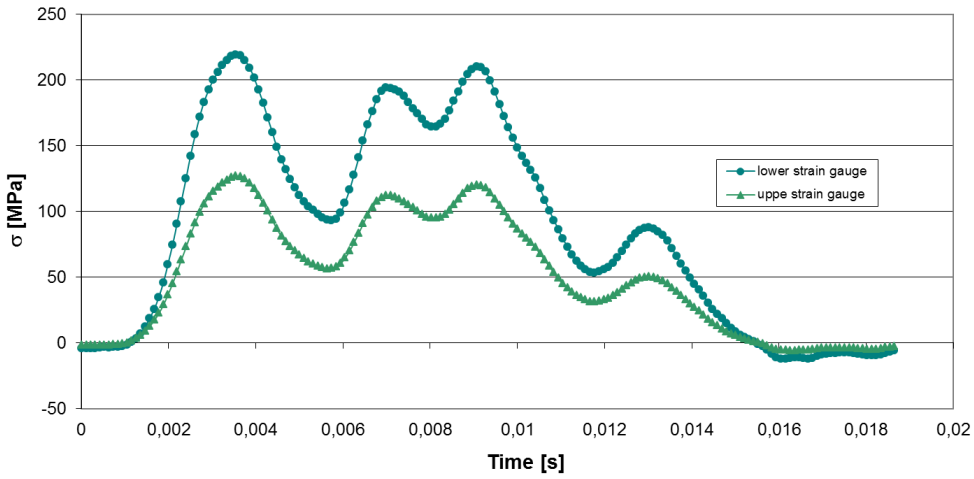

(a) Stress-time curve for a blow with the drop height H=0.3 m for NPRA shoe 1

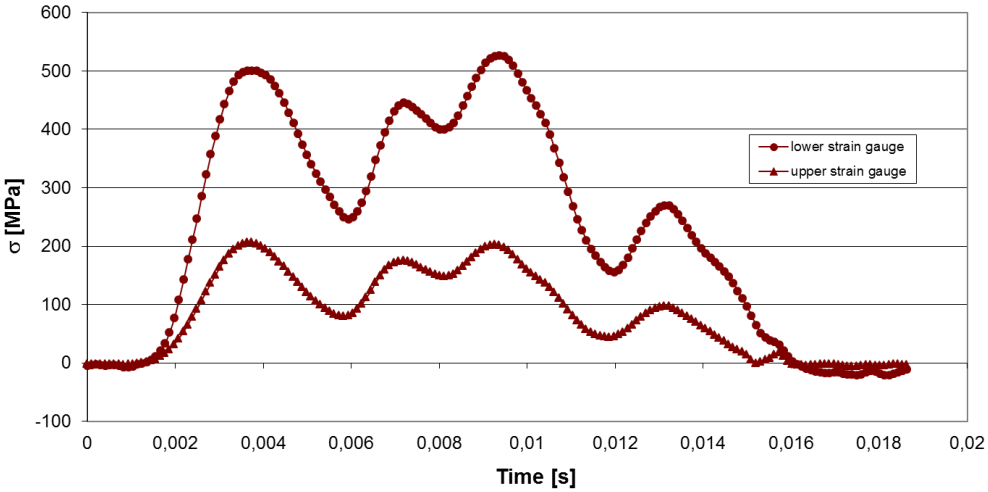

(b) Stress-time curve for a blow with the drop height H=1.4 m for NPRA shoe 1

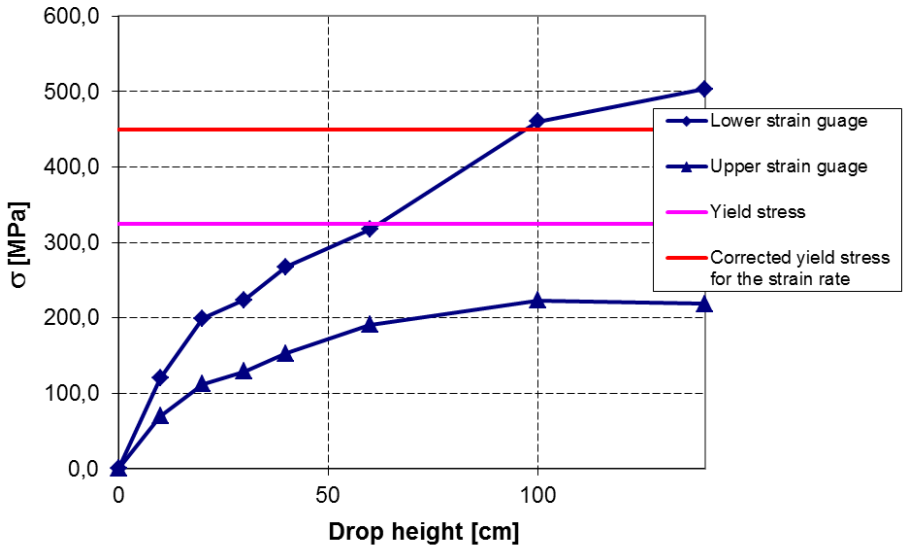

(c) Maximum stress from each series plotted against the drop height

Figure 5-14: The figure shows the measured stresses at 0.3 m and 1.4 m drop heights (a) and (b) and the maximum stress measured for each drop height (c). Data from NPRA shoe no. 1. (The steel area of the shoe at the lower strain gauge location was 26,546 mm^2 and at the upper 47,066 mm^2.)

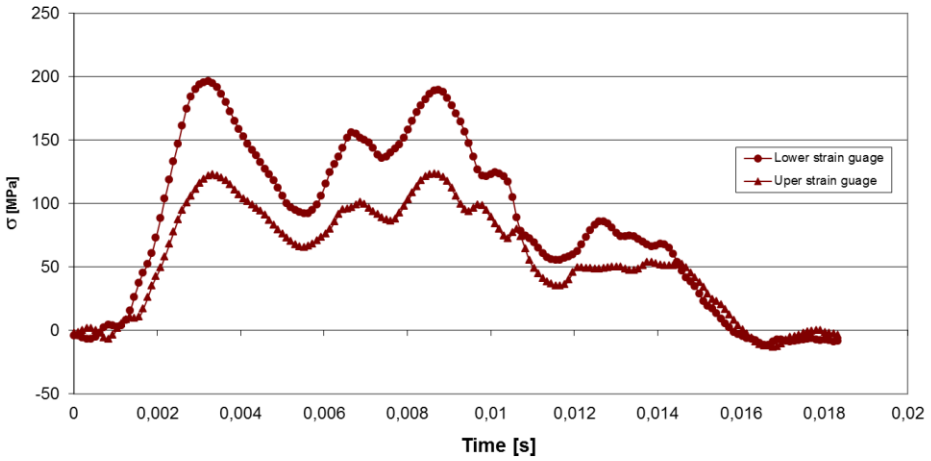

(a) Stress-time curve for a blow with the drop height H=0.3 m for RUUKKI shoe

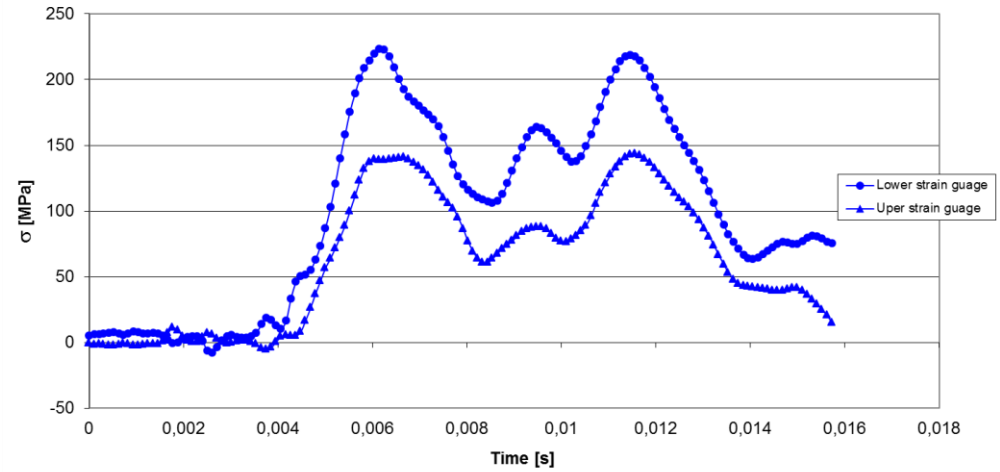

(a) Stress-time curve for a blow with the drop height H=0.5 m for RUUKKI shoe

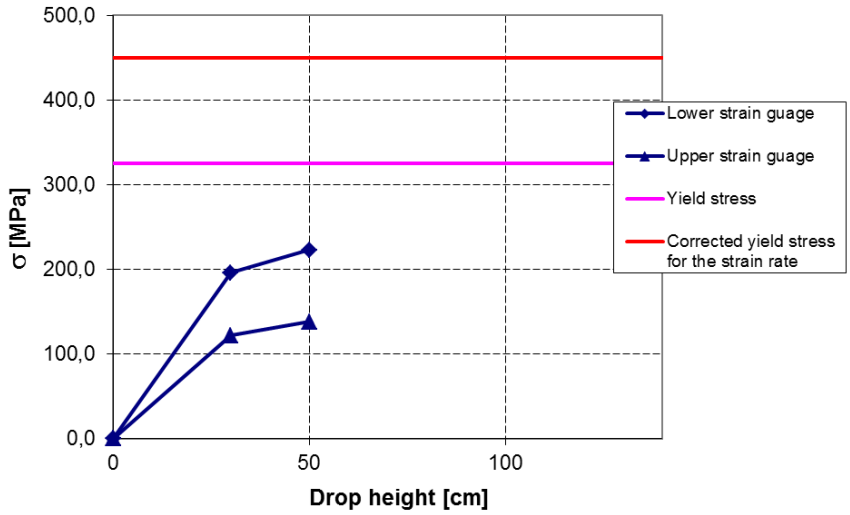

(c) Maximum stress from each series plotted against the drop height (at a higher drop height than 0.5 m the stress measurements were not reliable)

Figure 5-15: The figures show the measured stresses at 0.3 m and 0.5 m drop heights (a) and (b) and the maximum stress measured for each drop height (c). Data from RUUKKI shoe no. 3. (The steel area of the shoe at the lower strain gauge location was 37,385 mm^2 and at the upper 40,823 mm^2.)

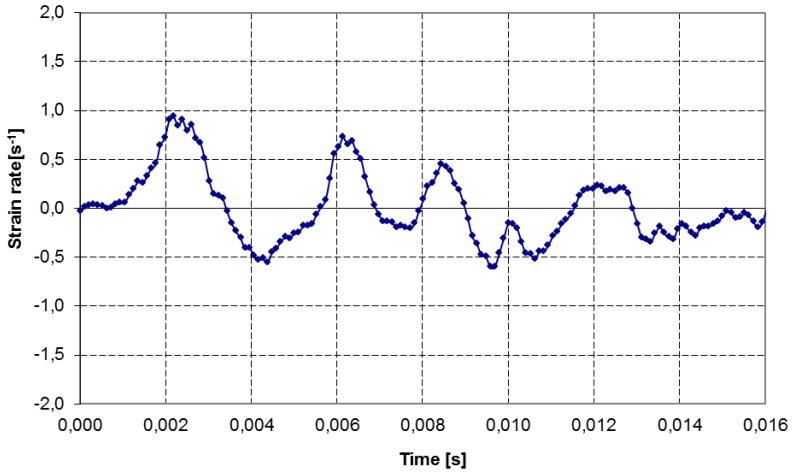

(a) drop height 40 cm

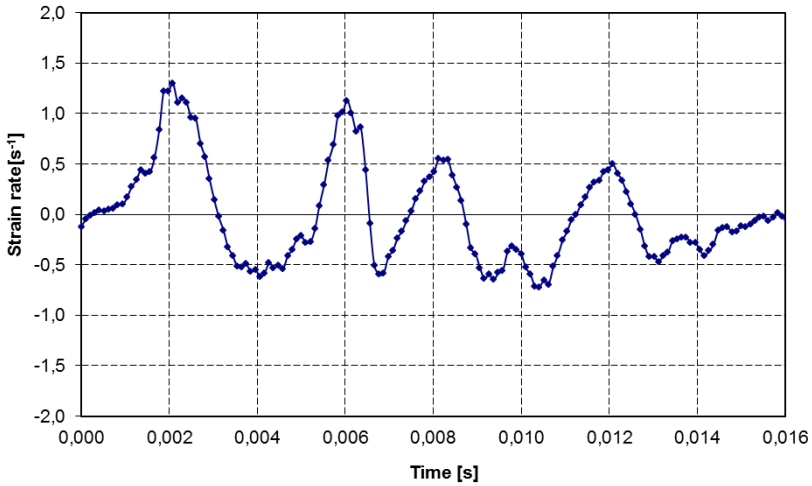

(b) drop height 60 cm

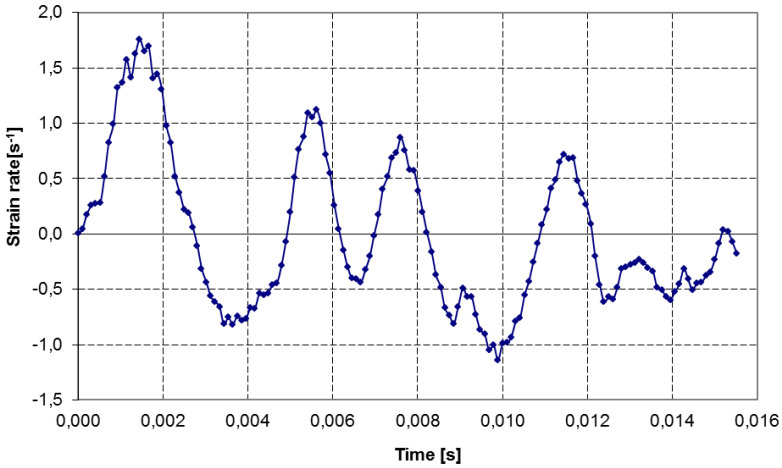

(c) drop height 140 cm

Figure 5-16: Strain rate measured at different drop heights.

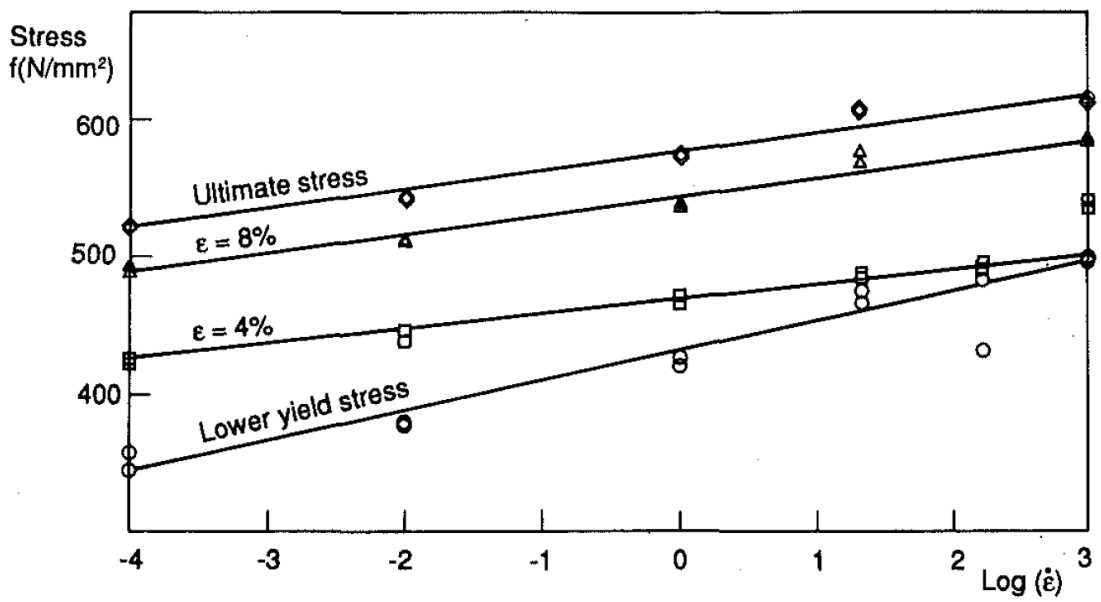

Figure 5-17: Trends found when testing strain rates on St52-3N steel, note that one of the axes is logarithmic [11].

Strain rates for three different drop heights are shown in Figure 5-16. It was noted that the values are high enough to have an effect on the steel's yield stress, and that the strain rates increases with an increase in drop height. The latter is because the stress increases more at the same time interval with higher drop height. In Figure 5-17 trends found in experiments made on St52-3N steel are shown that are comparable to the steel used in piles, note that one of the axes is logarithmic. From the figure it can be seen that the yield stress (Lower yield stress) increases rapidly with increasing strain rate.

5.6 *Related costs of the full scale test*

Three tests were performed in the form of driving three piles each with its own shoe on rock. Shoe no. 1 and no. 2, NPRA shoes, were designed in accordance with the guidelines in the Norwegian Piling Handbook. Shoe no. 3 was a model designed by RUUKKI, and all related costs of shoe no. 3 are covered by RUUKKI.

Material costs shoe 1 and 2.

- Hollow rock shoe for pre-dowelling, 2 pcs at NOK 4,345…….NOK. 8,690
- Pile pipe, Ø813x14.2 mm, 9 m at NOK. 1,207…….....NOK. 10,863
- Dowels, 2 pcs at NOK 1,000……..…….....NOK. 2,000
- TOTAL…….....NOK. 21,553

Driving of steel piles, PDA measurements of shoe no. 1, no. 2 and no. 3.

- Entreprenør-Service …….....NOK. 80,000
- Multiconsult …….....NOK. 38,000
- Mesta …….....NOK. 9,000
- TOTAL……..….NOK. 127,000

6 Theoretical calculation using the finite element method

6.1 Material models

All finite element analysis of the full-scale test was carried out using the software ABAQUS version 6.92 [5]. The basic model consists of different parts: hammer, impact pad, impact cap, ribs, and the pile and shoe together. See Figure 6-1. The rock in the base model is modelled as a rigid surface with the same form as the shoe blank's end face and an edge for lateral support. All measurements of pile and pile shoe are taken from the physical measurements made during test. As the model consists of parts with different characteristics, different material models have been applied for the various components.

Pile pipe and pile shoe

As pile driving has resulted in strain rates up to about 1.8 s^{-1} a Johnson-Cook model [11] that takes this into account has been used. The Johnson-Cook model is usually calibrated against material tests to determine the parameters to be included in the model, but this was not done and the model has been adapted by means of tests on similar materials from literature and from the material certificate for pile 1 Yield stress in the Johnson-Cook model is generally given by:

$$\sigma_y = \left[A + B(\varepsilon_p)^n\right]\left[1 + C\ln\left(\frac{\dot{\varepsilon}_p}{\dot{\varepsilon}_o}\right)\right]$$

A, B, n and C are material constants in the model. A is the yield stress, B and n determine the hardness of the material and C controls the effect of strain rate. ε_p and $\dot{\varepsilon}_p$ are equivalent plastic strain and equivalent plastic strain rate respectively. $\dot{\varepsilon}_o$ is equivalent plastic strain rate used in the tests that define A, B and n. Normally material tests are made at various speeds for the lowest rate, usually quasistatic, gives $\dot{\varepsilon}_o$.

Part	E GPa	ρ Kg/m^3	υ	A MPa	B MPa	C	n	$\dot{\varepsilon}_o$ s^{-1}
Base plate	210	7850	0.3	328	1037.32	0.012	0.71	5.10^{-4}
Rib	210	7850	0.3	425	1037.32	0.012	0.71	5.10^{-4}
Shoe	210	7850	0.3	365	1037.32	0.012	0.71	5.10^{-4}
Pile pipe	210	7850	0.3	434	1037.32	0.012	0.71	5.10^{-4}

Table 6-1: Parameters used in the Johnson-Cook model in ABAQUS [5].

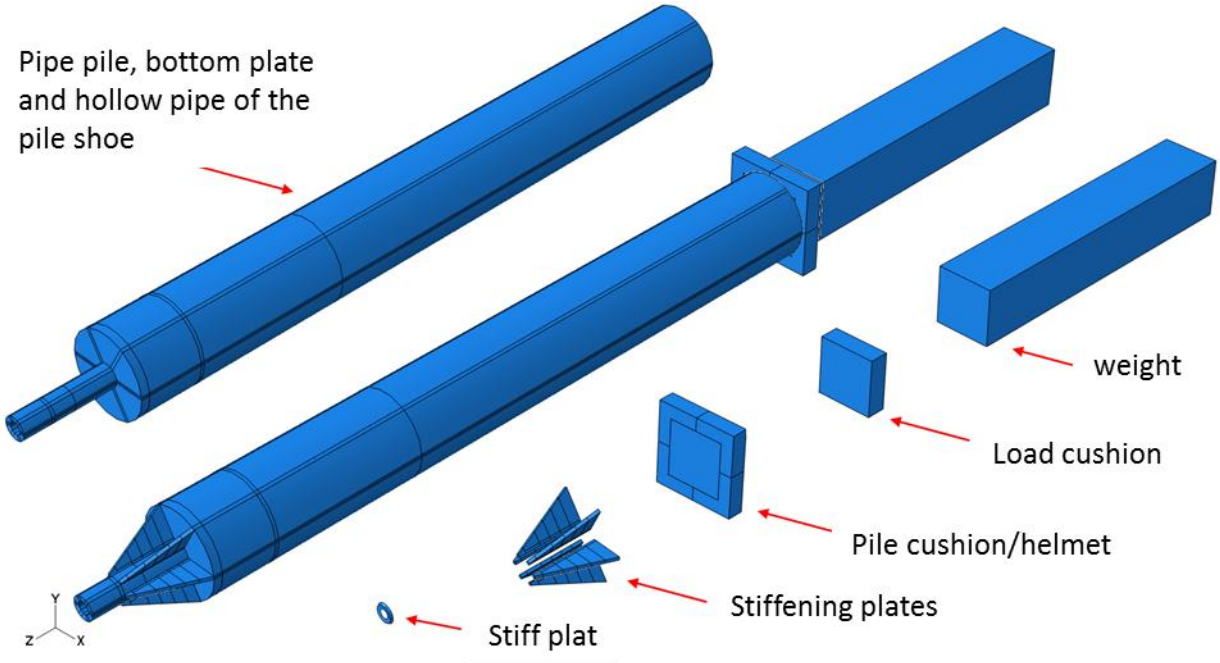

Figure 6-1: Different individual parts of the model. In the middle is the composite model [5]

From Figure 6-2 it is evident that for the shoe and base plate the model comes close to the certificate f_u, suggesting that the constructed curve is probably a good representation of the real curve. It is assumed that the strain at f_u in the material certificate is at 0.015. The curve for ribs ends with a f_u 12% higher than that specified. This is because the relationship f_y / f_u is considerably higher for the ribs than the other components, but the model is still a sufficiently good approximation. The same applies to the pile pipe.

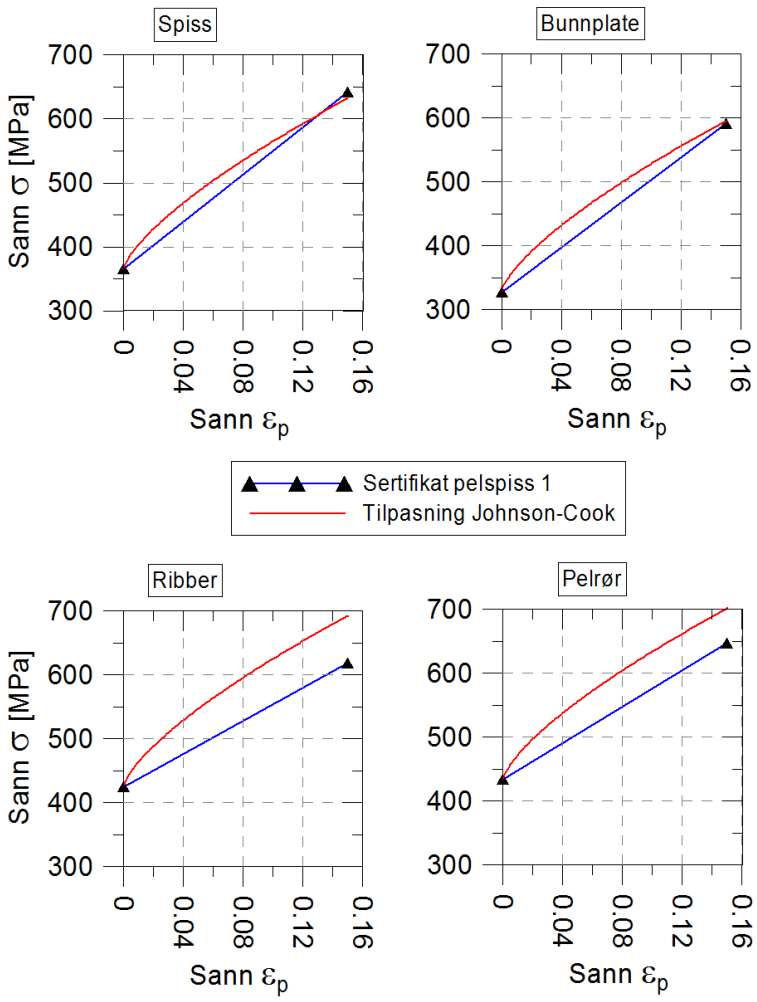

Figure 6-2: Material data provided by the certificate in relation to the Johnson-Cook model [5].

In practice, one can take out stresses or other values anywhere in the analysis, but as a starting point data is taken from the same points as those physically measured from the pile during the test. In addition, values are taken from the rigid plate and the values near the pile head, see Figure 6-3. The forces in the rigid plate represents the driving resistance.

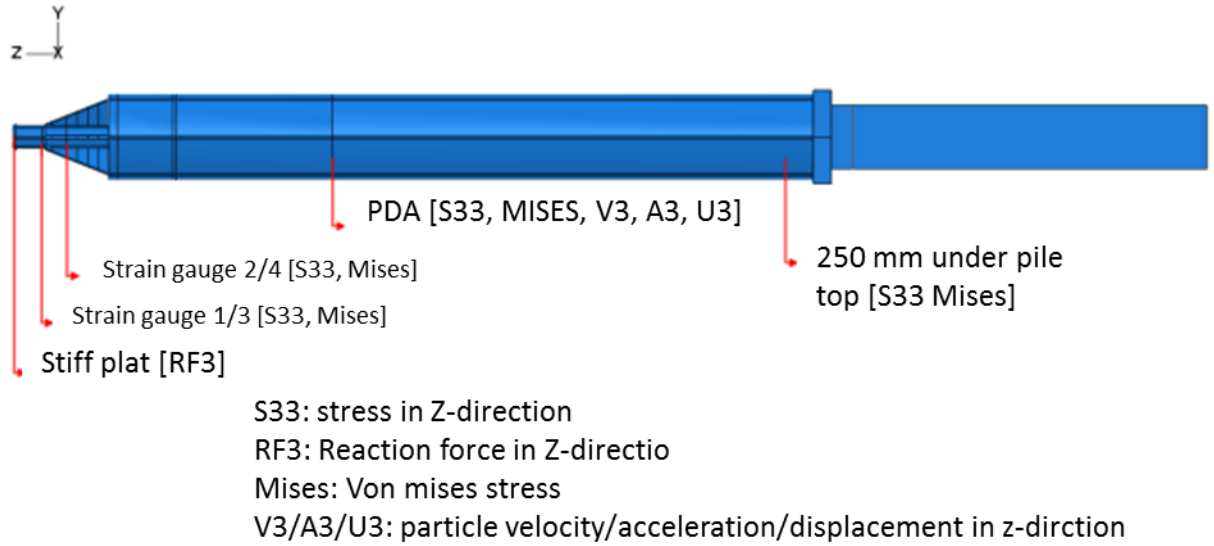

Figure 6-3: Where and what data is logged in the basic model [5].

The rock is modelled as a cylinder with a diameter of 1 m and height 1 m. Many different analyses were made to determine which material parameters gave the best agreement between tests and analyses. Density and transversal contraction were not varied and were set to $\rho = 2850$ kg/m^3 and $\upsilon = 0.2$ for all analysis. Results from this analysis along with experience gained from the analysis made with the rock modelled as a spring were used to optimize the material parameters. The parameters found to give the best result were as follows:

E=16,500 MPa, υ =0.2, ρ =2850 kg/m3.
The rock is modelled as elastic material with yield stress f_y = 100 MPa, and then behaves perfectly plastic.

6.2 Comparison of results with the physical test

Good correlation between test data and analysis was achieved especially in the shoe tips. There are some differences between the plots, among others the curve from the test sinks deeper after the first stress peak, while the analysis is slightly higher at the second stress peak. The differences are small, and are assumed to come from inaccuracies in the modelling. The results compared with the test are then as in Figure 6-4 to Figure 6-8.

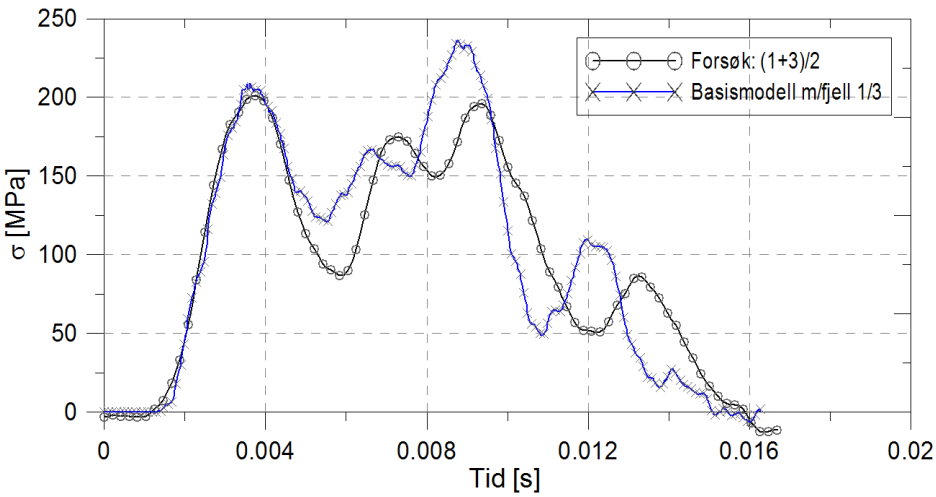

Figure 6-4: Comparison between test and analysis, stresses in the lower strain gauge. From the test: Drop height 30 cm, series 2, blow 10 [5].

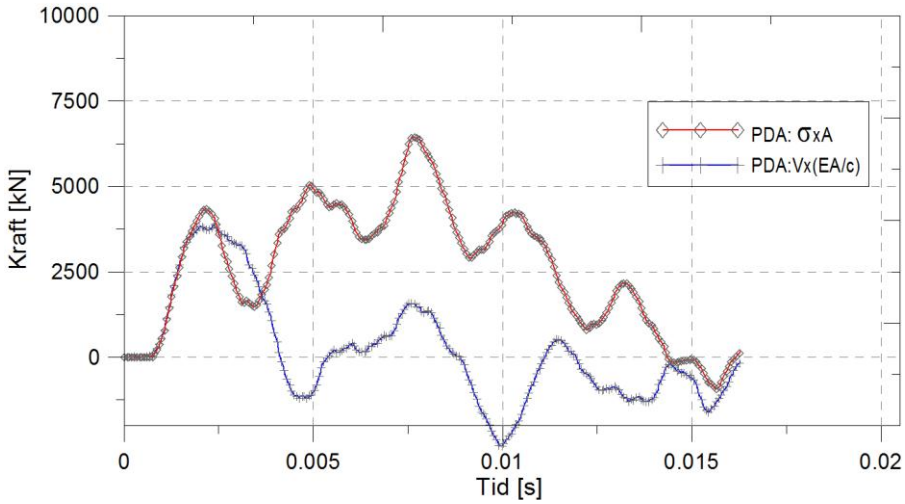

Figure 6-5: Force from stress measurements, and from particle velocity multiplied by Z. All measurements in the PDA position [5].

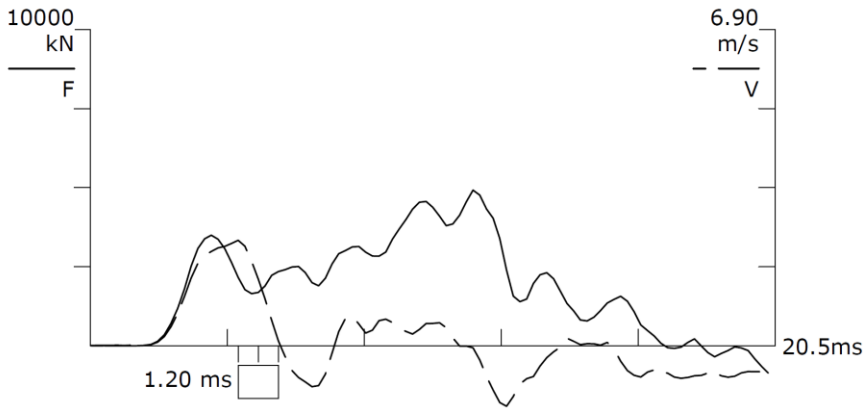

Figure 6-6: PDA plot number BN 179 from the test for comparison with Figure 6-5 [5].

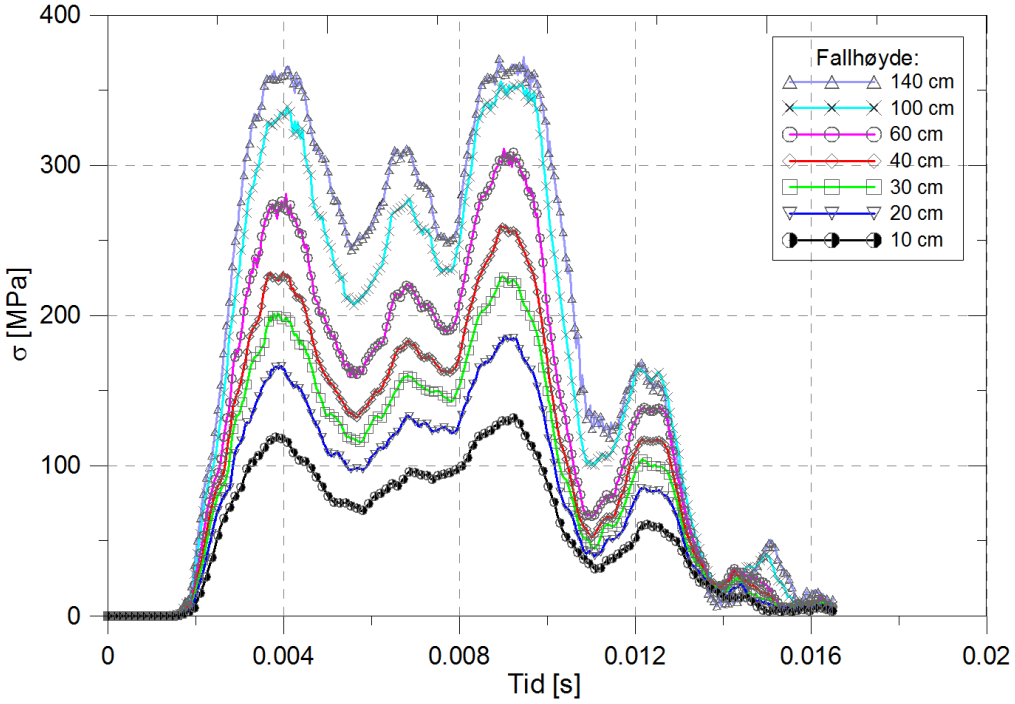

Figure 6-7: Stresses in the tip at different drop heights with rock volume [5].

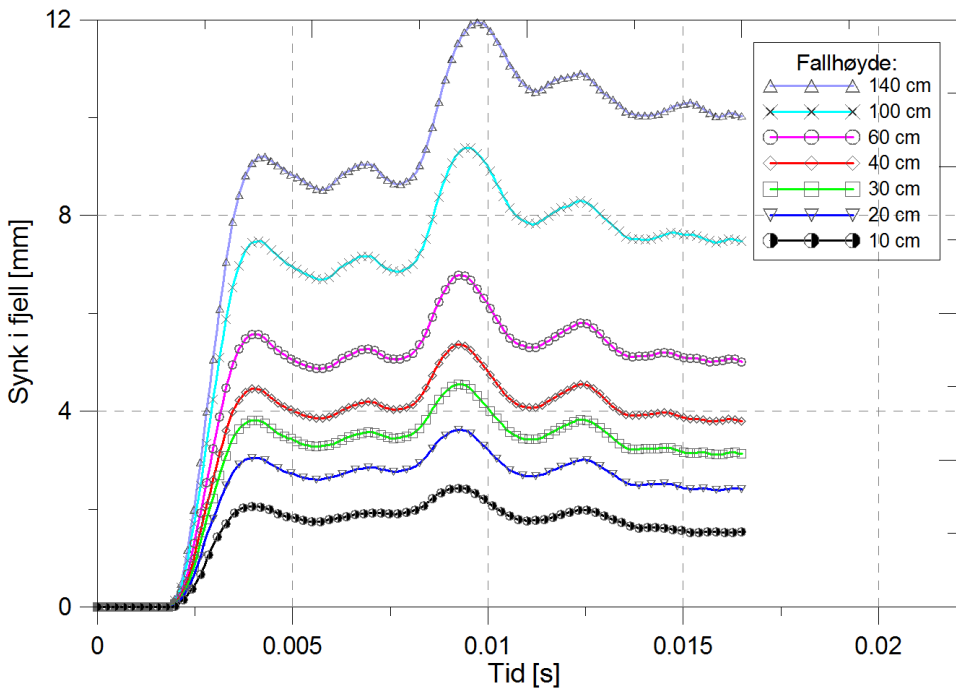

Figure 6-8: Penetration in the rock for different drop heights [5].

The drop in the rock is too high, especially for the highest drop heights. For drop height 1.4, the estimated drop in ABAQUS is 8 - 12 mm but the measured drop is about 1 mm.

Contour plot from ABAQUS

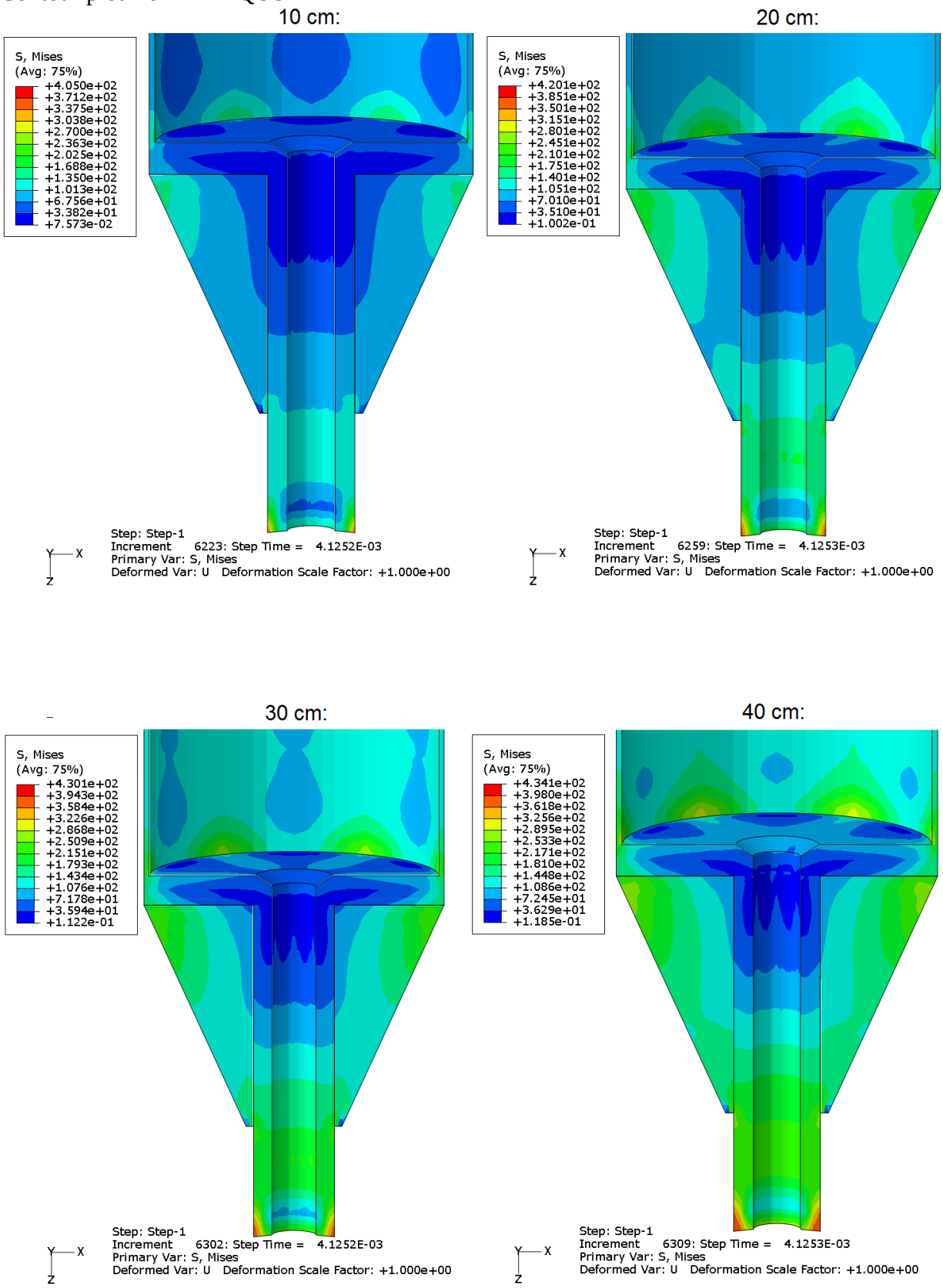

Figure 6-9: Stresses in the shoe at the first stress peak [5]

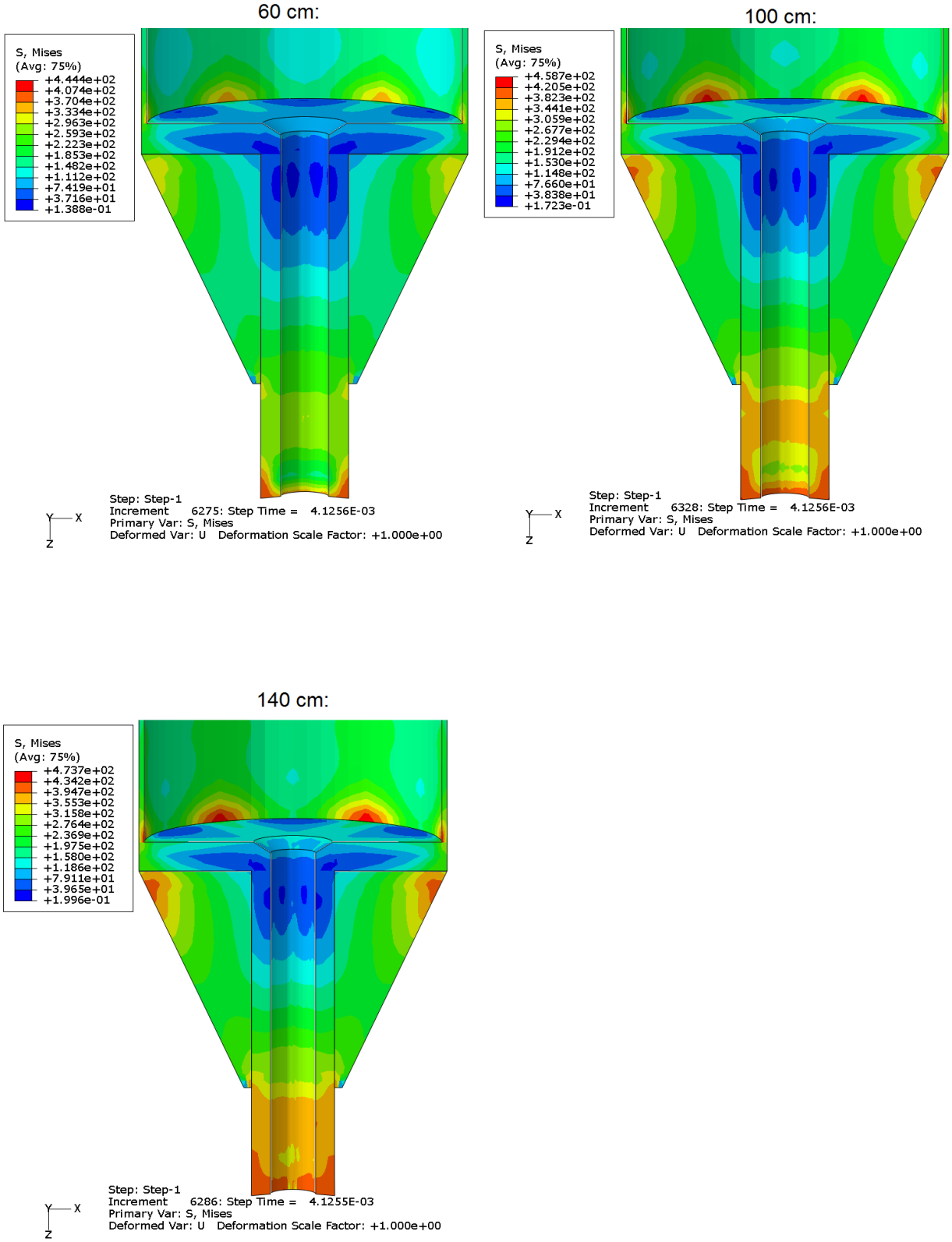

Figure 6-10: Stresses in the shoe at the first stress peak [5]

The stress concentrations in the pile pipes are where the stiffening plates are attached to the base plate. There are also stress concentrations in the stiffening plates at the top near the pile pipe and at the bottom near the hollow bar. Stress is also higher in the hollow bar below the stiffening plate.

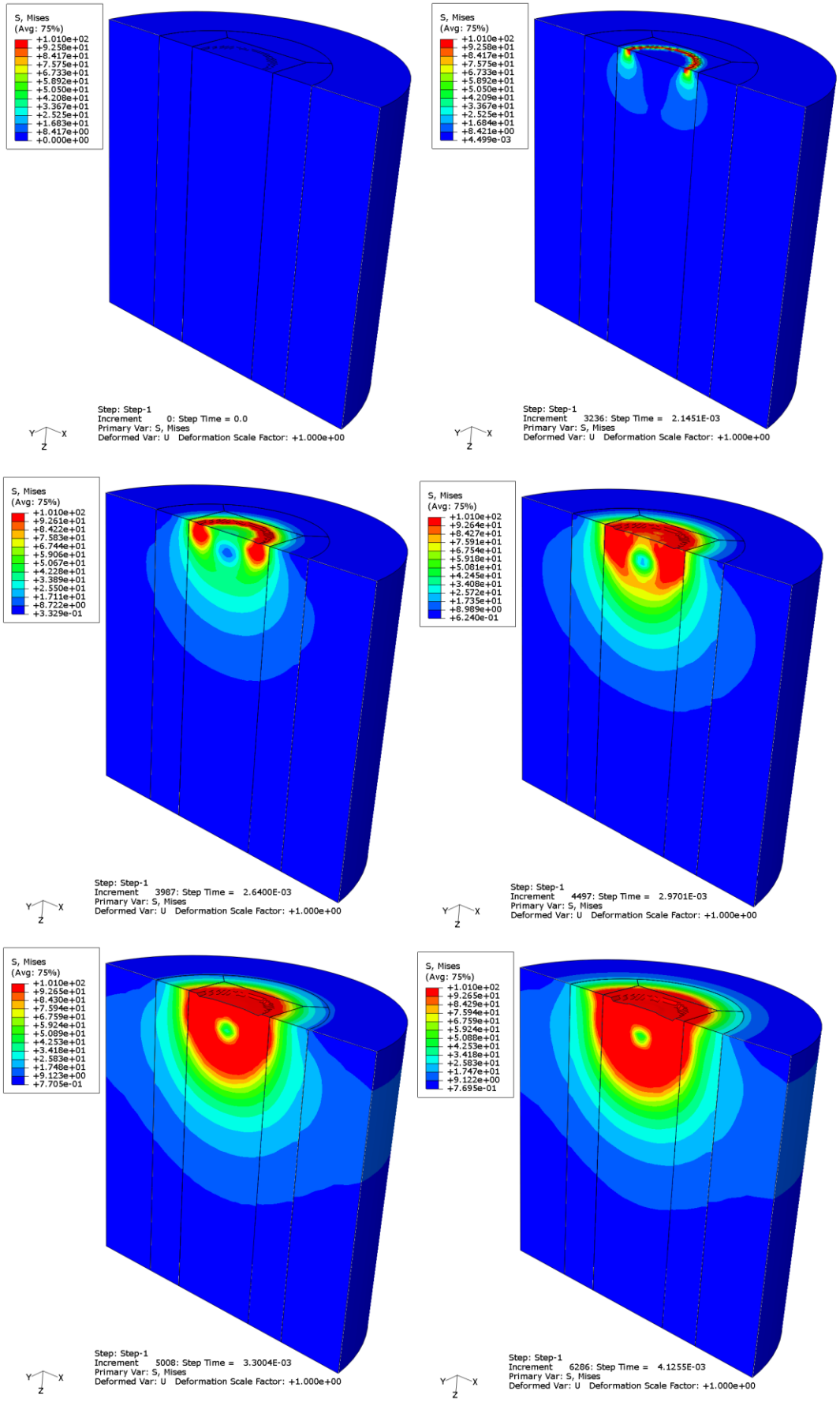

Figure 6-11: Stresses in the rock at the load drop height 140 cm [5]

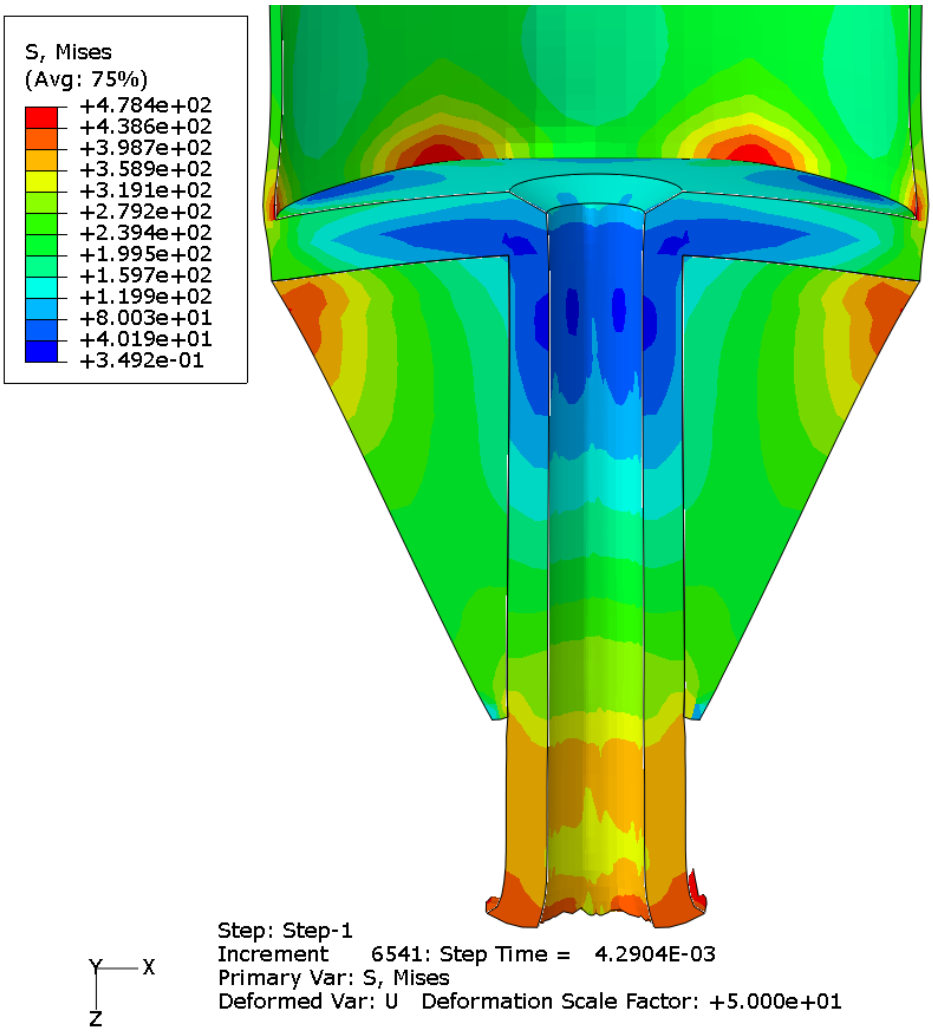

Figure 6-12: Up scaled deformations, drop height 140 cm, Scale: 50x [5]

7 Laboratory tests with small scale pile shoes

In the thesis of Sveinung J. Tveito [5] small scale tests were made in the SIMLab at NTNU. Structural Impact Laboratory (SIMLab) works to develop methods and tools for the development of structures exposed to shocks and collisions. SIMLab's equipment is used to test materials and components with fast loading rates and stress changes. Other test rigs are used for testing structures to recheck numerical models.

The experiments were conducted to investigate whether the end face of the hollow bar had a significant bearing on penetration into the rock, and to examine the effect of predrilling in the rock.

A simplified model of the pile shoe with hollow bar that had the same relationship between the diameter and thickness as those in situ was used. In the small scale test the pile shoes were driven on flat concrete surface. Load level, stress velocity and the hollow bar were scaled down according to the in situ test.

The test was performed with a hammer of 251.5 kg, with a fixed drop height of 1.5 m. During the test the hammer dropped through a hollow bar positioned on a concrete block. The penetration in to the concrete surface was measured with a measuring tape for each blow.

A rig was designed for the hammer, which was a steel cylinder with steel grade S355J2, this was held up by an electromagnet. The electromagnet was hung from a crane. Switching off the current caused the magnet to release and the hammer dropped. After each blow the magnet was connected to the power again, lowered and attached to the hammer. The hammer was then raised to the correct drop height of 1.5 m.

In order to hold the hammer stable during the fall guide rails were attached to the hammer. These had only a few millimetres of clearance to the guide pipe to the hammer. The guide pipe was held vertically and horizontally by a forklift truck and a wooden support. The guide pipe rested on wooden support which stood on a concrete block, Figure 7-1 and Figure 7-2.

The concrete block had the width, length and height: W = 306 mm, L = 2000 mm and H = 805 mm. The concrete had a strength f_{cck} = 60 MPa and modulus of elasticity E = 39,000 MPa. The same concrete block was used for all 4 test series. The concrete block was placed on a 10 mm rubber mat.

For two of the shoes there was a predrilled hole with a diameter of Ø30 mm in which a dowel made of a reinforcement bar with a diameter of Ø28 mm was placed.

All the samples were from the same hollow bar. Steel grade of the hollow bar was S355J2G3. Hollow bars were cut in 200 mm lengths. They were then machined to the required geometry. The geometry is shown in Figure 7-1 and the dimensions are shown in Table 7-1:.

	Form of end face	H [mm]	h [mm]	D [mm]	d_y [mm]	d_i [mm]	t	d_y/t
Shoe 1	Straight	200	50.1	71.4	58.1	32.2	12.95	4.49
Shoe 2	Concave	200	49.7	71.4	58.1	32.2	12.95	4.49
Shoe 3	Concave	200	49.7	71.4	58.1	32.2	12.95	4.49
Shoe 4	Straight	200	50.1	71.4	58.0	32.2	12.90	4.50
NPRA shoe	Concave				219	119	50	4.38
Ruukki shoe	Straight with build-up weld.				240	100	70	3.43

Table 7-1: Dimensions of the small scale pile shoe tips

Area scaled down shoe: 1,835 mm^2
Area NPRA shoe: 26,533 mm^2 gives a scaling down of approximately 1/14
Area Ruukki shoe: 37,366 mm^2 gives a scaling down of approximately 1/20

Four test series were performed:

1. Hollow bar with the straight end face driven against solid concrete
2. Hollow bar with the concave end face driven against solid concrete
3. Hollow bar with the straight end face driven against concrete with predrilled hole and dowel
4. Hollow bar with the concave end face driven against concrete with predrilled hole and dowel

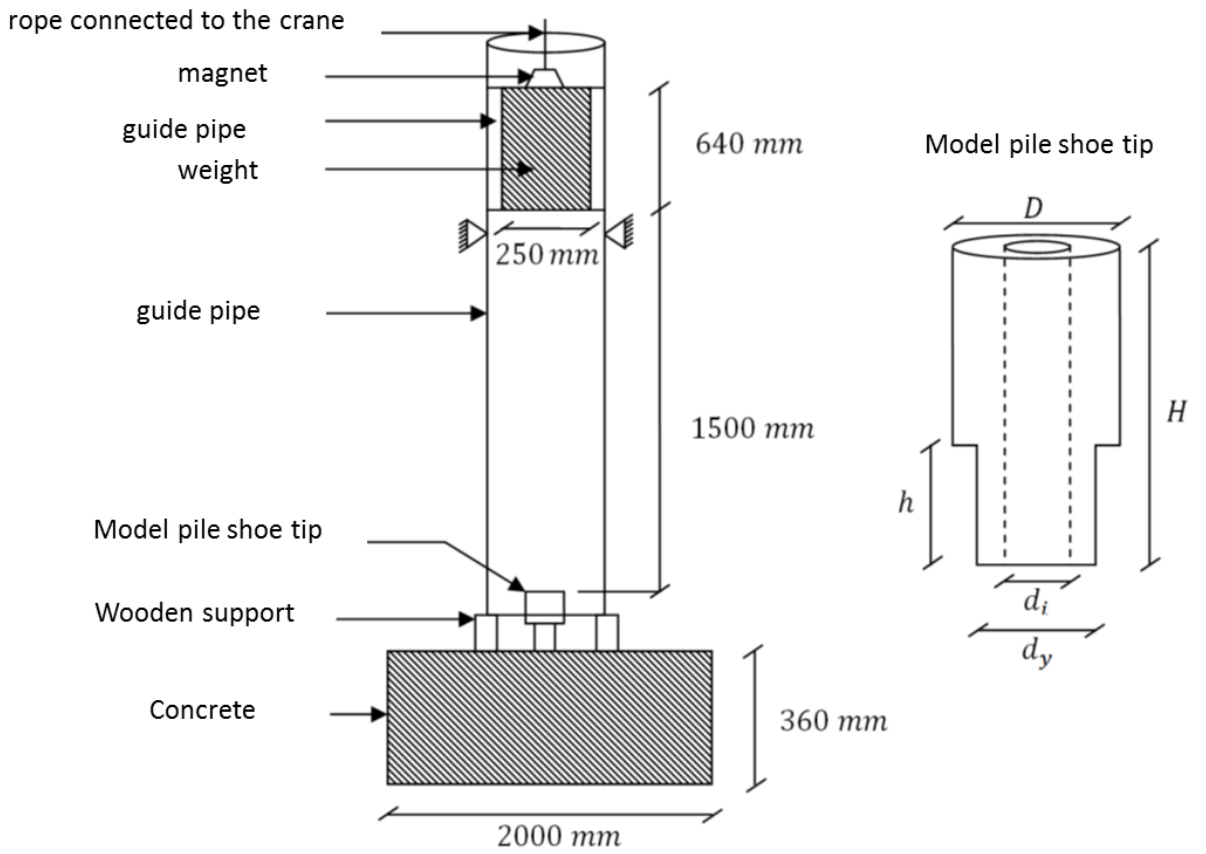

Figure 7-1: On the left, set up of the test rig and to the right geometry of the model pile shoe tip.

Figure 7-2: Test rig set up for the small scale test.

Results

Hollow bars 1 and 4 with a straight end face received large deformation during driving. On hollow bar 1 one side was particularly bent and in some places bits were missing. On the hollow bar 4 large pieces were knocked off and there were some plastic deformations.

Hollow bars 2 and 3 with concave end faces were less and slightly deformed. On hollow bar 2 some steel was torn off along the edge.

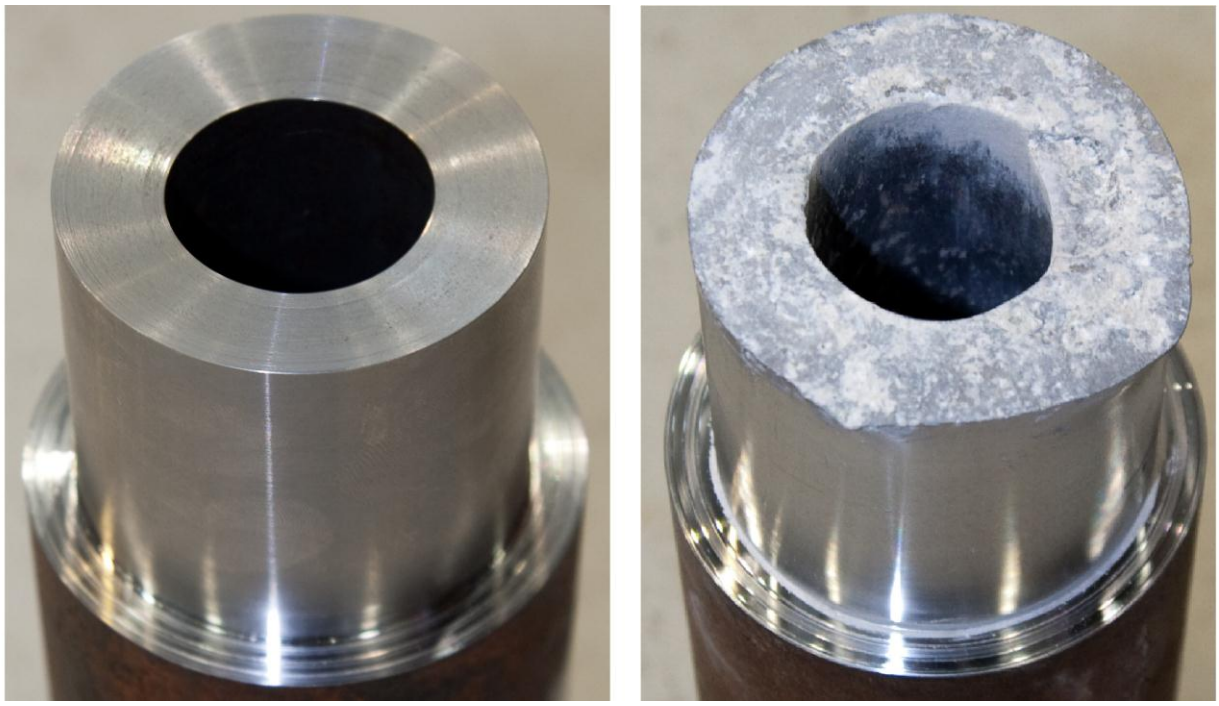

Figure 7-3: Before and after photos of the straight shoe, test series 1

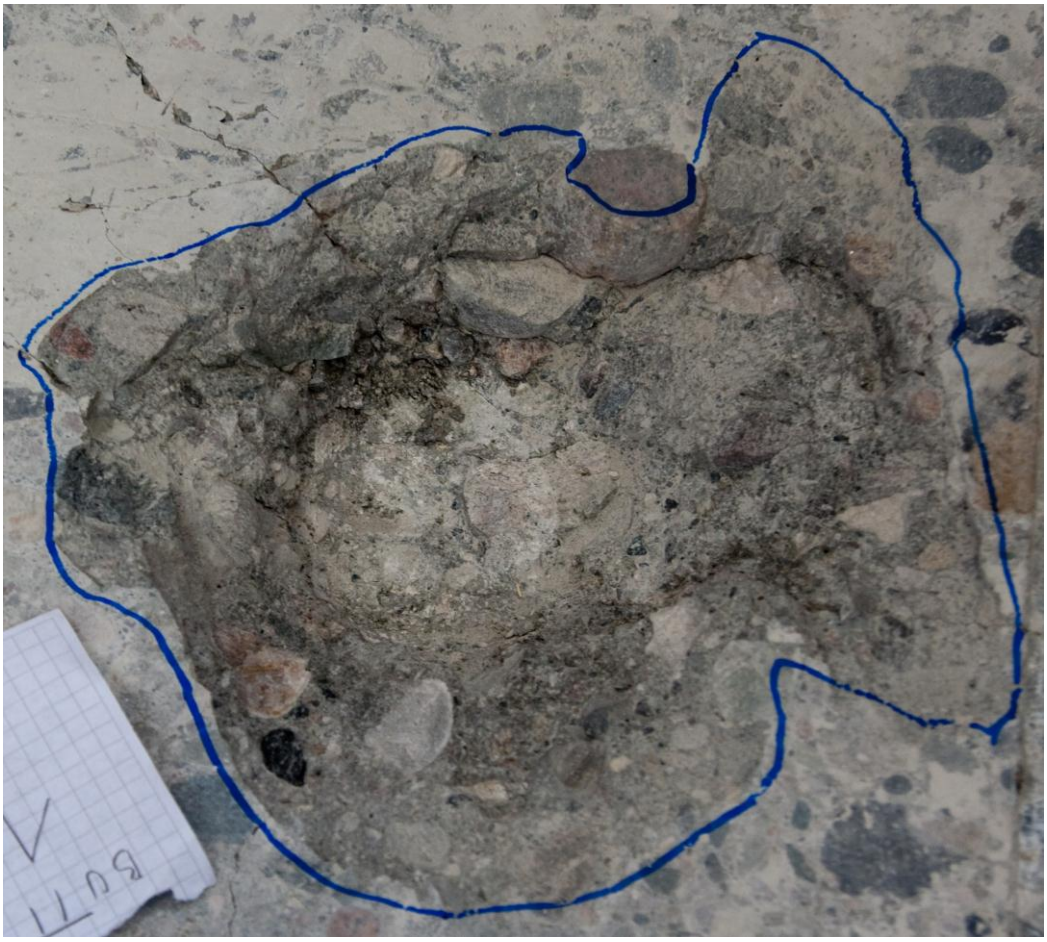

Figure 7-4: Crater made by the straight shoe, test series 1

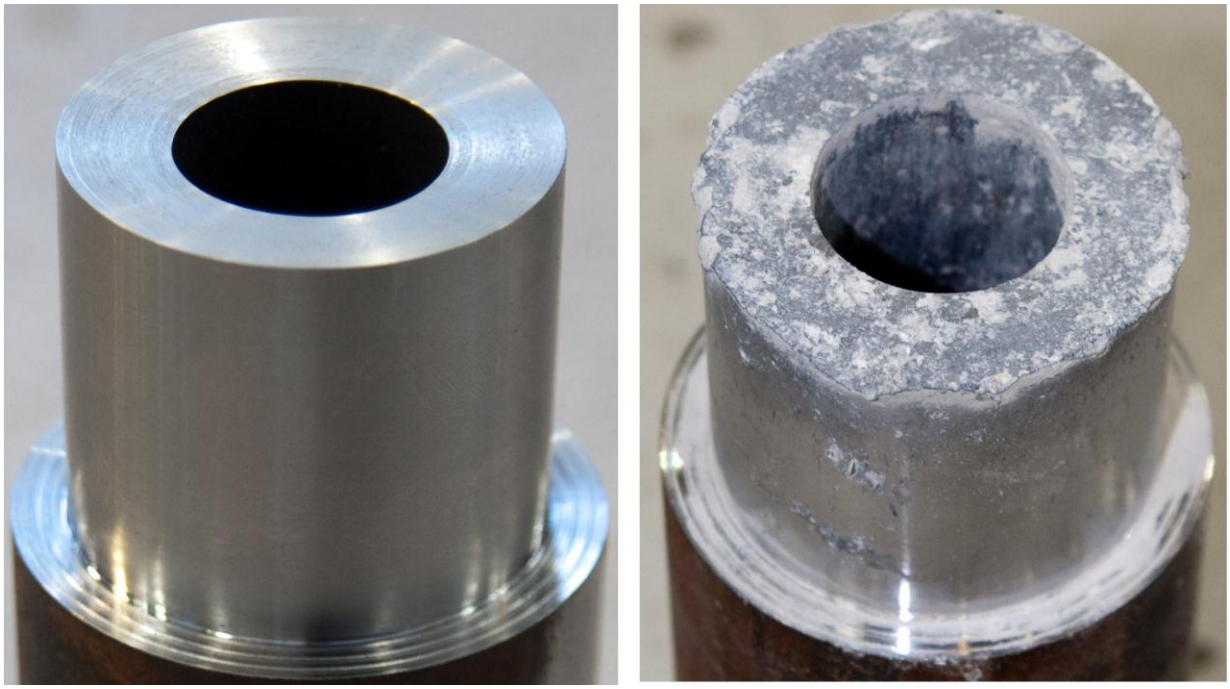

Figure 7-5: Before and after photos of the shoe with the concave end face, test series 2

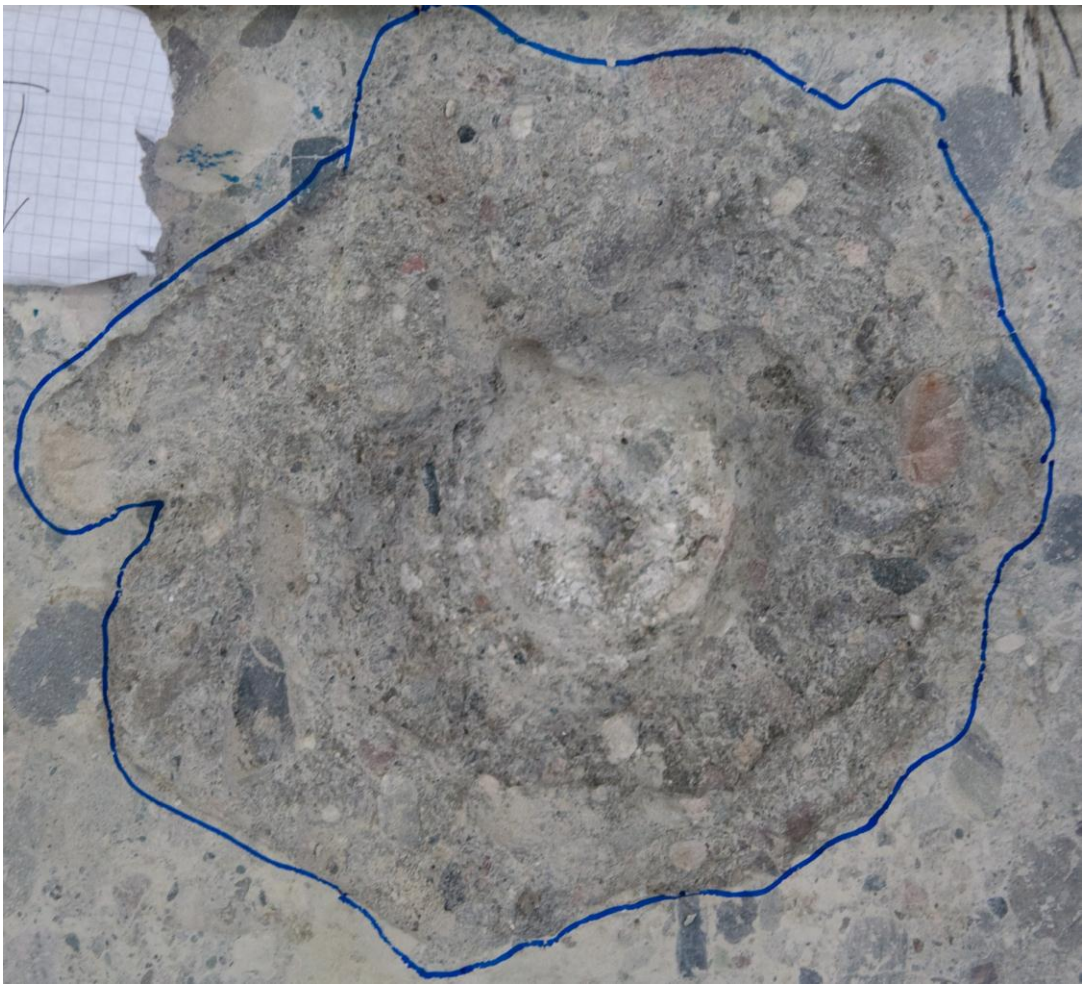

Figure 7-6: Crater made by the shoe with the concave end face, test series 2

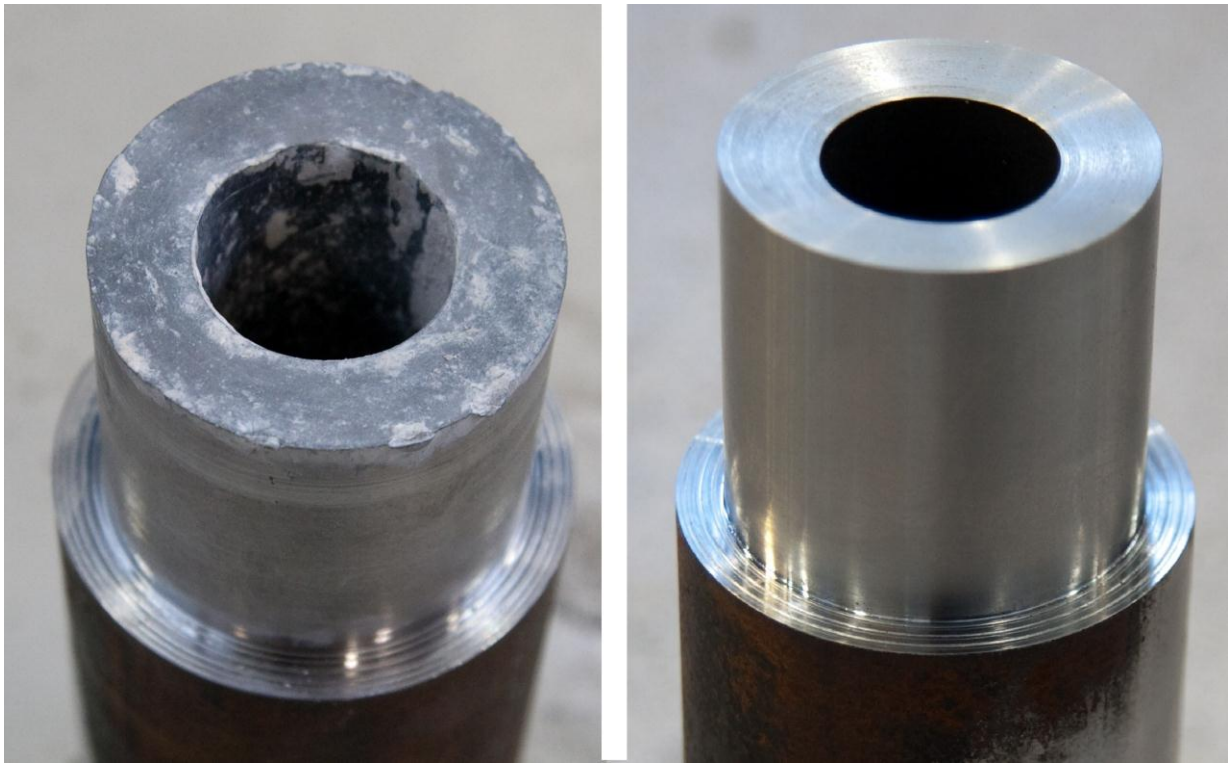

Figure 7-7: Before and after photos of the shoe with the concave end face and predrilling, test series 3

Figure 7-8: Crater made by the shoe with the concave end face with predrilling, test series 3

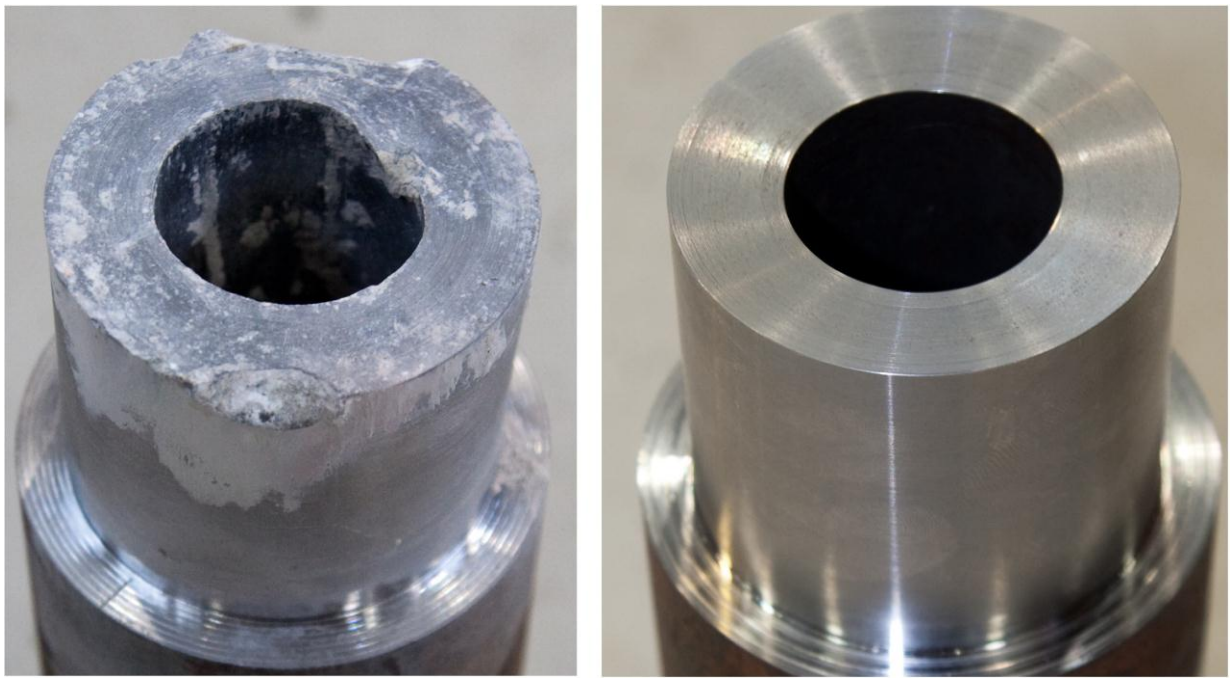

Figure 7-9: Before and after photos of the straight shoe with predrilling, test series 4

Figure 7-10: Crater made by the straight shoe with predrilling, test series 4

	Hollow bar 1 Straight [mm]	Hollow bar 2 Concave [mm]	Hollow bar 3 Concave with dowel [mm]	Hollow bar 4 Straight with dowel [mm]
dy after driving	62	60	58.8	60
Δ dy	3.9	1.9	0.7	1.9
h after driving	49.5	48	49.5	47 to 49
Δ h	-0.6	-1.7	-0.2	-1.1 to -3.1
Crater Dmax	200	230	220	270
Crater Dmin	160	130	200	190
Crater Dmean	180	195	210	230
Crater depth	45	55	60	62

Table 7-2: Summary of the small scale tests

The shoe with the clear minimum damage was hollow bar 3. This had a concave end face and was driven in the predrilled holes with dowel. Shoes that were driven with the dowel had the best penetration and the concrete was crushed with the largest mean diameter.

There are some errors that may have affected the results. All shoes were driven in the same concrete block. The depression in the concrete block became bigger and bigger for every shoe. Finally, the concrete block split in to two. The last tests may have been affected by previous driving and weaknesses in the concrete may have occurred.

The drop height was not adjusted to the depression, i.e. the drop height varied between 1.5 and 1.56 m. Neither was friction taken into account and a degree of efficiency on the hammer less than 1.0 was chosen.

8 Summary of all tests

8.1 Driving stresses in pile shoe parts

We have calculated stresses using Abaqus, but to a lesser extent have verified stresses in the various structural components by means of the full scale test.

The full-scale test was successful, but later in the full-scale test we realised that it would have been an advantage to have fitted more strain gauges. We lacked strain gauges on the stiffening plates, the bottom plate and on the top edge of the pile pipe.

We would have benefitted from the following additional strain gauges:

- 3 strain gauges placed in the stiffening plate triangle on two of them (2 close to the hollow bar at the top and bottom and 1 close to the outer edge of the pipe, upper), i.e., 6 in total.
- 4 strain gauges on the base plate (2 above the stiffening plate and 2 in the field between the stiffening plates) - positioned so that vertical stresses were logged.
- 4 strain gauges on the pipe just above the base plate positioned in the same way on the base plate.

Then we could have evaluated the stress further. It would have been an advantage to measure the height inside the hollow bar before and after driving to evaluate if there is at any compression of the hollow bar.

Measurements with strain gauges of the NPRA shoes show that the hollow bar 270 mm from the shoe tip (bellow the stiffening plate) yields. The hollow bar 500 mm from the shoe tip does not yield.

When comparing the upper and lower strain gauges on the two maximum drop heights, we see that the stress in the upper strain gauges flattens out. This may indicate that there is greater deformation in the hollow bar so that the stiffening plate receives a larger share of the loads than at the lower drop heights. The stiffening plates were not instrumented, so that this theory has not been verified.

There are no reliable measurements for the Ruukki shoes at drop heights higher than 0.5 m. We have therefore not recorded measurements whether the steel yields or not. The steel area of the Ruukki shoe is slightly larger than the NPRA shoe, so the stress level is naturally slightly lower at the same drop height.

Based on the calculation for NPRA shoe, the stress plots show that the hollow bar attained yield stress below the stiffening plates.

8.2 Dynamic amplification factor

Dynamic amplification factor according to the Norwegian Piling Handbook 2001 [2] section 4.6.2.

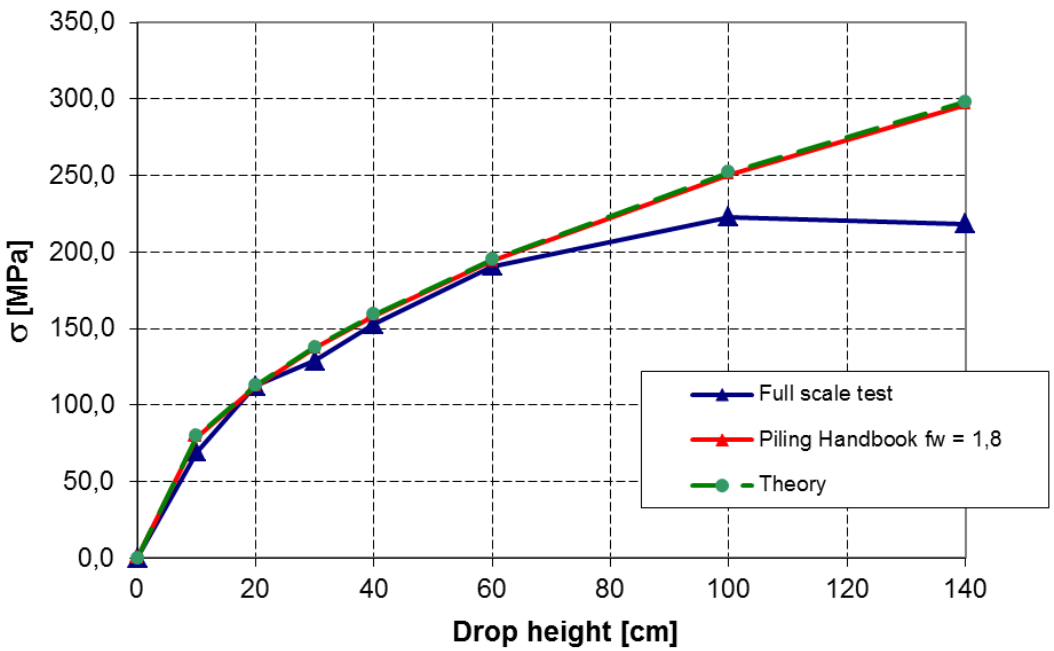

Figure 8-1: Comparison of the theoretical stress and full scale test stress at 1.8 stress amplification factors. Data from NPRA shoe no. 1 and the upper strain gauges.

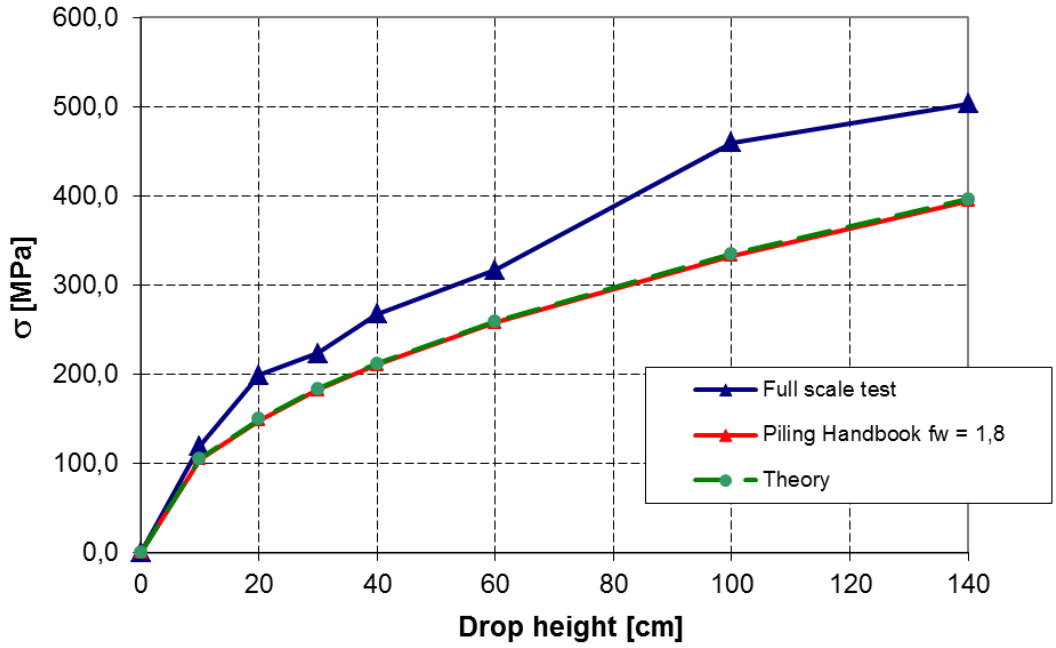

Figure 8-2: Comparison of the theoretical stress and full scale test stresses at 1.8 stress amplification factors. Data from NPRA shoe no. 1 and the lower strain gauges.

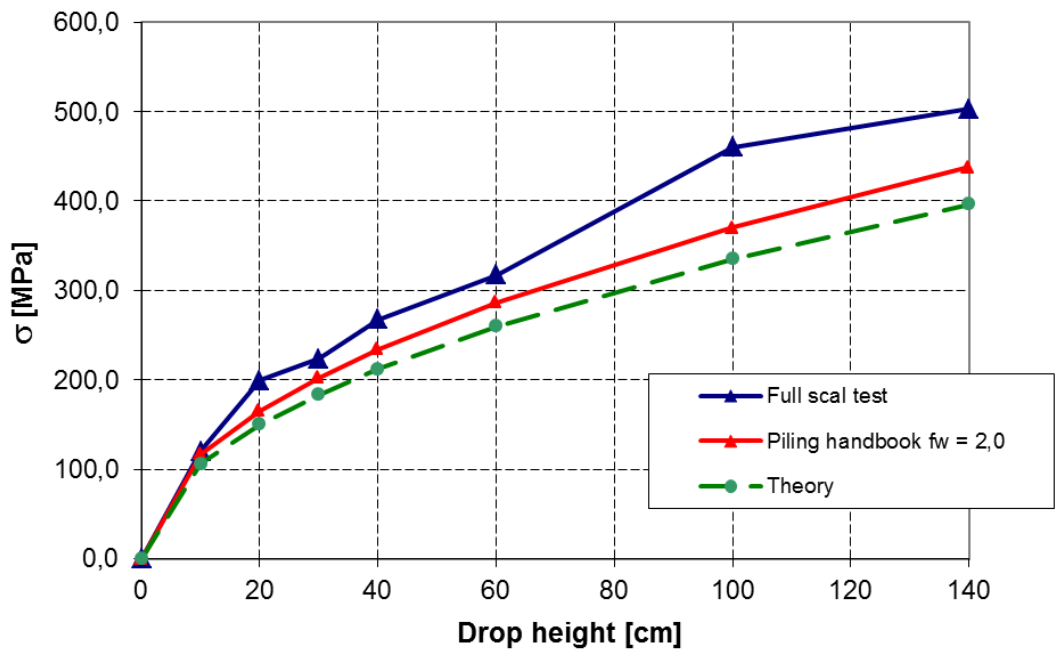

Figure 8-3: Comparison of the theoretical stress and full scale test stresses at 2.0 amplification factors. Data from NPRA shoe no. 1 and the lower strain gauges

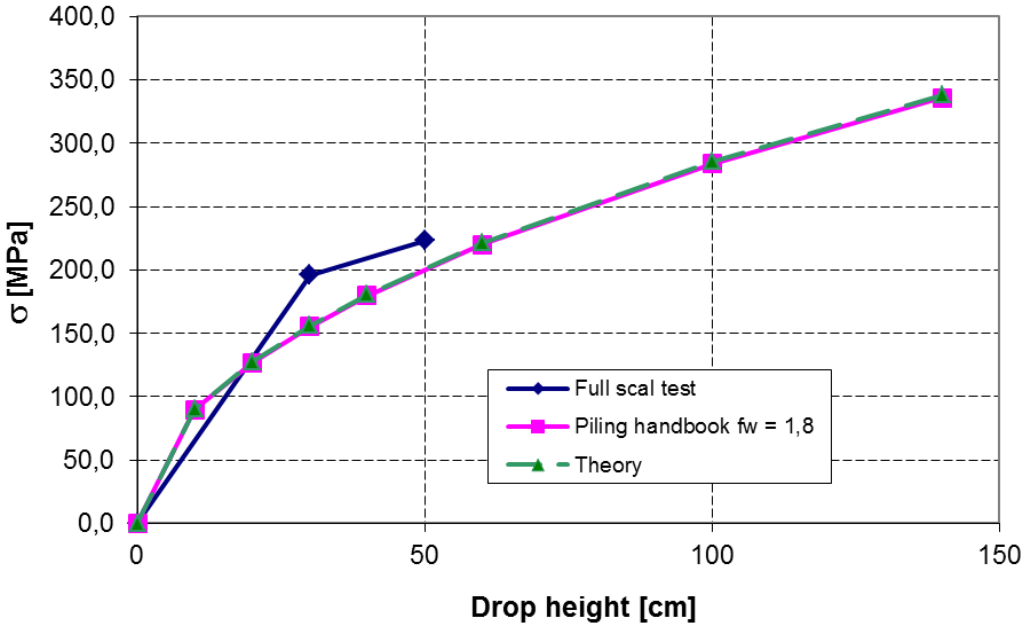

Figure 8-4: Comparison of the theoretical stress and full scale test stresses at 1.8 stress amplification factors. Data from Ruukki shoe no. 3 and lower strain gauges.

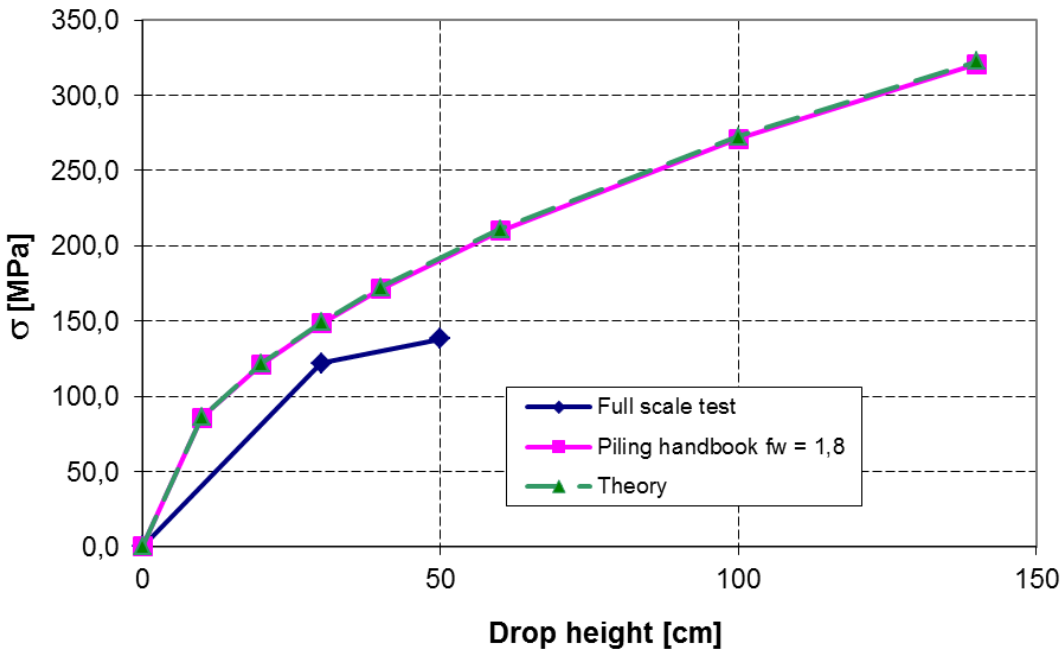

Figure 8-5: Comparison of the theoretical stress and full scale test stresses at 1.8 stress amplification factors. Data from Ruukki shoe no. 3 and the upper strain gauges.

The full-scale test is at the extreme limit in relation to actual driving conditions. In the full scale test, we have a very short steel pile that does not stand in loose soil. There is therefore no dampening in relation to the friction against the loose soil. The pile hammer is driven under

very controlled conditions on a vertical pile. We have measured the efficiency of the hammer up to 1.4. It is therefore natural that the stress has a high amplification, also higher than that described in the Norwegian Piling Handbook [2].

We see in Figure 8-1 to Figure 8-5 that both the RUUKKI shoe and the NPRA shoe exceed the values for amplification in the Norwegian Piling Handbook. How different areas between the pile shoe and pile pipe affect the result has not been evaluated.

8.3 Stresses in steel with rapid load application as during pile driving

In the Norwegian Piling Handbook (1991) [3] section 9.5 it states that the steel's yield stress may be exceeded by 25% due to rapid load application, as during final driving of piles. The same is stated in the new Norwegian Piling Handbook (2005) [2] section 4.7. There is also supporting references about stress to be exceeded during rapid loading in the literature studies.

Driving with hydraulic drop hammer occurs over a very short period of time. Loading takes place between 0 and 0.02 s. In this short period the pile and the shoe are subjected to a powerful impulse load, and there are strains in the steel over an extremely short time. The yield stress of the steel is related to rate of deformation. It is therefore possible to accept a higher von Mises stress in the results than conventional steel yield stress. The following figures are a result of research [10]. In Figure 8-6: the stress - strain diagram of steel is shown at different strain rates.

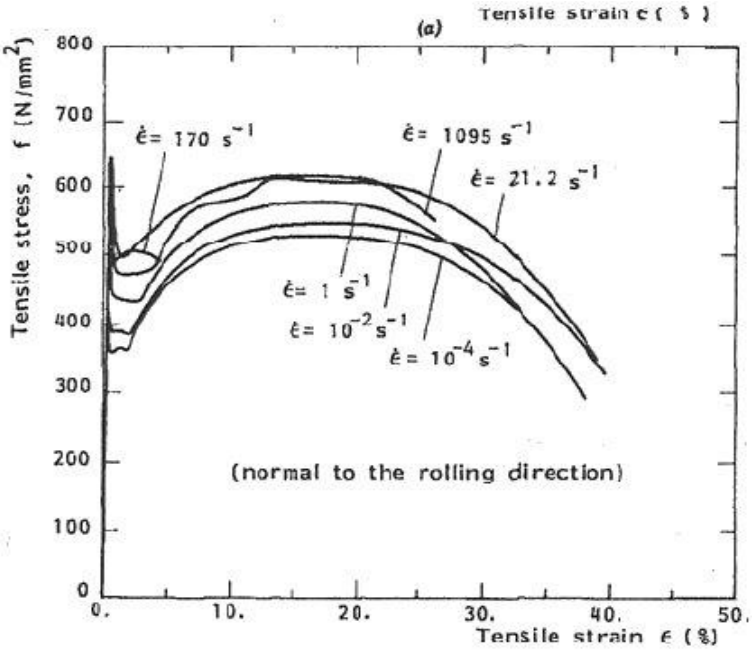

Figure 8-6: Stress- strain diagram at different strain rates [10]

The stress - strain diagram shows that both yield stress and fracture stress in the steel will be higher with an increasing strain rate. This increase occurs linearly with the logarithm for the strain rate, as shown in Figure 8-7.

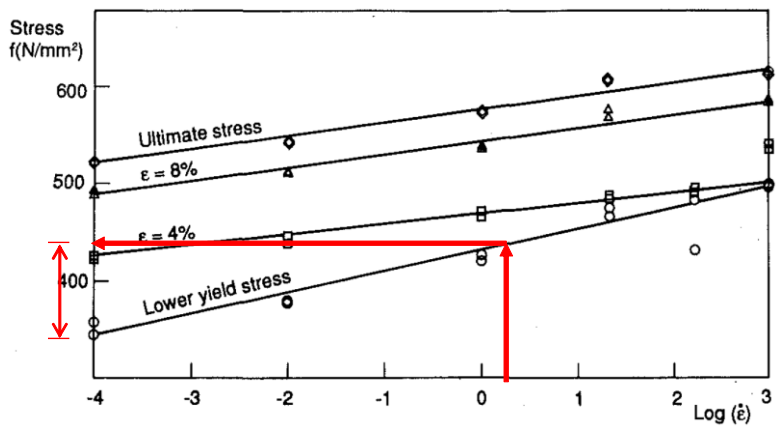

Figure 8-7: Trends found when testing strain rates on St52-3N steel, note that one of the axes is logarithmic [11].

When a pile is dimensioned, one should consider how one wants the forces to go. As part of the pile shoe begins to yield, it will deform and the forces will stored. If one wishes to use thinner stiffening plates, it would be sensible to use adequate area in the hollow bar and in the shoe and not take advantage of the extra capacity that one gets through rapid loading as the curves show above.

9 Conclusions and recommendations

A pile shoe against the rock bears the pressure. It can therefore withstand some deformation and will still be adequate from a construction standpoint. As long as there is no failure between the hollow bar and base plate it will work in a permanent state when the steel pipe is filled with concrete. For geotechnical aspect it has been common to dimension the steel elastically, and not make use of the plastic capacity of the steel. A shoe with little plastic deformation, in our opinion, has a better penetration capacity in the rock.

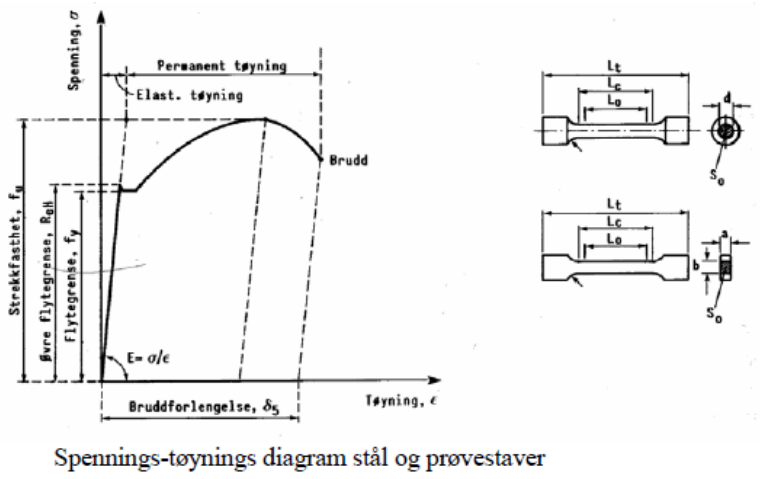

Figure 9-1: The stress diagram for the tie rods show that although the steel achieves plastic strain the steel will still be sustainable up to failure. Elastic strain ξ = Eσ is added to the plastic strain of repetitive loads.

It is not desirable to have a lot of plastic deformation during pile driving, and our assessment is that the NPRA shoe had a better performance than the Ruukki shoe in the full-scale test. When we measure the elastic and plastic deformations with movement measurements during pile driving, it will be a source of error if there is a lot of plastic deformation in the steel. If the

build-up weld deformed and lies outside the hollow bar the movement measurements for calculating the bearing capacity will not be correct.

The designer of the pile shoe can influence the force path in the pile shoe using the various dimensions of the structural parts. Since rather big force runs through the hollow bar during pile driving, then one must use a heavy base plate and hollow bar. When the base plate deforms little, there will be less force out on the stiffening plates.

Large welds are expensive to produce, and it is therefore desirable to minimise the welding thickness between the stiffening plates and the base plate and between stiffening plates and the hollow bar. Between the stiffening plates and the base plate must be a fillet weld (full penetration welding) since it is the transfer of pressure forces. The thickness of the stiffening plate must be reduced in order to reduce the throat measurement of the weld here. There was no buckling on the stiffening plate on the Ruukki shoe in the full-scale test. When we look at the stress that occurred in Figure 9-2 shows an example where the stiffening plate has buckled on a pile with a diameter of Ø = 610 mm, here the thickness of the stiffening plates is t = 15 mm and the base plate thickness 60 mm. This gives t = 0.025 Ø and T = 0.1 Ø.

For diameter Ø800 mm we recommend t = 25 mm and T = 80 mm.
This gives t = 0.030 Ø and T=0.1 Ø. Recommendation in the Norwegian Piling Handbook currently is t = 0.035 Ø and T = 0.1Ø.

We recommend chamfering of the corners of stiffening plates. Large stress concentrations occur where the triangle in the corner goes out to zero. 20 mm chamfering of the corners is therefore recommended. See Figure 9-3 where this is done.

Figure 9-2: Buckling of the stiffening plates with thickness t = 15 mm Photo: Hannu Jokiniemi.

9.1 Proposed changes to the Norwegian Piling Handbook

Norwegian Piling Handbook [2] table 4.8: The table for the amplification factor for shock waves f_w gives values for depressions greater than 5 mm and less than 1 mm. With stop driving the drop is usually between 1 and 3 mm. The table is therefore difficult to interpret in this area. We have called the factor f_w "amplification factor for the stress waves" in this report, but it can also be given a name in the Norwegian Piling Handbook too.

We have seen that the design of the end face is important. We would recommend that the Norwegian Piling Handbook advises that the face is concave (hollow ground). This is already described in Bjerrum NGI publication in 1957 [7].

There are concentrations of stress in the upper and lower corners of the stiffening plate where the plate is attached to the hollow bar and top plate. We would suggest that there is a recommendation to 20 mm chamfering on corners of the stiffening plate, Figure 9-3.

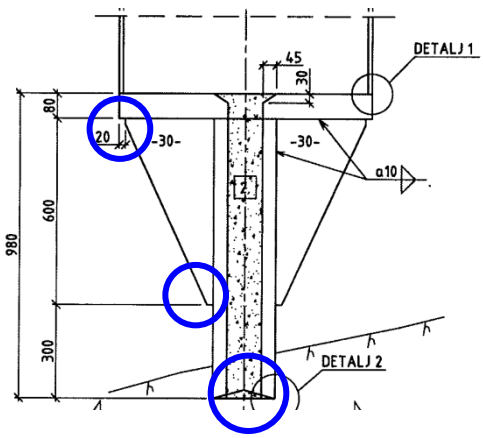

Figure 9-3: Pile shoe with hollow ground end face and chamfering of corners on stiffening plates

Stress changes with dimensions differences should also be mentioned under the stress waves. There is varying stress in the shoe and pipe if there are different areas in the shoe and pipe, section 4.1 about shock wave theory.

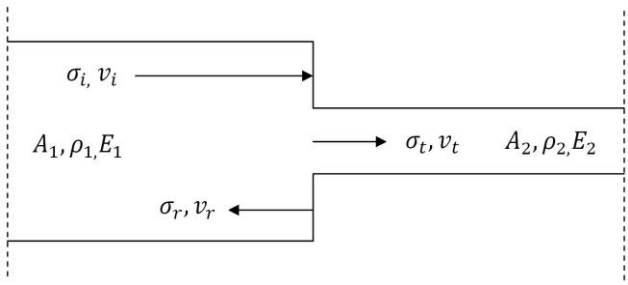

Figure 9-4: Discontinuity in the cross section

In the case when the density ρ and modulus of elasticity E are equal for the two materials the stress can be described with the following conditions:

$$\sigma_t = \frac{2A_1}{A_1 + A_2} \cdot \sigma_i \qquad \text{and} \qquad \sigma_r = \frac{A_2 - A_1}{A_1 + A_2} \cdot \sigma_i$$

9.2 Pile spacing

In the full-scale experiment, we noted that the shoe affected over a diameter in the rock by 800 - 1000 mm. The hollow bar diameter was 220 - 240 mm. This means that the rock was affected in a diameter of 3 - 4 times the outer diameter of the shoe.

We saw the same happened on the small scaled test. There we recorded craters in the concrete 180 - 230 mm and outer diameter of shoe was 58 mm. The concrete was thus affected in the same way as the full-scale test by 3 - 4 times the outer diameter of the shoe.

The conclusion is that with today's requirements in the Norwegian Piling Handbook of 3 to 5 times the pile diameter, one should have ample spacing between piles. The pile shoe's penetration into the rock should not affect the rock of the neighbouring pile.

10 Suggestions for further work

10.1 Design of pile shoe for piles with a diameter of 800 mm

10.1.1 Parameter study in Abaqus

The deformations in the rock have become too large in the calculations in Abaqus. New calculations should be made where the parameters of the rock are adjusted so that the deformation is correct.

Assessment of the discontinuity formula in Abaqus. How is the stress in the various structural parts dependent on the area? Is much reflected in the base plate which has a large area?

A parameter study should then be made where the dimensions of the pile shoe parts are changed:

- The base plate is calculated with T = 80 mm T = 60 and 100 mm would be interesting, maybe even increments in between.
- Stiffening plate t_r = 30 mm. It may be interesting to look at t_r = 20 mm with varying thickness of the base plate.
- Variable area of the hollow bar. We have estimated approximately 26,000 mm^2. It may be interesting to see 37,000 mm^2 and 20,000 mm^2.

There should be an assessment of safety in relation to adverse conditions such as sloping rock.

10.1.2 Thickness of the welding

There should be a back calculation of stresses calculated in Abaqus and/or measured in the full scale test to find the dimensions of welds between the hollow bar and stiffening plate.

10.1.3 Evaluation of hardening, shaping and build-up welding on the rock shoe

The full-scale test showed that the shoe with the concave end face and hardening was virtually unaffected by the hard driving. There was very little damage and deformation. What is the reason for this?

To study this further, we suggest further assessments:

- A metallurgical literature study and assessment of the hardening's effect on the steel. This may include a visit of a hardening workshop.
- Can we achieve sufficient brinell hardness using other steel types and thus prevent hardening?
- In the first step a small scaled test with shoes with a concave end face, where they have different treatment:
    a. Common S355-steel
    b. Hardened S355 steel
    c. Machined shoe with build-up welding so that it has a similar geometry as the shoe with a concave end face.
    d. Common S460-steel
- In the small scaled tests differences with material should be reduced. In later tests an attempt to insert gneiss into the concrete and driving the shoes against gneiss instead of concrete should be made.
- In the next step it may be necessary to make a new full-scale test.

10.1.4 What is the best end face on the hollow bar, concave or straight end face?

By a visual assessment of the shoes after driving it is clear that the shoe with a concave end face has less deformation and damage. In the small scaled test all shoes were treated equally. None of the shoes were hardened.

We see the same in the full-scale test. Here the shoes with the concave end faces are almost completely undamaged. The shoes are hardened and this will affect the result.

Shoes with the straight end face and build-up welds are the worst visually. Here the shoe is deformed and the build-up weld spread after driving.

For future work, we propose an initial step to undertake scaled down test with shoes of a concave end face. The next step may be full-scale tests.

10.2 The rock type and stress occurring in the shoe

We have made a full-scale test with the gneiss rock type. Other rock types will have different resistance to penetration. In a later full-scale test or scaled down test it will be interesting to consider other rocks than gneiss.

We have experience that the following rock types are difficult to drive in:

- Limeston in Porsgrunn (Steinar Giske)
- Rombphorfhy in Drammen (Grete Tvedt)

10.3 Full-scale test with solid shoes

When driving solid shoes the outer diameter is smaller than with hollow rock shoes. We cannot predrill the rock before driving the shoe. It may be interesting to see any different behaviour between hollow and solid shoes.

10.3.1 Other pile dimensions - can we just scale up and down?

We have only seen steel pipe piles with a diameter of 814 mm up until now in the R&D project. We do not have sufficient information to assess how stresses change with other pile dimensions. This would be interesting to see numerically, when we have a good model.

Pile diameters that may be relevant are: 600 mm, 1000 mm and 1200 mm.

11 References

/1/ Fredriksen F. and Ytreberg D. I., *Standardized hollow rock shoes – Static analysis and design.* Geovita and Aas-Jakonsen. 14.3.2008.

/2/ Norwegian Geotechnical Society and the Norwegian pile committee, *Norwegian Piling Handbook 2005.*

/3/ The Norwegian pile committee and NBR, *Norwegian Piling Handbook 2nd. ed. 1991.*

/4/ Forseth A. K., *Examination of steel pipe piles and standardized pile shoes.* Master Thesis June 2009. Norwegian University of Science and Technology, NTNU.

/5/ Tveito S.J., *Driving of steel piles with rock shoes against rock.* Master Thesis June 2010. Norwegian University of Science and Technology, NTNU.

/6/ NPRA, *Handbook 016 Geotechnics in road construction*. April 2010.

/7/ Bjerrum L., *Norwegian experience with steel piles to rock*. NGI-Publication no 23 Oslo, 1957.

/8/ NBG Norwegian Group for Rock Mechanics.,*Engineering Geology and Rock Engineering*. Handbook No 2. 2000.

/9/ Eiksund G, *Dynamic testing of piles*. PhD thesis 1994:31, Institute of Soil Mechanics, Norwegian University of Science and Technology, NTNU.

/10/ Langseth, M., Lindholm, U.S., Larsen, P.K. og Lian, B., *Strain Rate Sensitivity of Mild Steel Grade, St52-3N*. Journal of Engineering Mechanics. 1991, Vol.117.

/11/ Johnson GR, Cook WH, *A constitutive model and data for subjected to large strains, high strains, high strain rates and high temperatures*. Proc. 7th Int. Symp. on Ballistics. pp 541 – 547. The Hague, The Netherlands, April 1983.

Attachment

A. PDA report

Entreprenørservice AS
Att.: Harald Amble
Rudssletta 24

1309 RUD

Deres ref.: 25283 Vår ref.: 120535/JOT Oslo, 13. april 2010

PDA FoU Pelespiss
Rapportering av PDA målinger

Vi viser til utførte PDA-målinger i uke 14 i forbindelse med Forskning på pelespiss ved E6 Dal, Multiconsult AS ble forespurt av Entreprenørservice AS om å utføre målingene og oversender herved resultatene fra målingene rapportert i brevs form.

Det er utført målinger på tre stålrørspeler, P10A. Ruukki og P10B. Dimensjoner for pel og spiss er presentert i figur 1. Pelene er rammet på fjell i dagen. Peleramningen er utført av Entreprenørservice. Pelemaskinen som slo på pelen har et Junttan 9t akselererende lodd.

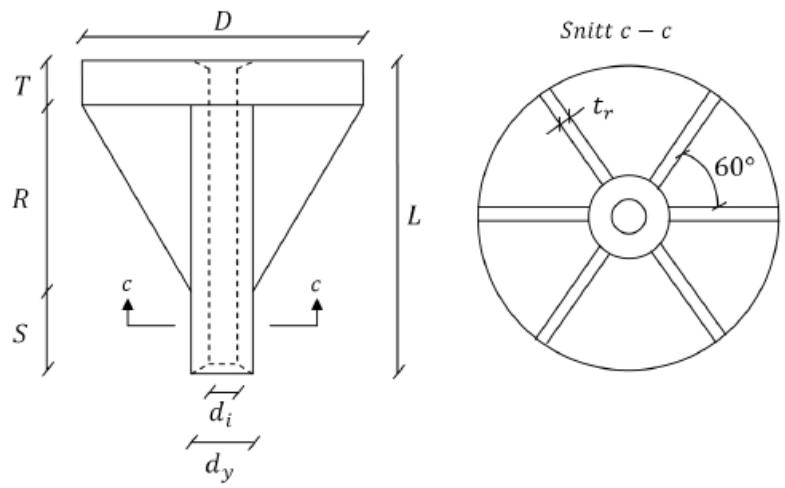

Figur 1: Pelspissenes mål

Tabell 1: Mål på pelspisser og total lengde av pel og spiss (L_{tot})

	D	T	R	S	L	d_y	d_i	t_r	L_{tot}	t_{pel}
	mm	*mm*	*mm*	*mm*	*mm*	*mm*	*mm*	*mm*	*mm*	*mm*
Pel 10 A	813	80	600	300	980	219	119	30	7450	14,2
Pel 10B	813	80	600	300	980	219	119	30	7520	14,2
Pel RUUKKI	813	70	600	260	930	240	100	20	6980	12,5

Figur 1. Dimensjoner for pel og spiss. (ref.III)

Rammingen ble utført i forbindelse med et forskningsprosjekt i regi av Vegvesenet/NTNU.

Pelen ble instrumentert med PAK PDA-utstyr (ref. /I/) av Multiconsult AS torsdag 8.april 2010. Det ble utført PDA målinger kontinuerlig ved ramming på pelene.

I tillegg ble nederste del av pel og pelespiss (steg) instrumentert med strekklapper for å måle spenninger i stålet (NTNU). Ved utvalgte slag ble det logget data fra strekklappene og også filmet med høyfrekvent kamera. For å sammenstille resultater fra strekklapper og PDA blir PDA rådata filer oversendt til NTNU i etterkant.

Det er presentert et plot fra PDA målinger for hver pel, plottene er gitt for følgende fallhøyder:

- Ett utvalgt slag med 10 cm fallhøyde
- Ett utvalgt slag med 20 cm fallhøyde
- Ett utvalgt slag med 30 cm fallhøyde
- Ett utvalgt slag med 60 cm fallhøyde
- Ett utvalgt slag med 140 cm fallhøyde

Hensikten med PDA-målingene var å dokumentere spenninger i stålet, energitilførselen fra pelehammer (virkningsgrad på loddet), og bæreevnen til pelene. I tillegg vil PDA målingene bli sammenstilt med resultatene fra strekklappene montert av NTNU.

Tabell 1 viser verdier som er tatt ut fra PDA målingene.

Bæreevne gitt fra PDA målingene skal kun betraktes som veiledende. Grunnet kort avstand til spiss gir målingene et litt vanskelig grunnlag for nøyaktig tolkning av refleksjonsbølgene. Resultatene fra PDA målingene gir følgende maksimum bæreevne:

P 10A = 13005 kN, P Ruukki = 9907 kN og P10 B 9818 kN.

PDA-målingene har dokumentert maksimalt tilført energi fra pelehammeren tilsvarende 128,9 kNm. Dette tilsvarer en virkningsgrad på 1,04 for fallhøyde 1.4 m. Det bemerkes at det ikke nødvendigvis er godt samsvar mellom fallhøyde gitt i tabellen og faktisk fallhøyde for slaget, dette gir i noen tilfeller svært høy virkningsgrad, og i andre tilfeller en lav virkningsgrad.

Det bemerkes også at anslag på en ujevnt kappet peletopp kan medføre redusert tilført energi og dermed redusert virkingsgrad på falloddet.

Tabell 1. *Registerte verdier for PDA målinger.*

Måling P 10A						
Fallhøyde HHK90	[m]	0.1m	0.2m	0.3m	0.6m	1.4m
Total lengde, L	[m]	7.450	7.450	7.450	7.450	7.450
Målelengde (givere til pelespiss), L_E	[m]	3,0	3,0	3,0	3,0	3,0
Lengde i jord, L_P	[m]	0,05	0,1	0,2	0,35	0,4
Loddvekt, W	[kN]	90	90	90	90	90
Tilført energi, E	[kNm]	8,5	16,0	34,1	56	128,9
Maks kraft (FMX) PDA	[kN]	3783	4922	6583	9020	12154
Virkningsgrad, η	[-]	0,96	0,91	1,29	1,06	1,04
Karakteristisk bæreevne, Q_k fra PDA med $J_C = 0,0$	[kN]	3757	5036	6775	9450	13005
Rammepenning, σ [1)]	[MPa]	106,2	138,1	184,7	253,1	341,1
Registrert synk pr.slag	[mm]	4,5	0,07	2	1	1
Slag nummer registrert i PDA [2)]	[-]	27	105	179	467	498
Filnavn		10A	10A	10A	10A	10A

[1)] Rammepenning registrert 3 m fra pelespiss.

[2)] Det er utført flere slag/ registreringer for å teste PDA-utstyr i forkant. Registrerte tall kan derfor avvike fra peleprotokoller.

Tabell 2. *Registerte verdier for PDA målinger.*

Måling P Ruukki						
Fallhøyde HHK90	[m]	0.1m	0.2m	0.3m	0.6m	1.4m
Total lengde, L	[m]	7450	7450	7450	7450	7450
Målelengde (givere til pelespiss), L_E	[m]	3,0	3,0	3,0	3,0	3,0
Lengde i jord, L_P	[m]	0,05	0,1	0,2	0,35	0,4
Loddvekt, W	[kN]	90	90	90	90	90
Tilført energi, E	[kNm]	10,3	18,1	28,7	47,5	97,7
Maks kraft (FMX) PDA	[kN]	4522	5690	6858	7461	9188
Virkningsgrad, η	[-]	1,17	1,02	1,08	0,90	0,79
Karakteristisk bæreevne, Q_k fra PDA med $J_C = 0,0$	[kN]	4324	5640	6898	7811	9907
Rammepenning, σ [1)]	[MPa]	143,8	181	218,1	237,3	292,3
Registrert synk pr.slag	[mm]	1	1	0,4	0,2	5,4
Slag nummer registrert i PDA [2)]	[-]	16	27	280	389	415
Filnavn		Ruukki	Ruukki	Ruukki	Ruukki	Ruukki

[1)] Rammepenning registrert 3 m fra pelespiss.

[2)] Det er utført flere slag/ registreringer for å teste PDA-utstyr i forkant. Registrerte tall kan derfor avvike fra peleprotokoller.

Tabell 3. *Registerte verdier for PDA målinger.*

Måling P 10B						
Fallhøyde HHK90	[m]	0.1m	0.2m	0.3m	0.6m	1.4m
Total lengde, L	[m]	7.525	7.525	7.525	7.525	7.525
Målelengde (givere til pelespiss), L_E	[m]	3,0	3,0	3,0	3,0	3,0
Lengde i jord, L_P	[m]	0,05	0,1	0,2	0,35	0,4
Loddvekt, W	[kN]	90	90	90	90	90
Tilført energi, E	[kNm]	9,7	24,8	29,6	41,9	109,7
Maks kraft (FMX) PDA	[kN]	4159	5693	6141	7529	11142
Virkningsgrad, η	[-]	1,1	1,4	1,12	0,79	0,89
Karakteristisk bæreevne, Q_k fra PDA med $J_C = 0,0$	[kN]	4356	5674	6070	7153	9818
Rammepenning, σ [1)]	[MPa]	116,7	159,8	172,3	211,3	312,7
Registrert synk pr.slag	[mm]	3,6	0,4	0,7	0,5	1,6
Slag nummer registrert i PDA [2)]	[-]	16	162	274	360	386
Filnavn		10B	10B	10B	10B	10B

[1)] Rammepenning registrert 3 m fra pelespiss.

[2)] Det er utført flere slag/ registreringer for å teste PDA-utstyr i forkant. Registrerte tall kan derfor avvike fra peleprotokoller.

For videre tolkning av resultat og oversendelse av rådata etc. anbefales direkte kontakt mellom Multiconsult og NTNU for diskusjoner, supplerende CAPWAP analyser (hvis ønskelig). Dersom ønskelig kan også Sigbjørn Rønning ved vårt kontor i Trondheim bistå ved diskusjon av resultater osv.

Referanser

/I/ Pile Driving Analyzer version 2004.096.003. *PDA-W Manual of Operation*. Pile Dynamics Inc., Ohio, USA

/II/ CAPWAP version 2000-1. *Case Pile Wave Analysis Program*. Pile Dynamics Inc., Ohio, USA.

/III/ e-post korrespondanse med Sveinung Jørgensen Tveito, NTNU.

Vennlig hilsen
for Multiconsult AS

Leif Olav Bogen

Joar Tistel

Vedlegg: PDA utskrift P 10A
PDA utskrift P Ruukki
PDA utskrift P 10B

Kontrollert av: SR

PDA utskrift P10A
0,1 m

Noteby A/S

FOU Pelespiss

PDA OP: JOT

PILE DRIVING ANALYZER ®
Version 2002.093
10A
813

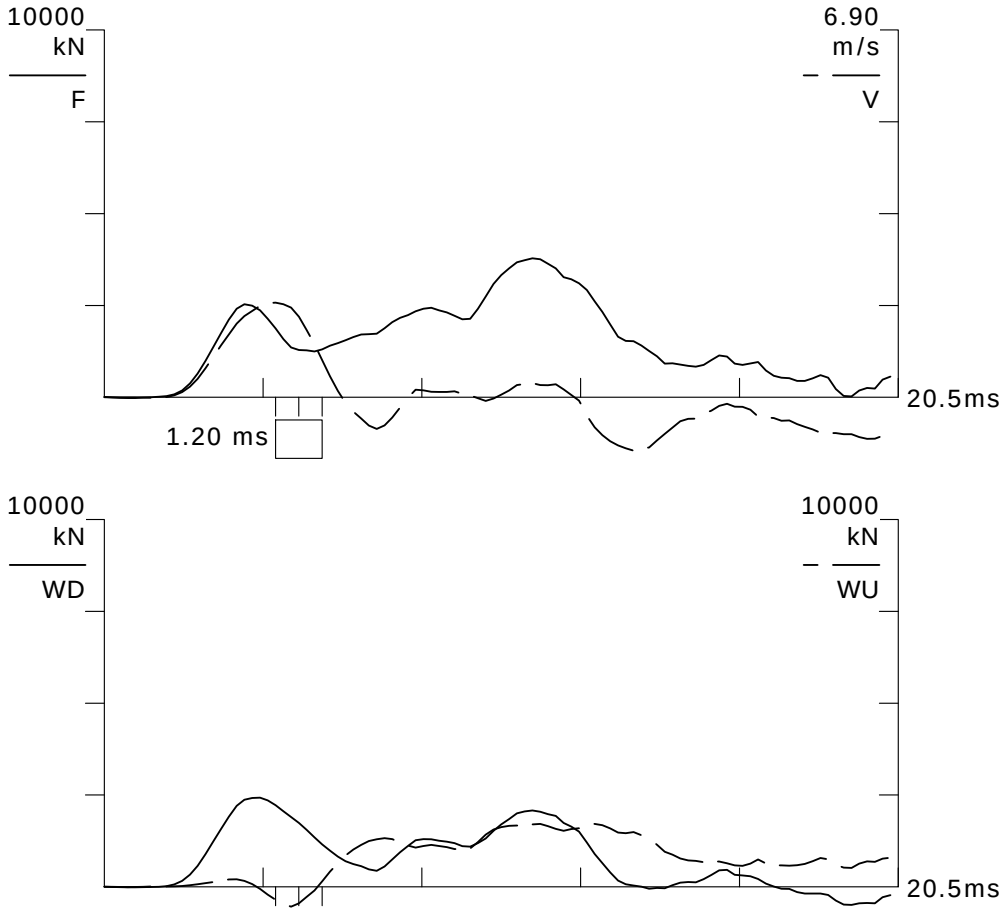

BN 27
08.04.2010 11:55:15

FMX	3783	kN
CSB	105.4	MPa
FVP	0.7	[]
RMX	3757	kN
QNV	0.00	[]
QNV	0.00	[]
QNV	0.00	[]
QNV	0.00	[]
QNV	0.00	[]

LE	3.0	m
AR	356.35	cm^2
EM	210000	MPa
SP	77.3	kN/m3
WS	5161.6	m/s
EA/C	1450	kN-s/m

F12 A12

F1: [6918] 92.1 (1)
F2: [9789] 91.9 (1)
A1: [52208] 1091 g's/v (1)
A2: [14131] 1005 g's/v (1)

PDA utskrift P10A
0,2 m

Noteby A/S

FOU Pelespiss

PDA OP: JOT

PILE DRIVING ANALYZER ®
Version 2002.093
10A
813

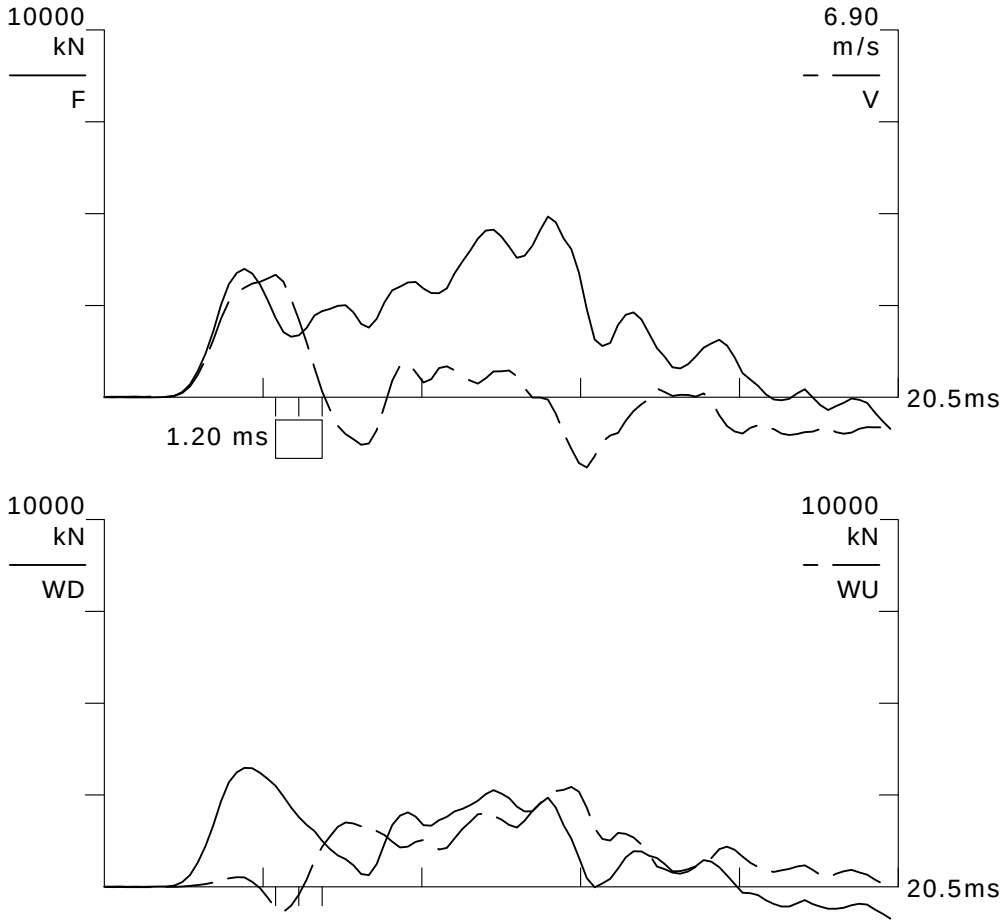

BN 105
08.04.2010 12:03:17

FMX	4922	kN
CSB	141.3	MPa
FVP	0.7	[]
RMX	5036	kN
QNV	0.00	[]
QNV	0.00	[]
QNV	0.00	[]
QNV	0.00	[]
QNV	0.00	[]

LE	3.0	m
AR	356.35	cm^2
EM	210000	MPa
SP	77.3	kN/m3
WS	5161.6	m/s
EA/C	1450	kN-s/m

F12 A12

F1: [6918] 92.1 (1)
F2: [9789] 91.9 (1)
A1: [52208] 1091 g's/v (1)
A2: [14131] 1005 g's/v (1)

PDA utskrift P10A
0,3 m

Noteby A/S

FOU Pelespiss

PDA OP: JOT

PILE DRIVING ANALYZER ®
Version 2002.093
10A
813

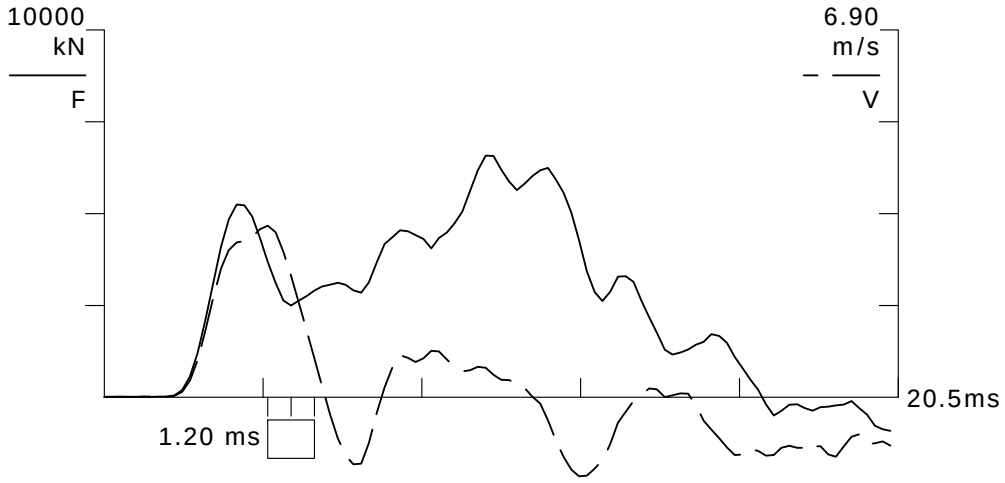

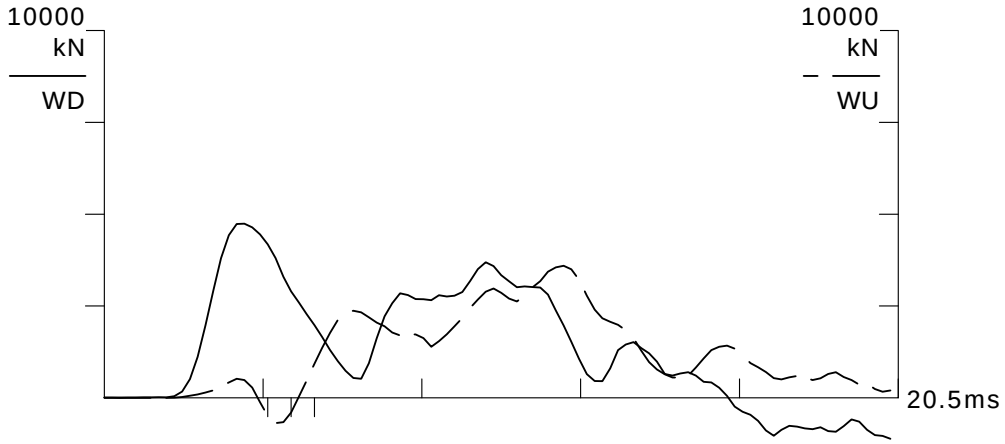

BN 179
08.04.2010 12:14:21

FMX	6583	kN
CSB	190.1	MPa
FVP	0.8	[]
RMX	6775	kN
QNV	0.00	[]
QNV	0.00	[]
QNV	0.00	[]
QNV	0.00	[]
QNV	0.00	[]

LE	3.0	m
AR	356.35	cm^2
EM	210000	MPa
SP	77.3	kN/m3
WS	5161.6	m/s
EA/C	1450	kN-s/m

F12 A12

F1: [6918] 92.1 (1)
F2: [9789] 91.9 (1)
A1: [52208] 1091 g's/v (1)
A2: [14131] 1005 g's/v (1)

PDA utskrift P10A
0,6 m

Noteby A/S

FOU Pelespiss

PDA OP: JOT

PILE DRIVING ANALYZER ®
Version 2002.093

10A

813

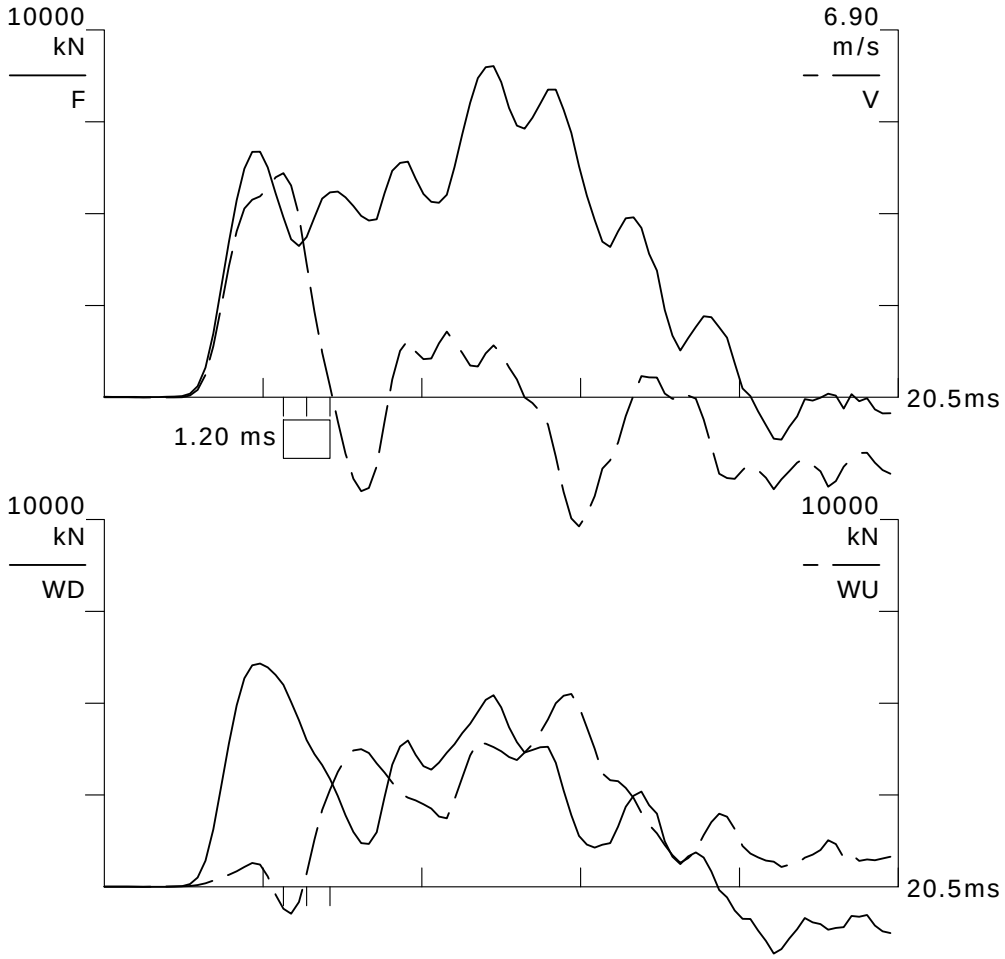

BN 467
08.04.2010 12:35:58

FMX	9020	kN
CSB	265.2	MPa
FVP	0.8	[]
RMX	9450	kN
QNV	0.00	[]
QNV	0.00	[]
QNV	0.00	[]
QNV	0.00	[]
QNV	0.00	[]

LE	3.0	m
AR	356.35	cm^2
EM	210000	MPa
SP	77.3	kN/m3
WS	5161.6	m/s
EA/C	1450	kN-s/m

F12 A12

F1: [6918] 92.1 (1)
F2: [9789] 91.9 (1)
A1: [52208] 1091 g's/v (1)
A2: [14131] 1005 g's/v (1)

PDA utskrift P10A
1,4 m

Noteby A/S

FOU Pelespiss

PDA OP: JOT

PILE DRIVING ANALYZER ®
Version 2002.093

10A

813

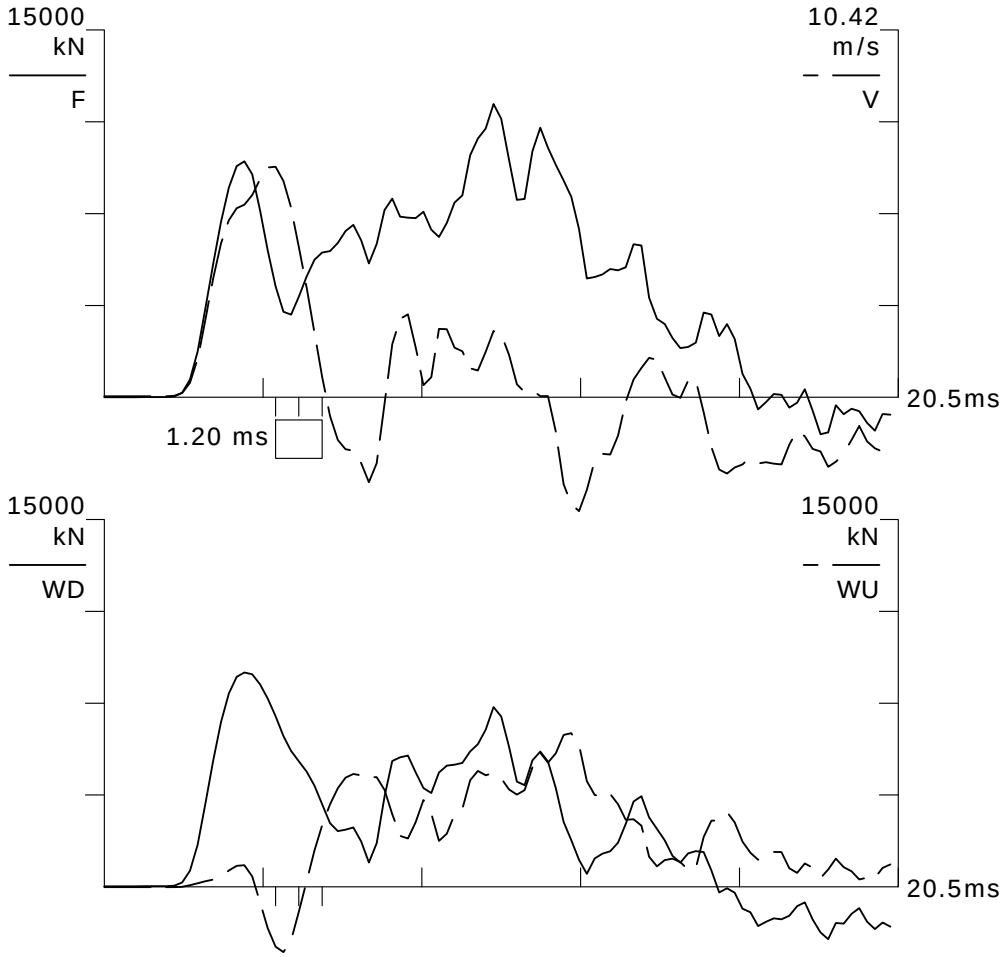

BN 498
08.04.2010 12:46:14

FMX	11980	kN
CSB	360.0	MPa
FVP	0.5	[]
RMX	12829	kN
QNV	0.00	[]
QNV	0.00	[]
QNV	0.00	[]
QNV	0.00	[]
QNV	0.00	[]

LE	3.0	m
AR	356.35	cm^2
EM	207000	MPa
SP	77.3	kN/m3
WS	5124.6	m/s
EA/C	1439	kN-s/m

F12 A12

F1: [6918] 92.1 (1)
F2: [9789] 91.9 (1)
A1: [52208] 1091 g's/v (1)
A2: [14131] 1005 g's/v (1)

PDA utskrift P Ruukki
0,1 m

Noteby A/S

FOU Pelespiss

PDA OP: JOT

PILE DRIVING ANALYZER ®
Version 2002.093
RUUKKI
813

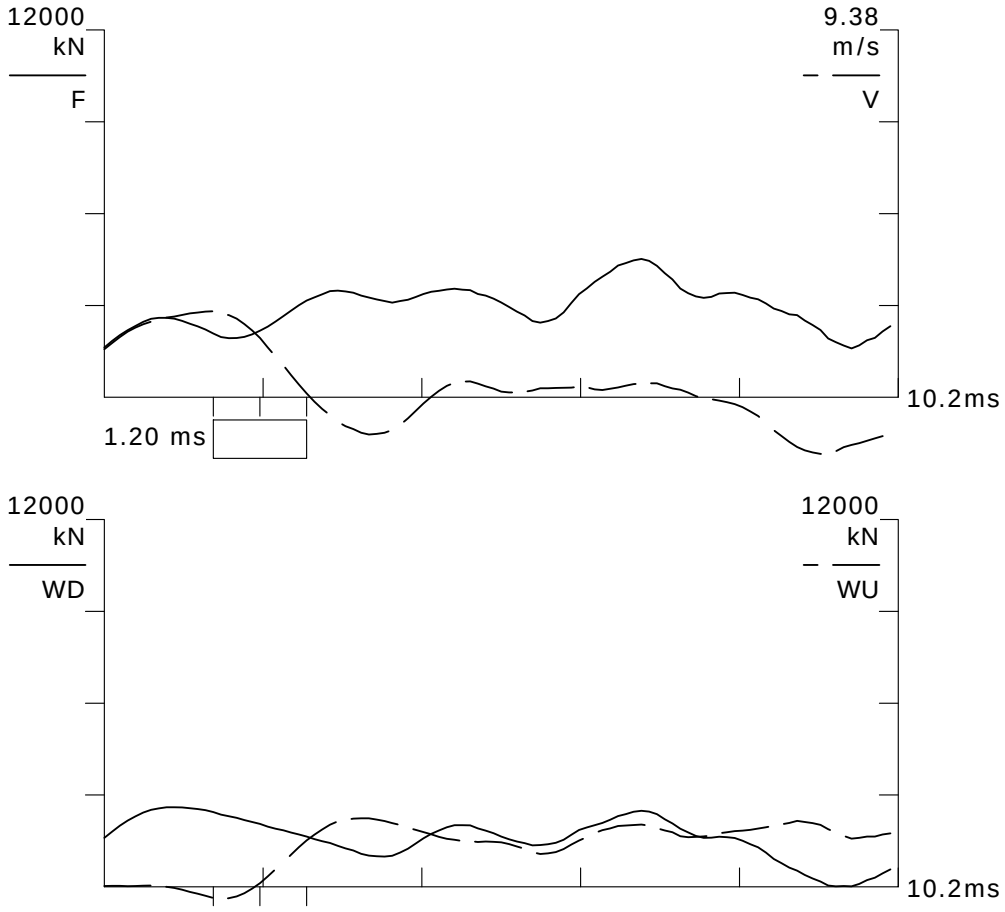

BN 16
08.04.2010 14:03:23

FMX	4522	kN
CSB	137.6	MPa
FVP	0.7	[]
RMX	4324	kN
QNV	0.00	[]
QNV	0.00	[]
QNV	0.00	[]
QNV	0.00	[]
QNV	0.00	[]

LE	3.0	m
AR	314.36	cm^2
EM	210000	MPa
SP	77.3	kN/m3
WS	5161.6	m/s
EA/C	1279	kN-s/m

F12 A12

F1: [6918] 92.1 (1)
F2: [9789] 91.9 (1)
A1: [52208] 1091 g's/v (1)
A2: [14131] 1005 g's/v (1)

PDA utskrift P Ruukki
0,2 m

Noteby A/S

FOU Pelespiss

PDA OP: JOT

PILE DRIVING ANALYZER ®
Version 2002.093
RUUKKI
813

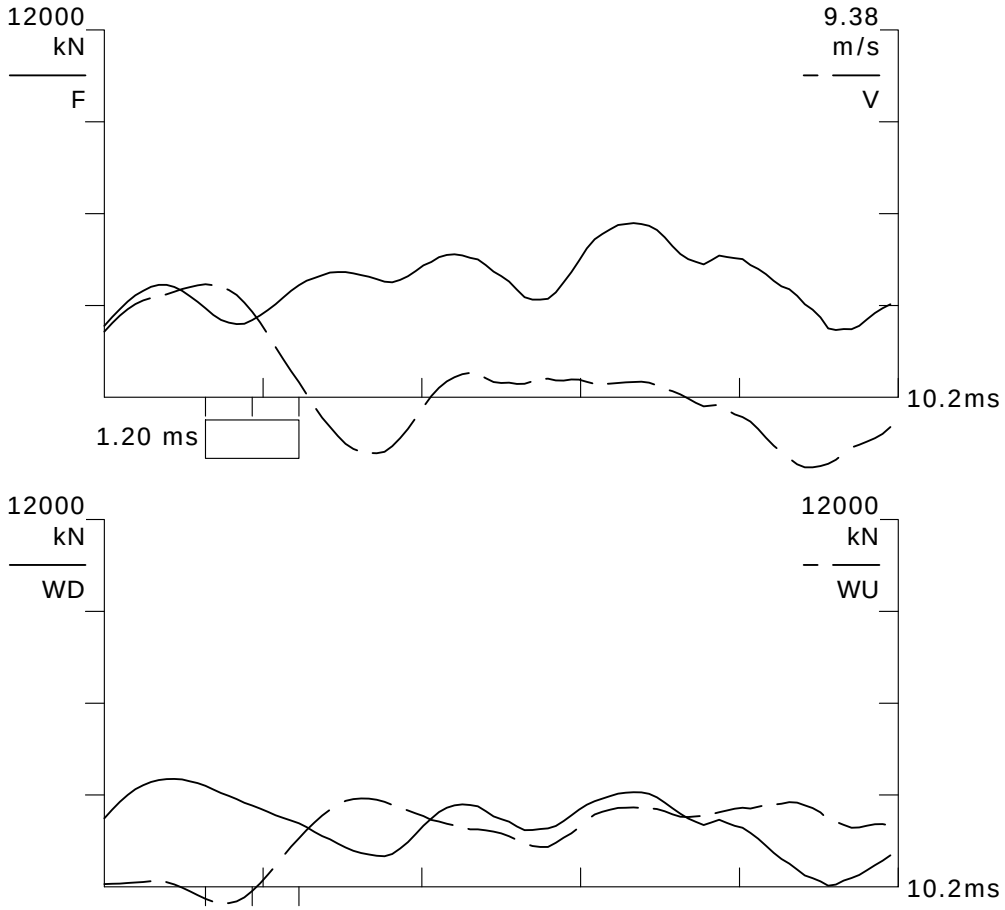

BN 27
08.04.2010 14:04:51

FMX	5690	kN
CSB	179.4	MPa
FVP	0.8	[]
RMX	5640	kN
QNV	0.00	[]
QNV	0.00	[]
QNV	0.00	[]
QNV	0.00	[]
QNV	0.00	[]

LE	3.0	m
AR	314.36	cm^2
EM	210000	MPa
SP	77.3	kN/m3
WS	5161.6	m/s
EA/C	1279	kN-s/m

F12 A12

F1: [6918] 92.1 (1)
F2: [9789] 91.9 (1)
A1: [52208] 1091 g's/v (1)
A2: [14131] 1005 g's/v (1)

PDA utskrift P Ruukki
0,3 m

Noteby A/S

FOU Pelespiss

PDA OP: JOT

PILE DRIVING ANALYZER ®
Version 2002.093
RUUKKI
813

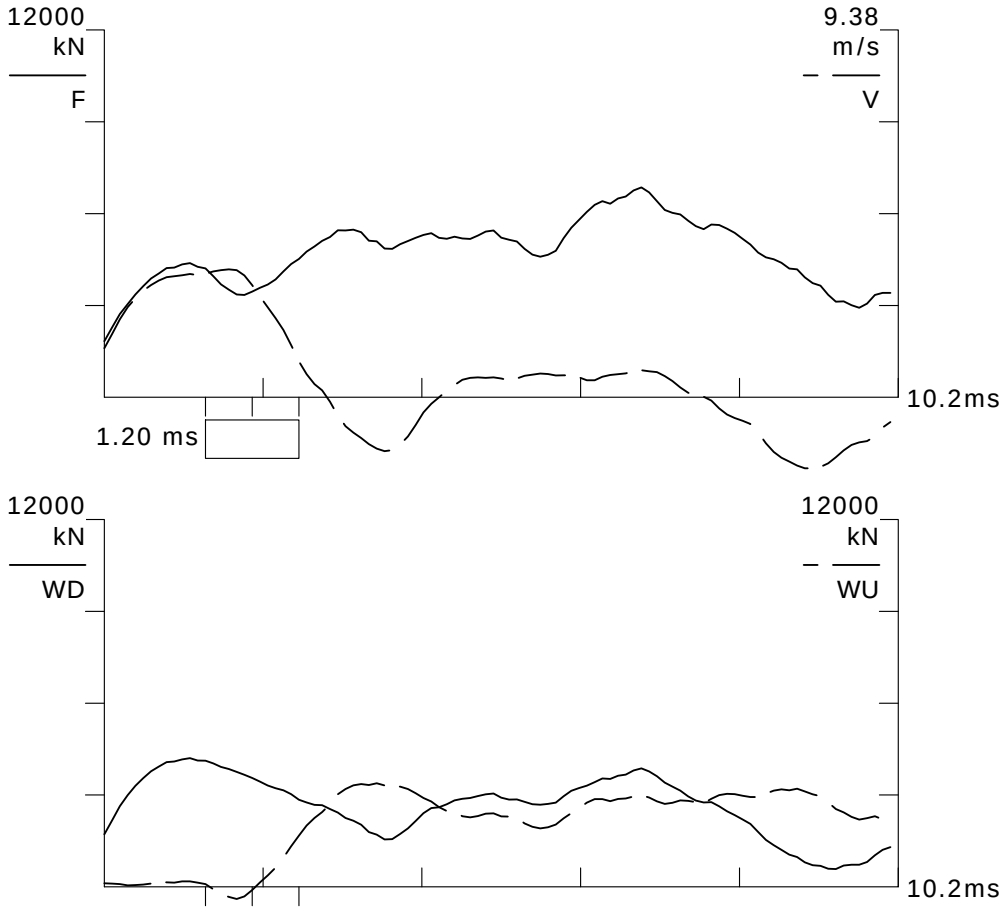

BN 280
08.04.2010 14:25:27

FMX	6858	kN
CSB	219.4	MPa
FVP	1.0	[]
RMX	6898	kN
QNV	0.00	[]
QNV	0.00	[]
QNV	0.00	[]
QNV	0.00	[]
QNV	0.00	[]

LE	3.0	m
AR	314.36	cm^2
EM	210000	MPa
SP	77.3	kN/m3
WS	5161.6	m/s
EA/C	1279	kN-s/m

F12 A12

F1: [6918] 92.1 (1)
F2: [9789] 91.9 (1)
A1: [52208] 1091 g's/v (1)
A2: [14131] 1005 g's/v (1)

PDA utskrift P Ruukki
0,6 m

Noteby A/S

FOU Pelespiss

PDA OP: JOT

PILE DRIVING ANALYZER ®
Version 2002.093
RUUKKI
813

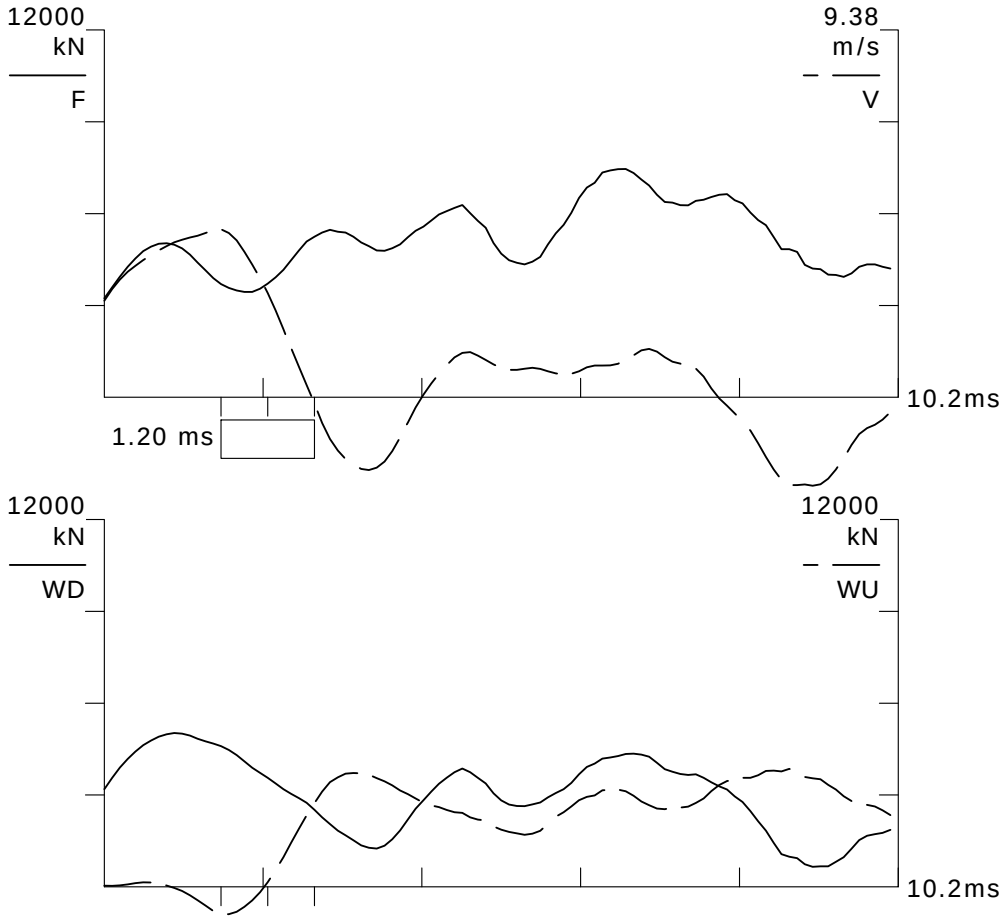

BN 389
08.04.2010 14:33:51

FMX	7461	kN
CSB	248.5	MPa
FVP	0.7	[]
RMX	7811	kN
QNV	0.00	[]
QNV	0.00	[]
QNV	0.00	[]
QNV	0.00	[]
QNV	0.00	[]

LE	3.0	m
AR	314.36	cm^2
EM	210000	MPa
SP	77.3	kN/m3
WS	5161.6	m/s
EA/C	1279	kN-s/m

F12 A12

F1: [6918] 92.1 (1)
F2: [9789] 91.9 (1)
A1: [52208] 1091 g's/v (1)
A2: [14131] 1005 g's/v (1)

PDA utskrift P Ruukki
1,4 m

Noteby A/S

FOU Pelespiss

PDA OP: JOT

PILE DRIVING ANALYZER ®
Version 2002.093
RUUKKI
813

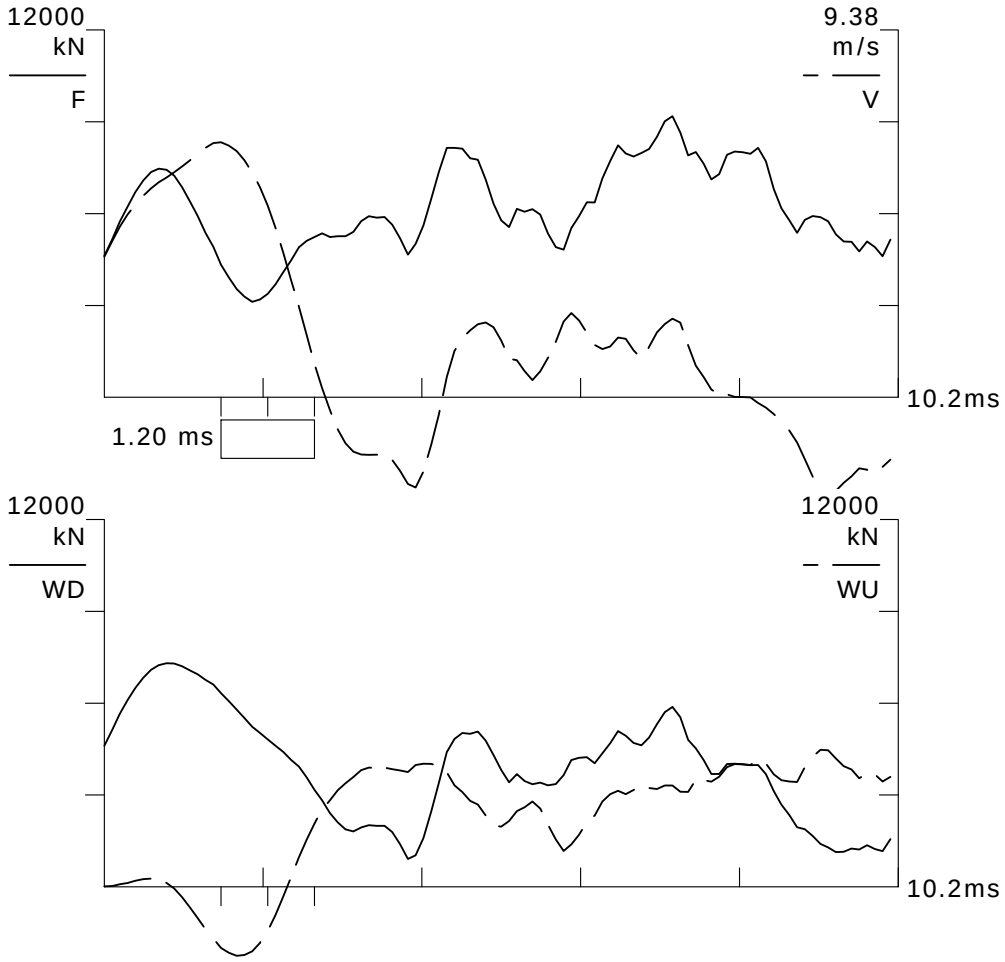

BN 415
08.04.2010 14:37:18

FMX	9188	kN
CSB	315.1	MPa
FVP	0.5	[]
RMX	9907	kN
QNV	0.00	[]
QNV	0.00	[]
QNV	0.00	[]
QNV	0.00	[]
QNV	0.00	[]

LE	3.0	m
AR	314.36	cm^2
EM	210000	MPa
SP	77.3	kN/m3
WS	5161.6	m/s
EA/C	1279	kN-s/m

F12 A12

F1: [6918] 92.1 (1)
F2: [9789] 91.9 (1)
A1: [52208] 1091 g's/v (1)
A2: [14131] 1005 g's/v (1)

PDA utskrift P 10B
0,1 m

Noteby A/S

FOU Pelespiss

PDA OP: JOT

PILE DRIVING ANALYZER ®
Version 2002.093

10B

813

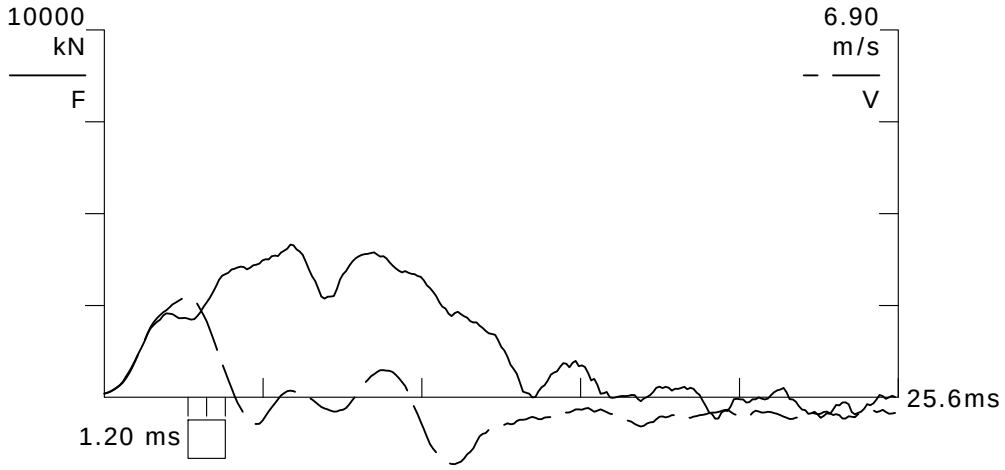

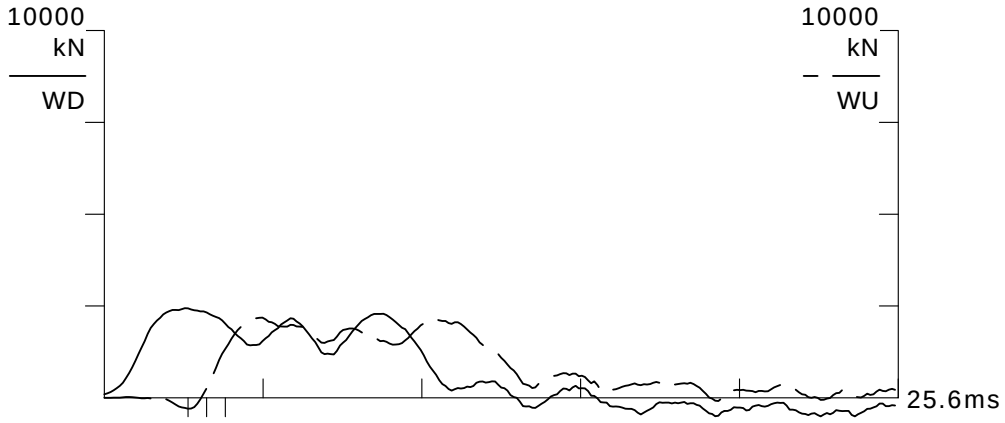

BN 16
08.04.2010 15:44:25

FMX	4159	kN
CSB	122.3	MPa
FVP	0.8	[]
RMX	4356	kN
QNV	0.00	[]
QNV	0.00	[]
QNV	0.00	[]
QNV	0.00	[]
QNV	0.00	[]

LE	3.0	m
AR	356.35	cm^2
EM	210000	MPa
SP	77.3	kN/m3
WS	5161.6	m/s
EA/C	1450	kN-s/m

F12 A12

F1: [6918] 92.1 (1)
F2: [9789] 91.9 (1)
A1: [52208] 1091 g's/v (1)
A2: [14131] 1005 g's/v (1)

PDA utskrift P 10B
0,2 m

Noteby A/S

FOU Pelespiss

PDA OP: JOT

PILE DRIVING ANALYZER ®
Version 2002.093

10B

813

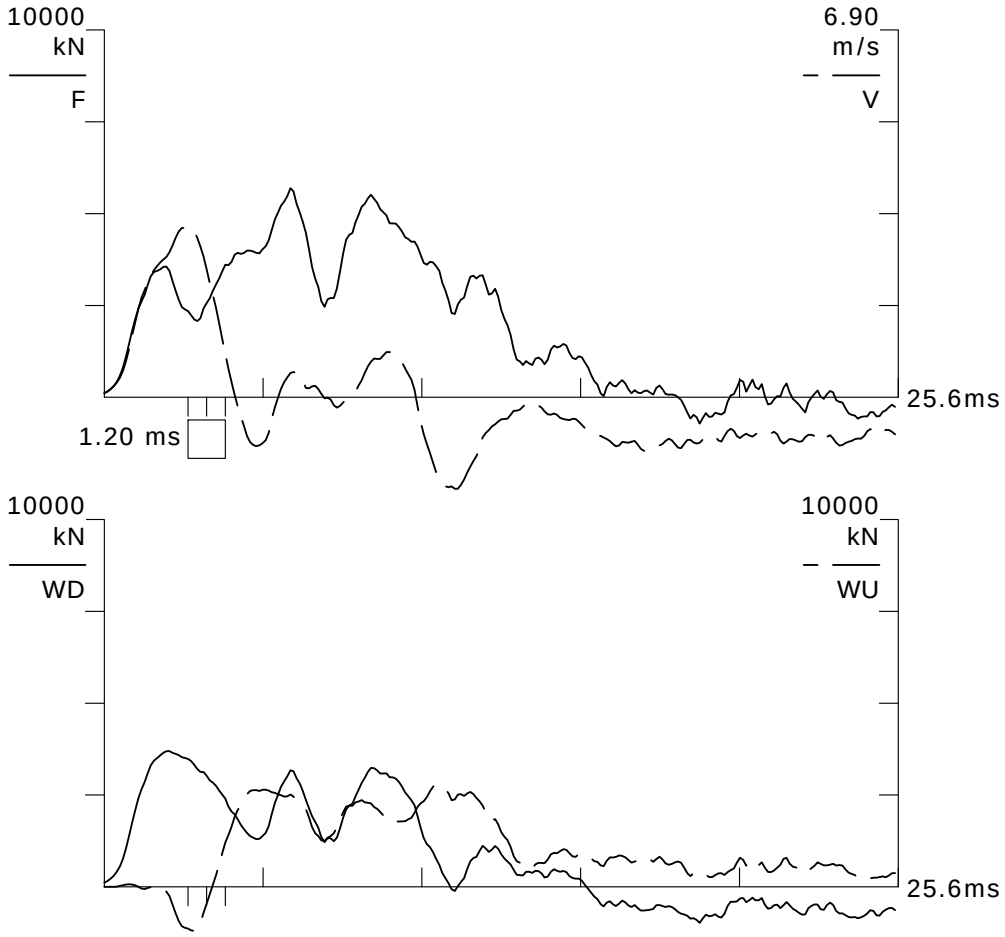

BN 162
08.04.2010 15:53:37

FMX	5693	kN
CSB	159.2	MPa
FVP	0.5	[]
RMX	5674	kN
QNV	0.00	[]
QNV	0.00	[]
QNV	0.00	[]
QNV	0.00	[]
QNV	0.00	[]

LE	3.0	m
AR	356.35	cm^2
EM	210000	MPa
SP	77.3	kN/m3
WS	5161.6	m/s
EA/C	1450	kN-s/m

F12 A12

F1: [6918] 92.1 (1)
F2: [9789] 91.9 (1)
A1: [52208] 1091 g's/v (1)
A2: [14131] 1005 g's/v (1)

PDA utskrift P 10B
0,3 m

Noteby A/S

FOU Pelespiss

PDA OP: JOT

PILE DRIVING ANALYZER ®
Version 2002.093

10B

813

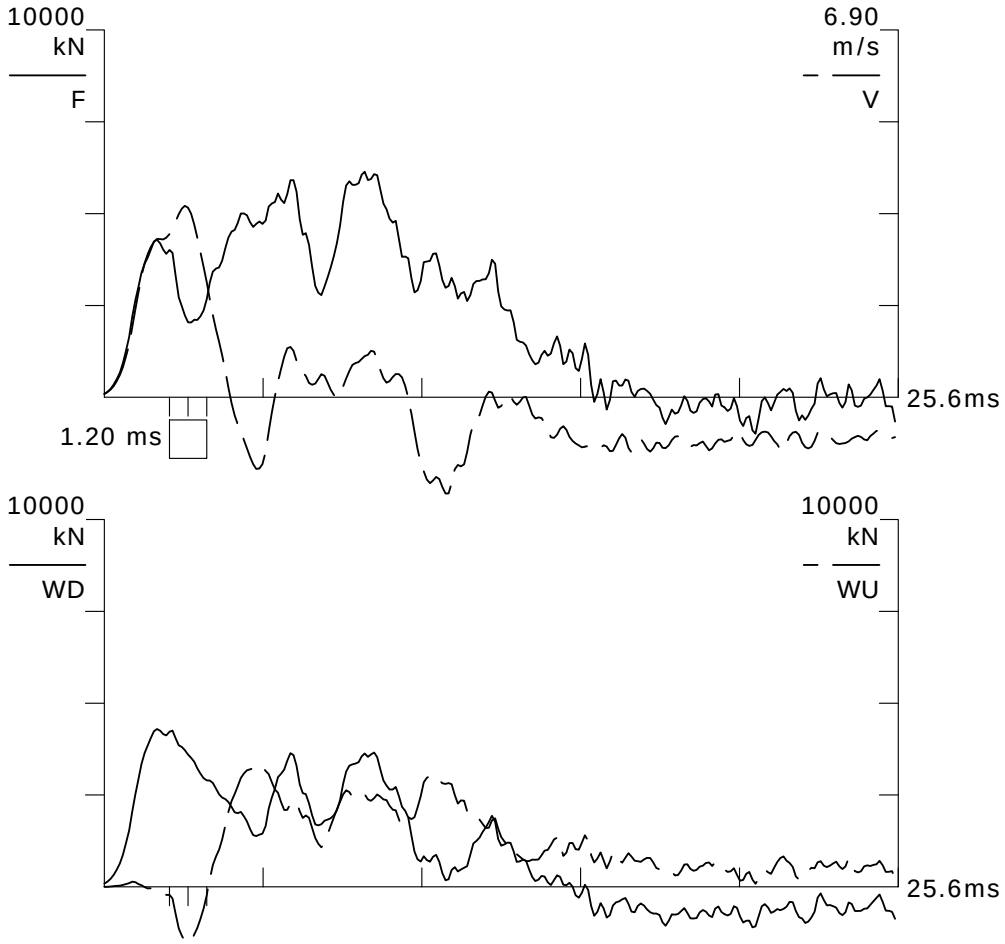

BN 274
08.04.2010 15:59:38

FMX	6141	kN
CSB	170.3	MPa
FVP	0.9	[]
RMX	6070	kN
QNV	0.00	[]
QNV	0.00	[]
QNV	0.00	[]
QNV	0.00	[]
QNV	0.00	[]

LE	3.0	m
AR	356.35	cm^2
EM	210000	MPa
SP	77.3	kN/m3
WS	5161.6	m/s
EA/C	1450	kN-s/m

F12 A12

F1: [6918] 92.1 (1)
F2: [9789] 91.9 (1)
A1: [52208] 1091 g's/v (1)
A2: [14131] 1005 g's/v (1)

PDA utskrift P 10B
0,6 m

Noteby A/S

FOU Pelespiss

PDA OP: JOT

PILE DRIVING ANALYZER ®
Version 2002.093

10B

813

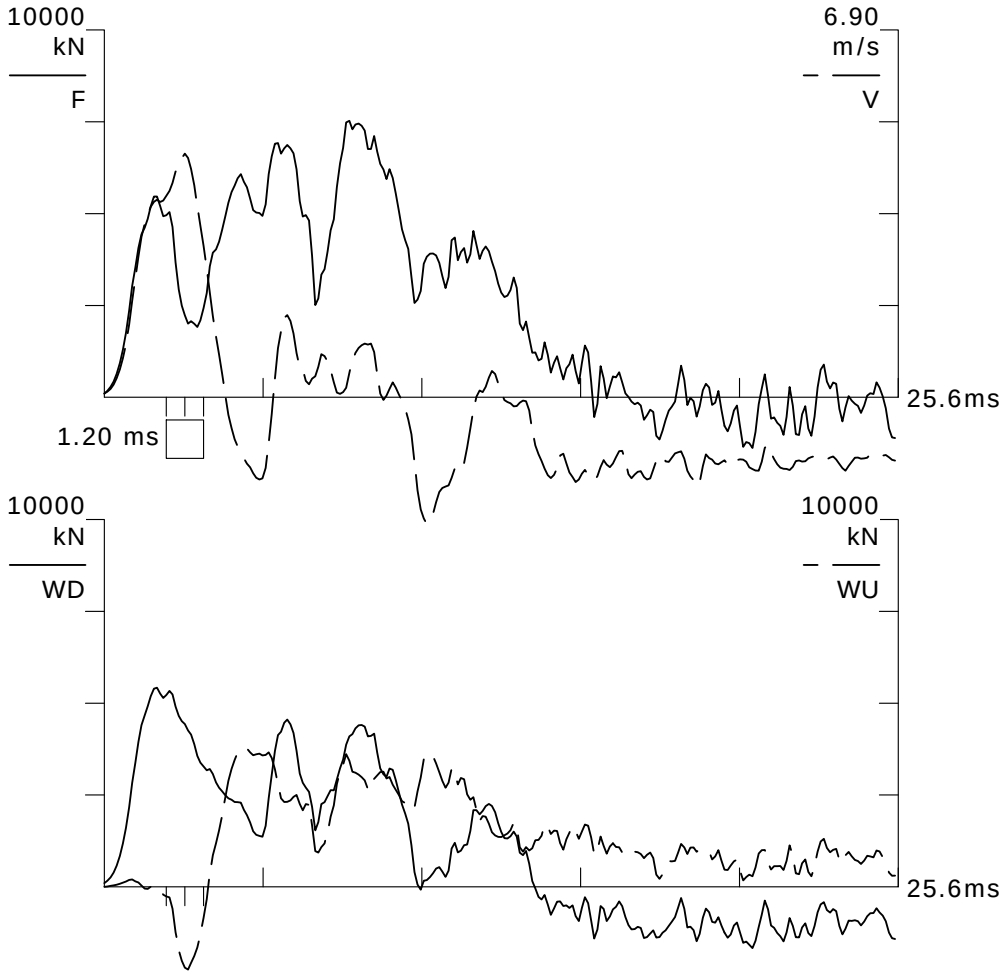

BN 360
08.04.2010 16:05:11

FMX	7529	kN
CSB	200.7	MPa
FVP	0.9	[]
RMX	7153	kN
QNV	0.00	[]
QNV	0.00	[]
QNV	0.00	[]
QNV	0.00	[]
QNV	0.00	[]

LE	3.0	m
AR	356.35	cm^2
EM	210000	MPa
SP	77.3	kN/m3
WS	5161.6	m/s
EA/C	1450	kN-s/m

F12 A12

F1: [6918] 92.1 (1)
F2: [9789] 91.9 (1)
A1: [52208] 1091 g's/v (1)
A2: [14131] 1005 g's/v (1)

PDA utskrift P 10B
1,4 m

Noteby A/S

FOU Pelespiss

PDA OP: JOT

PILE DRIVING ANALYZER ®
Version 2002.093

10B

813

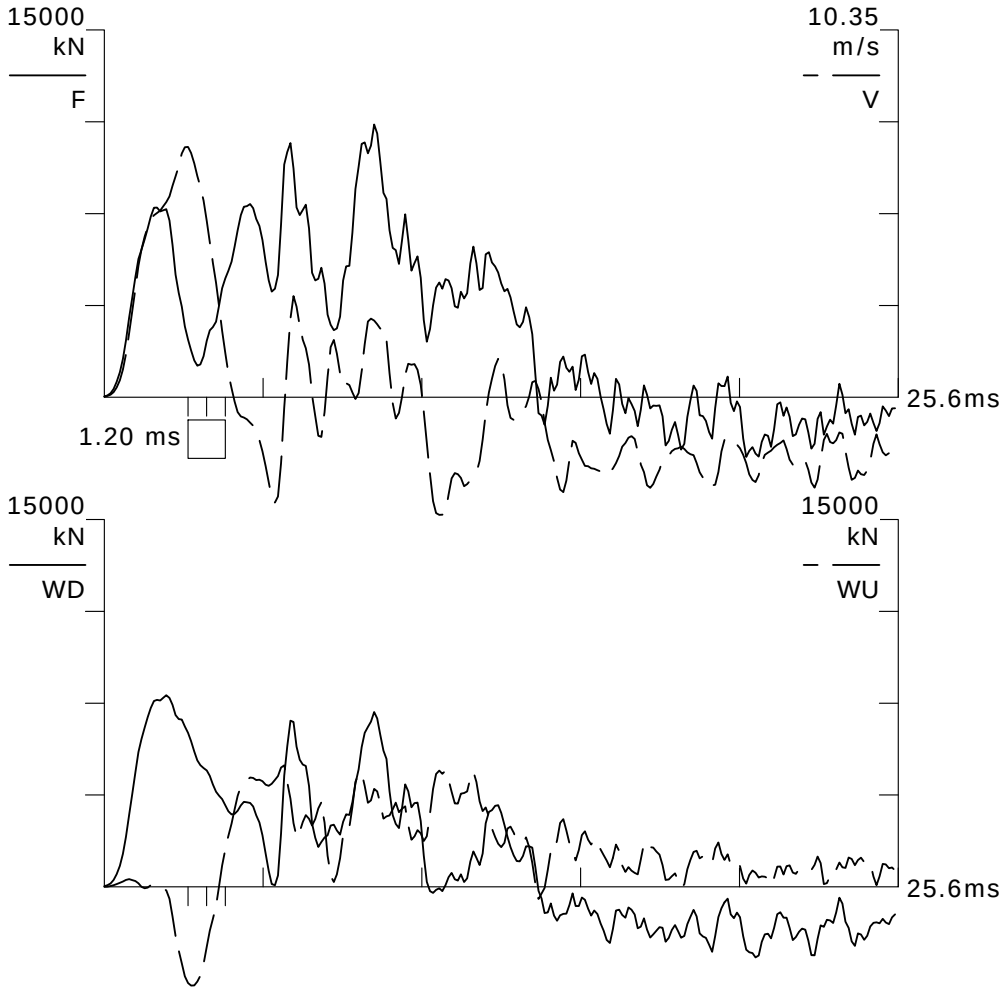

BN 386
08.04.2010 16:07:50

FMX	11142	kN
CSB	275.5	MPa
FVP	0.2	[]
RMX	9818	kN
QNV	0.00	[]
QNV	0.00	[]
QNV	0.00	[]
QNV	0.00	[]
QNV	0.00	[]

LE	3.0	m
AR	356.35	cm^2
EM	210000	MPa
SP	77.3	kN/m3
WS	5161.6	m/s
EA/C	1450	kN-s/m

F12 A12

F1: [6918] 92.1 (1)
F2: [9789] 91.9 (1)
A1: [52208] 1091 g's/v (1)
A2: [14131] 1005 g's/v (1)

Attachment

B. Pile driving procedure and pile driving protocol

Guide lines for driving the piles during the test

	Drop height, H(cm)	Minimum number of series (@ 10 blows)	penetration per series of blows≤ (mm)
Step 1	10	1	2
Step 2	20	1	2
Step 3	30	1	2
Step 4	40	1	2
Step 5	50	1	2
Step 6	60	1	2
Step 7	70	1	2
Step 8	80	1	2
Step 9	100	1	2

Pile driving protocol for pile shoe nr. 1

Drop height, H(cm)	Number of blows	Penetration (mm)	Drop height, H(cm)	Number of blows	Penetration (mm)
10	10	43			
	10	45			
	10	55			
	10	43			
	10	11			
	10	5			
	10	3			
	10	2			
20	10	1			
	10	7			
	10	2			
30	10	10			
	10	14			
	10	16			
	10	21			
	10	19			
	10	10			
	10	7			
	10	6			
	10	5			
	10	6			
	10	4			
	10	4			
	10	3			
40	10	3			
	10	3			
	10	3			
50	10	7			
	10	9			
	10	5			
	10	5			
	10	4			
	10	8			
60	10	5			
	10	9			
100	10	11			
140	10	16			
	10	10			

Pile driving protocol for pile shoe nr. 2

Drop height, H(cm)	Number of blows	Penetration (mm)	Drop height, H(cm)	Number of blows	Penetration (mm)
10	10	36	40	10	4
	10	16		10	5
	10	4		10	5
	10	6		10	4
	10	5		10	5
	10	3		10	3
	10	3		10	5
	10	6		10	2
	10	7	50	10	1
	10	9	60	10	5
	10	7		10	4
	10	4		10	5
	10	6	100	10	6
	10	4		10	13
	10	4	140	10	16
	10	8			
	10	5			
	10	8			
	10	6			
	10	4			
	10	4			
	10	3			
	10	2			
20	10	4			
	10	3			
30	10	7			
	10	7			
	10	9			
	10	16			
	10	10			
	10	8			
	10	11			
	10	8			
	10	5			
	10	7			
	10	3			
	10	3			
	10	4			

Pile driving protocol for pile shoe nr. 3

Drop height, H(cm)	Number of blows	Penetration (mm)	Drop height, H(cm)	Number of blows	Penetration (mm)
10	10	10	50	10	3
	10	16		10	3
	10	2	60	10	3
20	10	10		10	2
	10	9		10	1
	10	10	100	10	13
	10	9		10	19
	10	3	140	10	54
	10	4			
	10	3			
30	10	5			
	10	5			
	10	6			
	10	9			
	10	5			
	10	14			
	10	6			
	10	7			
	10	10			
	10	18			
	10	25			
	10	29			
	10	25			
	10	16			
	10	3			
	10	8			
	10	4			
40	10	5			
	10	2			
	10	0			
	10	3			
	10	4			
	10	5			
	10	5			
	10	3			
	10	2			

Norwegian Public Roads Administration

Norwegian Public Roads Administration
Publications
Box 8142 Dep.
N-0033 Oslo
Tel. (+47 915)02030
E-mail: publvd@vegvesen.no

ISSN: 1892-3844